Università degli Studi di Milano
Scuola di dottorato in Fisica, Astrofisica e Fisica Applicata - Ciclo XXVIII

and

Université Pierre et Marie Curie - Paris 6
École Doctorale 564 Physique en Île-de-France - Promotion 2012

Dynamics with selection

Supervisor: **Sergio CARACCIOLO**
Supervisor: **Jorge KURCHAN**

PhD Candidate:
Tommaso BROTTO

Commission:

Enzo MARINARI	Rapporteur
Riccardo ZECCHINA	Rapporteur
Marco COSENTINO-LAGOMARSINO	Examiner
Stefano ZAPPERI	Examiner
Sergio CARACCIOLO	Supervisor
Jorge KURCHAN	Supervisor

Abstract (italiano)

Il soggetto di questa tesi è la dinamica delle popolazioni. Ne studiamo le caratteristiche in assenza o in presenza di una struttura spaziale, e ciò si riflette nella suddivisione del manoscritto in due parti. Nella prima, in cui consideriamo la competizione come avvenire tra tutti gli individui contemporaneamente, proviamo che una condizione di bilancio dettagliato è soddisfatta in diversi regimi evolutivi (e non solamente, come noto, nel regime di successional-mutations). Mostriamo che la dinamica adattativa di una popolazione presenta numerosi aspetti in comune con la dinamica vetrosa fuori equilibrio, il ruolo della temperatura essendo giocato dal numero di individui nella popolazione. Suggeriamo numerose applicazioni di una tale analogia. Successivamente, consideriamo l'evoluzione di popolazioni monomorfe interagenti. Mostriamo come l'accoppiamento causi una separazione delle scale temporali adattative, e sia possibile istituire una gerarchia nel grado di adattazione tra le popolazioni.

Nel caso di popolazioni che competono nello spazio, la dinamica evolutiva è fortemente modificata dalla località delle interazioni. I meccanismi di selezione sono meno efficaci nel favorire la fissazione del fenotipo più adatto. Proviamo quantitativamente che un maggiore tasso di mutazione comporta uno svantaggio evolutivo, dal momento che la presenza di mutanti rallenta la crescita spaziale di una popolazione. Mostriamo come, se il tasso di mutazione è variabile, la selezione favorisce non solo un alto tasso di riproduzione, ma anche un basso tasso di mutazione.

Abstract (français)

Le sujet de cette thèse est la dynamique des populations. Nous en étudions les caractéristiques en absence ou en présence d'une structure spatiale, et cela se reproduit dans la subdivision du manuscrit en deux parties. Dans la première, où nous considérons la compétition comme se manifestant entre tous les individus en même temps, nous prouvons qu'une condition de bilan détaillé est vérifiée dans des différents régimes d'évolution (et non seulement dans le cas de successional-mutations). On montre que la dynamique adaptative d'une population présente de nombreux aspects en commun avec la dynamique vitreuse hors-équilibre, le rôle de la température étant joué par la dimension de la population. Des nombreuses applications d'une telle analogie sont suggérées. Dans la suite, nous considérons l'évolution de populations monomorphes interagissants. Nous montrons comment le couplage génère une séparation des échelles temporales d'adaptation, et il est possible qu'une hiérarchie soit créée selon les degrés d'adaptation des populations.

Dans le cas de populations en compétition dans l'espace, la dynamique évolutive est fortement modifiée par la localité des interactions. Les mécanismes de sélection sont moins efficaces pour ce qui est de favoriser la fixation du phénotype le mieux adapté. Nous montrons de façon quantitative comment un taux de mutation plus élevé occasionne un désavantage évolutif, car la présence de mutants ralentit la croissance spatiale d'une population. On montre que, si le taux de mutation est variable, la sélection favorise non seulement un taux de reproduction élevé, mais aussi un taux de mutation réduit.

Contents

Definitions **1**

I Well mixed **7**

1 Adaptation **9**
Chapter Teaser . . . 9
1.1 Stochastic evolutionary models . . . 10
1.1.1 Moran model . . . 10
Genetic drift . . . 11
Constant selection . . . 13
1.1.2 Wright-Fisher model . . . 13
1.1.3 Galton-Watson model . . . 14
1.2 Time-scales . . . 15
1.2.1 Fixation times . . . 15
Fixation time in presence of selection . . . 15
Fixation time in presence of genetic drift . . . 16
1.2.2 Comparisons . . . 17
A first comparison: selection vs drift . . . 17
A second comparison: mutation vs selection . . . 18
1.3 Speed of adaptation . . . 19
The Gaussian shape of the travelling wave . . . 20
1.3.1 Successional mutations . . . 20
1.3.2 Clonal interference . . . 21
1.3.3 Concurrent mutations . . . 23
More involved calculations . . . 24
1.3.4 Infinite population size . . . 26

2 Population Temperature **29**
Chapter Teaser . . . 29
2.1 Population as a thermal system . . . 30
2.1.1 Detailed Balance . . . 30
2.1.2 Glasses . . . 32
Real glasses . . . 32

Correlation . . . 33
Trap model and ergodicity breaking . . . 33
Canyon model . . . 35
2.1.3 Coarse grained population dynamics . . . 35
2.2 Population glass . . . 38
2.2.1 Boolean satisfiability . . . 38
Physical interpretation . . . 39
2.2.2 M population, $1/M$ temperature . . . 41
Correlations and the glass-phase transition . . . 43
2.2.3 Test of detailed balance . . . 46
Crooks relation . . . 46
A test of the Crooks relation . . . 48
2.3 Phenomenology of population thermodynamics . . . 50
2.3.1 Kovacs effect . . . 50
Memory effects . . . 51
2.3.2 Parallel tempering . . . 52
2.3.3 Rejuvenation in fluctuating environment . . . 55

3 Coupled models **59**
Chapter Teaser . . . 59
3.1 Fitness REM . . . 60
3.1.1 REM . . . 61
3.1.2 A single model . . . 63
3.2 Interacting models . . . 64
3.2.1 Two systems . . . 65
A time-scale separation mechanism . . . 67
Limited jumps . . . 70
3.2.2 More systems . . . 72

II Space and Mutation **79**

4 Space as a limiting resource **81**
Chapter Teaser . . . 81
4.1 Constant population size in space . . . 82
The wandering island of individuals . . . 82
4.2 Freely growing population . . . 84
4.2.1 Drift in space . . . 85
Linear front . . . 85
Circular front . . . 87
4.2.2 Deterministic growth . . . 88
Linear growth . . . 88
Circular growth . . . 89

5 The selective effects of mutation **91**
Chapter Teaser . . . 91
5.1 Mutational Eden Model . . . 92
5.1.1 Active and inactive phases . . . 93
5.1.2 Front properties . . . 95
5.2 Selective advantage of stability in well-mixed . . . 96
5.3 Selective advantage of stability in space . . . 100
5.3.1 Speed of growth . . . 100
Saturation effects . . . 101
5.3.2 Mutation rate evolution . . . 102

Conclusions **107**

A Computations of the entropy **109**

Preface

Every organism has a finite lifetime. This finiteness engenders the need for reproduction, in order for the organism to survive, albeit in an indirect way, through its offspring. The finiteness amount of resources, space, and time, makes so that no individual can reproduce countless times. There is competition, to survive and to reproduce. According to the environment and external and internal elements, an individual is more or less favoured in this process. As time goes by, history will tell who wins, and survives, and who loses, and is condemned to extinction. Not everyone can live forever, only one can dominate, but its authority might be questioned at any time by a new, stronger outsider. Selection is the word.

This thesis is about one issue: competing reproducing populations. The term population is far from being naively used. The fact that the competition takes place at the level of the populations, rather than at the one of the individuals, is of extreme relevance. It is an uncontested result, in game theory and evolutionary biology, that a selfish individual is favoured against an altruist, but that a selfish population is going to be flushed away by a population of individuals that cooperate [1, 2]. We will encounter several examples during this work in which the dynamics at the level of the individual is qualitatively and quantitatively distinct from the one of a population. Even when the single individual is simply diffusively changing its internal state (see e.g. subsection 2.2), or randomly mutating (see e.g. chapter 5), an adaptive dynamics can emerge in the population, simply as an effect of the presence of reproduction and selection.

This work is concerned with population intended in a very broad way. Actually, the term population has already a biological characterization. Biological systems are particularly suited to fit the paradigm of group of single entities, reproducing, and competing for survival. Spanning from viruses, to bacteria, to multi-cellular organism, all the way up in complexity to humans, the whole ensemble of biological systems fits into this pattern. However, one can consider all the discussions that will follow, for example, as if they were set in the framework of computer science, or economics. As long as reproduction and selection can be recognized as leading actors in the dynamics, no matter how different they might be in practice from their biological counterparts, the results that we will derive will apply unaffected. A population can then be a portfolio of assets, being duplicated and then selected on the basis of their value on the market. Or a series of running programs, each one capable of generating copies of itself, and competing on the basis of its computational performance. The author personal interests, and its belonging

to the class of biological entities, made him choose as the preferred application that of biological populations.

The number of experiments devoted to the study of the evolution of populations is countless, and indeed every biological study has to face evolution as a part of its object of study. Viruses and bacteria, in particular, are the main candidates, given their characteristics: they are microscopic, numerous, they reproduce and evolve extremely fast, thus allowing for repeated experiments, and are economically affordable to generate and maintain. The most remarkable evolutionary experiment is the *E.coli long-term evolution experiment* by R. Lenski and collaborators [3, 4], who have been following the evolution of twelve identical populations of bacteria, uninterruptedly, since 1988. We will not be concerned with any particular experiment in the specific, since our approach is species-independent, and wishes to preserve the level of generality that only a theoretical study can guarantee. Many of the results we will obtain in our analysis, however, have found, or will find in the future, confirmation in the experiment.

In our effort to be as general as possible, we tried to minimize the number of specifications and ad-hoc assumptions. However, a cube cannot be distinguished from a sphere without going into the details, and one needs such details in order to play dice and hope for some gain.

The work is divided into two parts, separated by one main difference in the content. The first part refers to an a-spatial settings, while the second one retains a notion of space as a fundamental characteristic of the models analysed. The manuscript tries to be as complete and organised as possible. The content is homogeneous, and should be considered as one. Since, however, this is a thesis work, and credits should be given, the first chapters of every part are devoted to a general introduction to the subject, and collect several results provided by other authors, in order to give a general understanding of the main issues, and setting a basis for the future discussions. The second (or third) chapters of each part, instead, are more specific, and correspond, when not explicitly said otherwise, to original contributions provided by the author. These can also be found, partially, in two papers in publication, see [5] and [6].

We will describe, in the following, the content of each chapter. For each one of these, we provide here a summary of the contents, combined with a discussion on the results, in order to make the reader aware since the beginning about the main achievements obtained, and the interconnections linking the different sections of the manuscript. We considered redundant the presence of an additional introduction at the beginning of each chapter. Instead, as an overview, but also in the desire of intriguing the reader, persuading him to a more willing lecture, each chapter opens with a teaser. The most important results contained in each chapter are summed up in the form of open questions, sometimes voluntarily cryptic and tendentious, with a reference to the section or subsection in the chapter where the answer should be looked for.

Finally, the quotes at the beginning of each chapter are a tribute to Jorge Louis Borges, passionate reader of the fictitious literature.

The rest of this preface is dedicated to an overview of the main ideas and results contained in this work, following the subdivision of chapters.

- ▷ A sort of chapter zero is dedicated to provide the definitions for terms and concepts used in this thesis. Given the very abstract perspective of this work, every concept requires to be defined in its characteristics and limits of application. Several terms find their current use at least both in the physicists and biologists communities, often with different meanings. Sometimes these differences are apparent and relevant, sometimes they are more subtle, but still important. Even before reading the rest of this preface, dedicated to the introduction to the other chapters, the reader is advised to check this chapter zero and the definitions there within, in order to give to the concepts that follow the right interpretation.

- ▷ Chapter one, *Adaptation*. This chapter is concerned with adaptation, namely the capacity of a population of evolving to fitter states. In order to provide the mathematical instruments necessary to treat population dynamics under a physicist's perspective, the first section describes the main stochastic models used in the literature. Great attention and detail is paid to the Moran model, it being the key model used in this work, but more than a few words are spent also for its relatives, the Wright-Fisher and the Galton-Watson model. The features and peculiarities of these models are highlighted throughout. In the framework of the Moran process, we set the first analysis of a competition for survival, computing the probability for fixation in a two competing lineages setting. The general result is applied to find the explicit expression for such a probability in the case of a competition ruled by stochastic dynamics alone, or in the presence of selection favouring one of the two lineages over the other. We also see how these results are not model dependent, showing that a very similar expression is obtained using a Wright-Fisher model.

  A second section is present, concerning the typical time-scales required for fixation. Again, purely random and selection-driven dynamics are analysed and compared. A feature that will be encountered all along the work, i.e. that selection accelerates evolution, is clearly showed to be present since from the simplest model, in the Moran two lineages competition. We see the emergence of one of the key regime of adaptive evolution, the successional mutations regime. Its features are described carefully, and a limit on its domain of applicability is provided in terms of some parameters of the population, namely its size, its mutation rate and the selective advantage provided by mutations.

  The final section of the chapter is dedicated to the computation of the speed of adaptation. As long as the successional mutations regime is present, adaptation is significantly speeded up by augmenting the population size, its velocity being proportional to the number of individuals in the population. Beyond a certain threshold, however, such a relationship changes from being linear to be logarithmic. Indeed, we have the emergence of two different effects, characterizing this new regime of evolution, and both concurring in reducing the speed of adaptation: concurrent mutations and clonal interference. Their main characteristics are described in the corresponding sections, and we provide ways to compute the speed of adaptation in these two cases. Even though results do not converge to the same exact

expression, while solving the problem with different approaches, the logarithmic dependence in the population size is confirmed by all of them. Discrepancies are substantially due to the approximations made in each one of the approaches, that are necessary to allow the problem to be solvable. Finally, the unrealistic limit of infinite population is investigated. Though in principle a valid approximation for very large population, we show how in practice it turns out to be a very poor solution to the biological problem of finding the speed of adaptation for a realistic population, since it predicts an infinite value for the velocity. This is a clear proof for the difficulties that have to be faced when a continuum approach is to be adopted;

▷ Chapter two, *Population temperature*. The chapter is entirely devoted to draw a parallel between a population and a thermal system. A population is hotter when smaller, and decrease its temperature by increasing its number of individual.

The first section begins by showing how a two lineages Moran process satisfies detailed balance, and how an equilibrium distribution for the fitness of populations can be derived. Such equilibrium distribution is formally identical to the Gibbs energy distribution of a thermal system. All this is considered to be valid in the successional mutations regime only. A long parenthesis, regarding glasses, is opened at this point. The main features of glasses will be indeed encountered in the setting of population dynamics, and need to be clarified and discussed. In particular, we deal with the behaviour of the decay of correlation, and with the different possibilities of glassy landscapes. The main out-of-equilibrium characteristics of glasses, the emergence of new time-scales and the property of aging are deeply described. This parenthesis on glasses achieved, we turn our focus on showing how an extension of the detailed balance equivalence for a Moran process can be achieved, even outside the domain of validity of the successional mutations regime. The key issue is the presence of a time-scale separation, typical of out-of-equilibrium processes, that allows to use a procedure of coarse graining on the fast degrees of freedom of the system.

The second section is dedicated to prove the validity of such claim. Needing a time-scale separation, we focus our attention to a particular model of glassy system. We introduce then boolean clauses, and the class of satisfiability problem. A population is built up by individuals consisting in realizations of sets of boolean variables, which determine the individual's fitness. Such fitness is evaluated as the logic outcome of the individual internal variables, with respect to a given boolean clause. With individuals changing their internal state diffusively (thus in a non-adaptive fashion) we follow the adaptive dynamics of the population. In particular, we compute the correlations among individuals in the population and we see that a glass-liquid transition can be observed, not in the temperature, but in the population size. Indeed, a phase diagram can be carried out. We provide a more careful check on the presence of detailed balance, for the dynamics of the population, in the form of a Crooks theorem, relating the response of the system to a pertur-

bation in an additional field. Our results show the presence of detailed balance, and this even in the presence of clonal interference and concurrent mutations. The averaging over the fast time-scales is shown to be necessary.

The third section presents a series of applications of the thermal-population equivalence. The applications stem all from the thermodynamical analogy, and are the counterpart of effects and phenomena that are present and have been studied in out of equilibrium physics, rather than being suggested by biological reasoning. The analogy and the consequences are far-reaching, and sometimes even counter-intuitive, when considered from a pure biological perspective. The first phenomenon studied has been known for long time in glasses, and it's called the Kovacs effect [7]. Its phenomenology repeats itself in the context of populations, where an increase in the energy corresponds to a decrease in the fitness. This similarity in behaviour suggests to push further the analogy, and that memory effects found in glasses should be noticeable even in the context of biological evolution. A population, kept at a given size for a given amount of time, should be optimized in such a way that, if let grow and then shrunk back to that size, it will conserve a record of the previous time, and turn out to be already optimize, even without additional time to adapt again. A concept stolen from computer science, but that can turn out to be of great importance in experimental biological set-ups, is that of parallel tempering. We show how the evolution of a bacterial population could be speeded up, by setting up a series of chemostat, and switching and adjusting them in a careful way. Finally, the effects of a fluctuation environment are investigated. In full agreement with the expected glass behaviour, we see that populations are rejuvenated by a changing environment, and that their adaptability can turn out to constitute an evolutionary advantage.

▷ Chapter three, *Coupled models*. The chapter deals with the study of the adaptative evolution of populations with epistatic fitness, in the successional mutations regime.

The first section is concerned with the evolution of a single population alone. A parallel between a monomorphic epistatic population and a model of disordered system, the Random Energy Model, is drawn. The latter is discussed in its main features, and the concept of freezing energy and equilibrium temperature are introduced. The focus is then brought back to evolving populations, and the rate of adaptation is obtained in term of the average fitness jump. The linear relation of the adaptation speed with the population size, already obtained in chapter 1, is confirmed.

The second section deals with interacting populations. The fitness is supposed to be multiplicative, and a simple interaction term should be imposed by hand. First, we focus on two interacting populations. The evolution is studied in the infinite population size, and an effective temperature is introduced, in order to parametrize the evolution. The two populations result to be self-organising in a hierarchy, i.e. in a fixed relation for what concerns both their effective temperatures (that is their degree of adaptation), and their evolutionary time-scales. The colder population

is also the one that evolves faster, and the time-scales between the populations diverge in the thermodynamic, or infinite genome, limit. Strangely enough, we see that this different pace in evolution is exploited by the slow population to increase its adaptation, by exchanging fitness with the fast one, and forcing it to undergo some fitness-decreasing evolutionary steps.

This situation is found also in the case of several interacting systems. It is possible to observe the formation of a 'chain of adaptation', with populations ordered with respect to their degree of adaptation, and exchanging fitness by gaining it from the population just above (slightly more adapted), and losing it in favour of the one just below. The time-scale separation, however, is not diverging at all levels of the chain, but only between the highest population and the other ones, with the rates of adaptation in the other layers remaining of the same order even in the infinite genome limit.

▷ Chapter four, *Space as a limiting resource*. Starting from this chapter, we see how the introduction of the notion of space modifies the modalities in which competition takes place. We start in the first section by studying the effects of our familiar fixed population size constraint in the space setting. We show how a population of diffusive individuals is kept together and localized in space by means of the reproductive forces. The population is also shown to act like a single wandering particle, with the same diffusion coefficient as one of its constituting individuals. All these features are an artefact of the fixed size constraint, that finds much less justification in the spatial case than in a well-mixed environment, and that we will abandon in the later discussions.

In the subsequent section we investigate the behaviour of an expanding population, in a linear and circular fashion. In perfect analogy to what we do in the chapter 1, we first study the case in which competition unfolds between two equally advantaged lineages, and then we introduce selection. We find again that fixation time is shortened when selection is present. We also see how the two settings, linear and circular, distinguish from each other, and how their differences should be individuated more in the expansion of the front that occurs in the latter case, rather than in a change in the microscopical dynamics at the level of the individual competition. The chapter closes with a summary and a discussion of the different results obtained for the effect of selection in the competition of two lineages, in the well-mixed and spatial case, linear and circular.

▷ Chapter five, *The selective effects of mutation*. This chapter focuses on the effects of mutation, and in particular on the mutation rate itself as an inheritable characteristic and an evolutionary element.

The first section is dedicated to study the effect of different mutation rates in the competition for space, without the possibility for it to evolve (i.e. the mutation rate is the same for all the lineages involved in the competition). The model adopted in this section is the Eden model, modified so to include mutations. Two lineages are

considered simultaneously, with mutations allowed only from one type to the other, and not vice-versa. This engenders an asymmetry in the system, leading to the inevitability of the eventual fixation of the non-mutating lineage. The quantitative differences in this fixation process lead to the individuation of a phase diagram, where a transition occurs according to the values of the fitness of the two lineages, and the mutation rate. The merging (or not) of domains seems to be the cause of the switching between the two phases. We investigate the non-trivial properties of the front in the presence of the inhomogeneities created by the coexistence of the two lineages.

The second section deals with the problem of assessing the selective advantage of stability in a well-mixed setting. A fully epistatic, constant size population model is studied. We show that the effects of mutation are substantially two. First, the dominant lineage does not account for the entire population, but constitutes only a part of it. A notion of effective population should be introduced, and the rest of the, less fit, individuals can be treated as a non-interacting cloud, i.e. not reproducing and not mutating. Second, the nature of competition between two fit lineages is changed. Instead of having the reproduction rate as the parameter ruling the evolution, we shall define an effective fitness, that takes into account also the mutation rate of each lineage. It is this effective fitness, and not fitness intended as the reproduction rate alone, that guarantees to a given mutant the advantage over the wild-type. In other words, we can show that stability can confer an evolutionary advantage, for well-mixed competitions. High fitness and stability are shown to correlate in an adapted population. We also show that all the thermodynamical analogy existing between populations and thermal systems can hold even when mutation rate is considered, providing that the temperature does refer to the effective population, and instead of the usual reproduction rate it is the effective fitness that is interpreted as (the logarithm of) the energy of the system.

In the third section the attention is drawn to the speed of the spatial growth in presence of mutations. We show that, as expected, mutations into a slower lineage slow down the growth of the main lineage, and the more, the higher the mutation rate is. Unexpectedly, however, the slow lineage contributes to a higher slow-down if its speed is just slightly lower than the main lineage one, rather than being much lower. This fact can be justified, as before, by the introduction of an effective fitness value. Finally, we will study the case where the mutation rate is seen as a selected and evolving element. A population is shown to be disadvantaged with respect to another one, simply by the fact that it is mutating faster. The retardation due to mutation is estimated quantitatively, in 2 and 3 dimensions, showing a smaller effect in the higher dimensional case. We see then that stability, i.e. a lower mutation rate, is selected by evolution, and that a correlation between high fitness and high stability is induced at the level of population, even in space. This can be clearly shown to be an effect absent at the individual level, and sustained by the presence of reproduction, adaptation being lost when individuals get far from the front, where reproduction occurs.

Definitions

Population dynamics is a field at the very border between statistical physics and biology. As it always happens in such situations, the two communities do not talk much to each other, and a common jargon is missing. We will then start this work by addressing this issue. In the following, we will try to be as specific and as general as possible, in the sense that we will define every object in the most precise way, but in avoiding all the specifications that will make its sense obscure for one of the two communities. So there will be no reference to, e.g., gene methilation or cadherin proteins. At the same time, while dealing with physics, we will try to provide introduction to key concepts. In the following, we give the definitions of the key concepts of our work.

Population: in our discussion, it will simply identify a collection of individuals. We will generally assume no interactions between single individuals, the only exception being constituted by the requirement of constant total population size. This is far from being a negligible constraint, and we will see that the dynamics at the level of the entire population will be drastically different from the one at level of the individual. The generic term **individual** might be intended as referring to cells, in the sense that the discussion will be carried on with a focus on biological systems, and colonies of cells (bacteria and viruses) are the straightforward field of application and analysis for studies in population dynamics. However, let us stress since now that our definition of individual is that of an entity able to reproduce and mutate, and possibly die. All the biochemical internal structure, along with all the possible complications that may arise in a feasible biological system, will be ignored. Typically, we will consider an individual as characterized by its reproduction rate only (λ in the text), as its only distinctive feature, and individuals with the same reproduction rate will be considered identical. Even when, like in section 2.2, some sort of internal structure will be introduced, it will only be significant in determining the fitness on the individual, and will be in no sense an attempt to reproduce any putative biological internal organization. In the true world, not all the populations might be able to reproduce, due to several factors, e.g. sexual maturity, environmental constraint, and so forth. In this sense, in literature, the concept of **effective population** is introduced, to indicate the fraction of the population that is capable and is actually involved in reproduction. In this work, when not explicitly stated, the effective population corresponds always to the entire population.

Genotype vs phenotype: it is common knowledge, encompassing by far the walls of the biology faculty, that every organism has an internal structure, that codes and provides the information for the development of its own characteristics and features. We will call this structure genome, with no other further specification, since we will not be concerned with it. However, the genome of an individual, or its genotype, it is not sufficient to determine what will be the final outcome of the interaction between genome expression and the environment. This outcome, namely the individual as it is, is what is called **phenotype**. We will always be speaking about an individual by considering its phenotype, neglecting its internal organization, and often considering, as the only phenotypic trait of interest, its reproduction rate.

Gene: from the chemical point of view, it is a sequence of molecules, or base-pairs, part of the genome of one organism. Its definition is much more accurate from the functional point of view, i.e. defining a gene as the constitutive unit of the genetic information. Oversimplifying, we will say that it contains the information for creating a protein, and therefore contribute, alone or along with other genes, to the determination of an individual's trait. Reality of course is more complicated than that, as the same sequence of base-pairs in a gene can be read in different ways, neglecting some of its parts, and thus give rise to different proteins, and different functions. The gene, namely the physical sequence, has a specific place, named locus, in the genomic chain. Therefore, when two genomes presents slightly difference sequences, in the same locus, containing the information for the development (with some differences) of the same trait, we refer them as variants of the same gene. In literature, the different variants of a gene are called **alleles**. One gene in a population can present only one allele, and in this case is defined **monomorphic**, or several different alleles, and it is termed **polymorphic**. The two terms can be used, in a wider sense, as referred to a population in its entirety. We see therefore that the true definition of a gene is the functional one, as the different alleles are actually physically different, even though we consider that they are all the same gene. An important property of a gene is its expression. Indeed the information contained in a gene can be or not used to create a protein, in respect of the actual need of the organism of that given protein. Genes can thus be switched off and switched on, and their state of activation can be extremely important in the correct development of the individual. In a sense, is not sufficient to have the information, but to be able to use it in the correct way. It is important to notice that is not only the gene that can be inherited, but also its activation state.

Fitness: in this work, fitness is synonymous of rate of reproduction of an individual, indicated by λ. The other definitions present in the literature defines the fitness as the average number of offspring that an individual can give birth to, which then corresponds to e^{λ}. We will come back to their distinction at the end of this chapter. Note that for finite population, where fluctuations count, fitness is a stochastic quantity, in the sense that an individual with fitness λ will give birth to an offspring on an *average* time of $1/\lambda$.

Lineage: when two individuals have exactly the same traits, we will refer to them as belonging to the same lineage, or that they are clones of each other. Typically, in a in-vivo population there is a dominant lineage, which is referred to as the **wild-type**, while the other existing types are called **mutants**. We might use these terms in the following.

Reproduction: the creation, from an individual, of another individual, which is the exact copy of itself. With this definition we are clearly stating that we will restrict ourselves to asexual reproduction only. Sexual reproduction (need of two individuals to give birth to a third one) is out of the scope of this work. Let us also stress that usually reproduction does not lead to the creation of an identical individual, as errors in the copy and replication of some individual genes may arise. In our study, we will neglect this eventuality, treating reproduction as an error-proof process, and consider all the mutations on the same level, regardless of whether they are occurring during replication or not. Since some parts of our study concern a null model of mutation and reproduction, we made the choice of considering the two processes as explicitly distinct.

Mutation: the change, in an individual, of one or some of its trait. This may, or may not, influence the fitness of the individual. In case of no consequences, the mutation is defined as *neutral*, while in the case of increase, or decrease, of the fitness of the individual, the mutation will be said to be *beneficial*, or *deleterious*, respectively. As we said before, we will in general consider mutation and reproduction as unrelated events. In nature, there are several types of different genetic mutations, ranging from the change of a single base-pair (called point mutation), to insertion or deletion of entire segments of genetic material, to extensive genome rearrangements, and so forth. But there are also other modifications that do not change the structure of the genome itself, but still have implication on the cell phenotypic state, e.g. the already mentioned activations and deactivations of genes. Many of these changes, even if not modifying the genome per se, can still have a character of heritability, and are referred to under the name of **epigenetics** (where the prefix 'epi' means 'over, outside of'). In this work, all the inheritable changes of a cell will be named as mutation, without distinction on their precise nature.

Genetic drift: the stochastic process of changing the respective frequencies of the alleles of a gene in a population. It is considered usually as a process distinct from mutation, that is normally associated with the creation, modification or deletion of a gene, in an individual. Genetic drift is instead see as a process that happens at the population scale. It can be seen as a sampling error, which will be non-zero for finite populations. For clarity, it is important not to confuse it with **genetic draft**, or hitch-hiking, which is an effect that has relevance in case of sexual population, and that we will not consider here.

Selection: in presence of different lineages in a population, the differences in their traits may lead to an advantage for some of them in the fight for survival. We will then say that selection favours one trait over another one. In a general sense, Darwinism is sometimes referred to as the *survival of the fittest*, considering fitness as a non-explicitly defined set of characteristics of an individual, providing higher chances to survive and reproduce. With our specific definition of fitness, however, we will see that fitness itself may not be the only quantity to consider. In chapter 5, for example, we will see how a small mutation rate in a lineage can play a fundamental role in its outliving the other faster mutating clones. In biology, people make sometimes the distinction between **positive** and **purifying** selection, to distinguish the case where selection operates in favouring individuals that underwent beneficial mutations, or vice-versa selecting against those with deleterious mutations.

Fixation: in the case in which different lineages are present in a population, it may happen that, due to selection, mutations or genetic drift, one of the lineages becomes dominant and ends up in constituting the whole population. We refer to this situation as fixation of the mutant, and the population is said to be **monoclonal**. No polymorphism is present. Using a more physical jargon, we will also speak of *condensation* of the population.

Epistasis: the interdependency in the effects that genes have in the behaviour of each other, in determining the phenotypic traits. Indeed, the relation gene $\rightarrow$ phenotypic effect is far from being linear and unique. Most of the times, the expression of one gene can enhance or weaken the effect of another one, or even change completely its behaviour. In this case, the organism is said to present epistasis. If a trait, say fitness, is obtained by such a complex interaction of genes, it is clear that the possibility of inheritance of such a trait will be reduced, as a simple mutation can make this whole house of card of interactions crumble down. We will speak then of **epistatic** fitness. The opposite case, when genes give each one a little contribution to fitness, and thus the effects accumulate one on top of the other, is called additivity, and we will speak of **additive** fitness.

Fitness landscape: a conceptual tool to visualize evolution, firstly suggested by Wright [8]. Individuals move, by mutating, in a landscape, where the height is given by the fitness of the individual. The other coordinates are normally supposed to represent the specific genomic state of the individual, and one supposes therefore a strict and precise mapping between the genome and the resulting fitness. In reality, such correspondence is far from being understood, and the study and comprehension of experimental fitness landscapes is an open field of study. From a theoretical perspective, the precise correspondence is usually ignored, and one simply assigns to every point in space $\mathbf{x}$ a given value of fitness $\lambda(\mathbf{x})$, the actual form of the function λ changing from model to model. Movement in this fitness landscape is done accordingly to mutations, which are supposed to shift an individual to a point in the neighbourhood of its actual position. While in the case of additive fitness the landscape is generally supposed to be fairly

smooth, in the case of epistatic fitness it is normally extremely rugged, and one can even wonder if such a representation should be abandoned. This visualization suffers also from two major drawbacks. Firstly, the landscape it is not supposed to vary upon time. Some studies approached this issue, and in this case the landscape is referred to with the evocative name of seascape. Secondly, the fitness is not supposed to be dependent on the actual distribution of the population, i.e. $\lambda(\mathbf{x})$ does not depend on the occupation number of the site in $\mathbf{x}$.

Adaptation: in the context of fitness landscape, adaptation is nothing but a coherent movement of the population distribution on the fitness landscape. If the rate of mutation is too high, or selection is absent, individuals are just scattered around and diffuse freely, the only constraint given by fixed population size keeping them together (see later in section 4.1). However, e.g. in the case of a smooth landscape with few mutations, the distribution of the individuals can stabilize to a stationary form after some time, while it is travelling on a slope leading to higher fitness. In this case, we will talk of a **travelling fitness wave**. In general, the velocity at which this travelling wave moves is referred to as the rate, or speed, of adaptation. The actual value of the velocity and the precise form of the wave is strongly dependent on the interplay between mutation and selection, and we will investigate this issue in section 1.3. When a maximum of fitness is reached, the population might stabilize around it, and in this case we will talk about **localization** [9–11]. The population will then generally start to condensate, and might reach fixation, i.e. localization in a single point of the landscape.

Chemostat: without entering in practical details, we can define a chemostat as a container (its volume being usually of some dm^3) filled with nutritive solution, inside which cells can live and reproduce. Two tubes are connected to the chemostat, one is used to inject nutrient, the other to remove waste products and cells in excess. The suspension of cells and nutrient in the chemostat is constantly mixed up. The most important characteristics of a chemostat are essentially two. First, by controlling the in- and out-flows, the population size can not only be kept constant, but its actual value can be fine tuned. Second, by mixing the solution, the chemostat presents homogeneous conditions in all its parts, and therefore cells experience all the same conditions, and each one is in competition with all the others. We will refer at this condition as **well-mixed** (it is essentially the same as fully-connected). The study of the competition of populations of fixed size, in well-mixed conditions, will be the central issue of the first part of this work.

Petri dish: another widely used device to grow cell colonies is the Petri dish. It consists of a plastic plate over which a nutritive medium is distributed. Cells can be implanted in one or more zones of the Petri dish, and let grow, in a quasi-2D fashion. Contrary to the chemostat, the conditions are very different from the well-mixed setup, as a cell only compete with its neighbours. The availability of space becomes very important, and it can constitute a limiting resource (as, for example, cells with no space around

them can become unable to reproduce). We will study the issues of competition in space in the second part, and we will see the striking differences of its behaviour compared to the well-mixed case.

About the different definitions of fitness Before dealing with the main content of this work, let us make a remark about the different definitions of fitness. We have λ, and $w = e^{\lambda}$, as the two possible definitions of fitness, the first indicating the rate of reproduction, the second the average number of offspring an individual generates. As already said, we will use the term fitness to refer to the first one. The two formulations give the same results, but let us set here, for clarity, the equivalence for a couple of expressions. The evolution of a deterministic growing colony is alternatively described by:

$$\dot{x}_i = \lambda_i x_i \qquad\qquad x_i(t) = w_i^t x_i(0) \tag{1}$$

if unbounded, or

$$\dot{x}_i = (\lambda_i - \langle\lambda\rangle) x_i \qquad\qquad x_i(t) = \left(\frac{w_i}{\langle w\rangle}\right)^t x_i(0) \tag{2}$$

if the population size is a constant. The average for a quantity a is defined, here and in the following, as

$$\langle a\rangle = \sum a_i x_i \tag{3}$$

and will be, in general, a time-dependent quantity, as it depends on the instantaneous distribution of the frequencies $x_i(t)$. Given this definition, the transformations $\lambda_i \to \lambda_i + k$, and $w_i \to k w_i$, with k constant for all the i, leave the system unchanged.

Part I

Well mixed

Chapter 1

Adaptation

Small like a rat, slow you adapt
Big as a cat, faster you act
Huge as a dog, only get log

Anonymous
Old Manchurian sayings

We have already defined adaptation, as a coherent movement of a population towards higher fitness. Adaptation in all these aspects will be the subject of study of this chapter, as its title might have suggested.

Chapter Teaser

- how to study two competing lineages in a constant size population, 1.1;
- what is a molecular clock, and how it can be justified by a neutral theory of evolution, 1.1.1;
- why life is under the constant threat of complete extinction, and the probability of such a dreadful event is far from being zero, 1.1.3;
- why increasing a population size M augments the speed of adaptation v, and $v \sim M$ for small populations, but for large ones $v \sim \ln M$ only, 1.3;
- how these adaptation regimes can be identified, and what are *successional mutations*, 1.3.1, *clonal interference*, 1.3.2, and *concurrent mutations*, 1.3.3;
- why infinite populations are completely different from finite ones, and their behaviour is totally unrealistic, 1.3.4.

1.1 Stochastic evolutionary models

A meaningful characterization of the dynamics of populations cannot be carried out if its intrinsic stochastic nature is not taken into account. In the real world, populations are always finite. One may wonder that for very large populations, like those of viruses or bacteria, the number of individuals is so high that an infinite population limit will provide good approximation of their behaviour, and mean field models are sufficient to guarantee an appropriate description. However, we will show that this is not the case, and that in complete generality the infinite size limit leads to a dynamics of a population that is not biologically feasible, see subsection 1.3.4. It is then necessary to deal with finite populations, whose evolution cannot be fully deterministic and in which fluctuations will definitely play a role. It is therefore compulsory to start our discussion with the description of the most common stochastic models used in the field.

1.1.1 Moran model

One of the simplest, but frequently used, stochastic model in the description of the dynamics of finite populations is the Moran model [12]. The name comes from P. Moran, who proposed it in 1958 [13]. One considers a population of M individuals. At every instant of time, each one of the individuals can reproduce or mutate. In case of reproduction, one other individual from the population is chosen at random and killed, i.e. replaced with the offspring generated in the reproduction event. In this way, and this is an important feature of the model, the population number is always kept constant.

Let us firstly consider the Moran model in an extremely simple case, when the population is made up of only two lineages, a and b types, and mutations are absent. We can describe the system by focusing on the number of a type individuals only, namely i, taking integer values in [0, M]. There are two absorbing states, $i = 0$, and $i = M$, that correspond to complete fixation of types b and a, respectively. For the other states, we will define the probability of transition from state i to state j as $\pi_{i\to j}$. Probability connecting the absorbing states are $\pi_{0\to i} = \delta_{0,i}$ and $\pi_{M\to i} = \delta_{M,i}$. All the entries in the matrix $\pi_{ij} = \pi_{i\to j}$, with $|i - j| > 1$ are zero, so that only $\pi_{i\to i+1}$, $\pi_{i\to i-1}$ and $\pi_{i\to i}$ will be finite.

We are interested in the probability of fixation of mutant a, namely in the probability p_i that, starting from a given number of mutants i, the system will end up in the absorbing state M, i.e. type a will reach complete fixation. To compute it, one can see that the evolution is simply given by:

$$p_i = \pi_{i\to i+1}p_{i+1} + (1 - \pi_{i\to i+1} - \pi_{i\to i-1})p_i + \pi_{i\to i-1}p_{i-1} \tag{1.1}$$

This represents the total probability of undergoing fixation at i (e.g. first term is the probability of jumping from i to $i + 1$ and undergo fixation at $i + 1$, and so on). It can be rewritten in a matrix form, as $p_i = \pi_{ij}p_j$ and the problem is reduced to calculate the eigenvector of the π_{ij} matrix.

Two probabilities are obvious, namely $p_0 = 0$, and $p_M = 1$. To compute the other ones, let us introduce:

$$z_i = p_i - p_{i-1} \qquad i = 1, ..., M \tag{1.2}$$
$$\gamma_i = \pi_{i\to i-1}/\pi_{i\to i+1} \tag{1.3}$$

These variables have some properties. First, $\sum_{i=1}^{m} z_i = p_m$. Then, with some algebra, one can see that eq. 1.1 can be rewritten as $\pi_{i\to i+1}(p_i - p_{i-1}) = \pi_{i\to i-1}(p_{i+1} - p_i)$, or equivalently $z_{i+1} = z_i\gamma_i$. Combining these two results one finds that:

$$p_i = \sum_{j=1}^{i} z_j = z_1 + \sum_{j=2}^{i} z_j = p_1 + p_1 \sum_{j=2}^{i} \prod_{k}^{j-1} \gamma_k = p_1 + p_1 \sum_{j=1}^{i-1} \prod_{k}^{j} \gamma_k \tag{1.4}$$

Using this expression for $\sum_{j=1}^{M} z_j = p_M = 1$, one finds that

$$p_1 = \frac{1}{1 + \sum_{j=1}^{M-1} \prod_k^j \gamma_k} \tag{1.5}$$

and consequently

$$p_i = p_1(1 + \sum_{j=1}^{i-1} \prod_{k}^{j} \gamma_k) = \frac{1 + \sum_{j=1}^{i-1} \prod_k^j \gamma_k}{1 + \sum_{j=1}^{M-1} \prod_k^j \gamma_k} \tag{1.6}$$

Up to this point, we have not specified the nature of the transition probabilities π_{ij}. Indeed, eqs. 1.5 and 1.6 are valid in a very general setting, that can include genetic drift and frequency-dependent fitness. We can think of them as valid also in presence of mutation, when the latter manifests itself only as a change from type a to type b and vice-versa (and only before fixation). A more general situation, extending this derivation to a case when the approximation of having only two lineages competing for fixation is not required, will be discussed in subsection 2.1.3. For the moment, let us stick to the present simple situation, and study some interesting particular cases.

Genetic drift Let us first discuss the case where no selection is present, and the dynamics is solely governed by genetic drift. Then, both the individuals, the one chosen for reproduction and the one chosen to die, are picked at random. Transition probabilities are

$$\begin{aligned} \pi_{i\to i+1} &= \frac{i}{M}\frac{M-i}{M} \\ \pi_{i\to i-1} &= \frac{(M-i)}{M}\frac{i}{M} \\ \pi_{i\to i} &= 1 - \pi_{i\to i+1} - \pi_{i\to i-1} \end{aligned} \tag{1.7}$$

So $\pi_{i\to i+1} = \pi_{i\to i-1}$, and consequently $\gamma_i = 1$. The probability of fixation, eq. 1.6, becomes simply

$$p_i = i/M \tag{1.8}$$

The interpretation of this result is very simple. We know that after some time the population will become monomorphic, since no mutations are present, and all the individuals will share the same common ancestor. Since all the individuals are equal, they all have the same probability of fixating in the population, thus equal to $1/M$, and the probability of fixation for type a will simply be the sum of this probability over the total number of a individuals present at the beginning.

This result is extremely simple, but has far-reaching consequences. Imagine indeed now to allow mutations, very separated in time, so every time a new mutant appears it has the time to fix or to disappear before another, different mutant is created. Let us call the rate of mutation per individual U, so mutations appear in the population at a rate UM. Successful mutations will then be created at a rate given by $r = MUp_1$. In the present case, when there is no selection, and dynamics is ruled by random drift, we have $p_1 = 1/M$, and therefore

$$r = U = \text{constant} \tag{1.9}$$

An historical remark is necessary. A constant mutation rate is the main result of a series of experimental observations by Pauli and Zuckerland in the 60's [14], after which they suggested the *molecular clock hypothesis*, which claims that the rate of evolution is constant in time. They found that the number of differences in the structure of some important proteins in organisms belonging to two different species are proportional to the time occurred since the separation of the two species. In other words, the number of accumulated mutations is linear in the time passed from speciation. The explanation of this experimental result, which lead us to obtain eq. 1.9, was provided in the 70's by Kimura [15], through its celebrated *neutral theory* of evolution. Kimura claimed that mutations are essentially neutral, and that genetic drift is at least as important as selection in evolution, in contrast with the current view of the time, which regarded randomness in evolution as a minor effect. Kimura's claim and findings raised a huge debate in those years about the relative importance of selection vs drift in evolution. As usually happens in science, the truth lies in between, and both effects are important. Notice also that in nature the two effects are interconnected. Since the environment is generally fluctuating, the definition of neutral or beneficial comes with a notion of time, and it is tipically transient. Therefore, a neutral mutation can be later, following some external changes, become a beneficial one, and be positively selected for. Thus, genetic drift acquires a great important in such it can allow an individual to explore widely the genome space, and provides the source for future possibly non-neutral, selected evolution. We will talk about the selective forces generated by fluctuating environments later on, in subsection 2.3.3.

Constant selection Let us now turn our attention to the case of constant selection, when individuals of type a and b have fitnesses λ_a and λ_b respectively. Going from an i to an $i+1$ state requires the reproduction of an a mutant, and the concomitant death of a b individual, picked at random among the $M-i$ wild-type clones. The probability $\pi_{i\to i+1}$ will be the product of the probabilities of these two independent events. So:

$$\begin{aligned}\pi_{i\to i+1} &= \frac{\lambda_a i}{M\langle\lambda\rangle}\frac{M-i}{M}\\ \pi_{i\to i-1} &= \frac{\lambda_b(M-i)}{M\langle\lambda\rangle}\frac{i}{M}\\ \pi_{i\to i} &= 1-\pi_{i\to i+1}-\pi_{i\to i-1}\end{aligned} \tag{1.10}$$

where $\langle\lambda\rangle = (i\lambda_a + (M-i)\lambda_b)/M$ is the average reproduction rate. Therefore $\gamma_i = \gamma = \lambda_b/\lambda_a$, and the probability of fixating the type a, after implantation of one mutant in a colony of type b is, recalling eq. 1.5:

$$p_1 = \frac{1}{1+\sum_{j=1}^{M-1}\gamma^j} = \frac{1-\gamma}{1-\gamma^M} = \frac{1-\frac{\lambda_b}{\lambda_a}}{1-(\frac{\lambda_b}{\lambda_a})^M} \tag{1.11}$$

We will discuss more about this probability and its consequences in section 2.1. For the moment, let us stress that, even if the invading mutant is selectively disadvantaged, namely $\lambda_a < \lambda_b$, the stochasticity of the process allows for a non-zero probability of fixation, even though it is exponentially suppressed in M.

In literature, it is common to rescale time so that the wild-type birth rate is 1, and define a *selection coefficient* s, to indicate the selective (dis)advantage of a mutant with respect to the wild type, as:

$$\lambda_{mut} = 1+s \tag{1.12}$$

In this notation, in the limit of $M\to\infty$, for a positive but small selection coefficient, the probability of fixation eq. 1.11 reduces simply to:

$$p_1 \sim s \tag{1.13}$$

This result is typically referred to by claiming that the probability of successful implantation of a mutant is proportional to its selective advantage. We will use this simplification in section 1.2.

1.1.2 Wright-Fisher model

The Moran model shares its title of most used stochastic process in finite populations with another process, the Wright-Fisher model, named after its inventors, already in the 30's [8]. The main difference with respect to the Moran model is that generations are not overlapping, in the sense that time is discretized, and at every time step all the individuals reproduce and are replaced by their offspring. In practice, at each time

step one extracts a number of offspring for each individual, according to its fitness. The exceeding number of generated individuals is eliminated by choosing among them at random the ones that will be discarded, in order to keep the population size constant, and then the ancestor population is completely substituted by these new M individuals. The Wright-Fisher model is then in some sense the parallelized version of the Moran model, and therefore preferred when simulating large populations. However, contrary to the Moran model, for the Wright-Fisher model obtaining analytical results is much more complicated, and the equivalent for the fixation probability of eq. 1.11 is not known exactly. The widely used approximation is expressed by means of the selection coefficient, and given by:

$$p_{1,WF} = \frac{1 - e^{-2s}}{1 - e^{2Ms}} \tag{1.14}$$

Comparing with the expression for the Moran model, one can see that there is only a factor 2 of difference. In the limit of large M and small selection coefficient, one can approximate $p_{1,WF} \sim 2s$.

1.1.3 Galton-Watson model

Another stochastic model that needs to be mentioned is the Galton-Watson model, that is simply the Wright-Fisher one without the restriction on the population size. In the Galton-Watson model, the population grows unbounded. One can show that the expected population size is given simply by $\langle M(t) \rangle = \langle \lambda \rangle^t$. We have an absorbing state at $M = 0$, and one can compute the extinction probability $p_{ext}(t)$, in the $t \to \infty$ limit. Its behaviour varies accordingly to the value of $\langle \lambda \rangle$. If $\langle \lambda \rangle \leq 1$, then $p_{ext} = 1$, while when$\langle \lambda \rangle > 1$, we have that $p_{ext} < 1$, but it is different from zero. Such an exponential growth is not feasible in reality, but one can nonetheless consider it as a good approximation for the first phases of the growth of a colony in a stable environment, or in the early evolution of a mutant lineage invading a monoclonal population, until its size becomes comparable to the total population size.

This even brief parenthesis on the Galton-Watson model is far for being irrelevant. Indeed, it shows that, even for a population in which the reproduction rate is as high as one offspring for each individual per generation, in the long time limit we are sure that the population will go extinct. It is then clear that in most of the cases of interest, when the growth is feasibly sub-exponential, in order to obtain non-trivial results for the evolution of a population, we are forced to impose the constraint of fixed population size. Extinction as an inevitable eventual ending for all non-constrained populations also sheds some little source of anxiety in considering the final destiny of humanity and life in general. We will not address such philosophical issues here. Let us only notice, for the worried reader, that a source of consolation, that may ease the sorrow and the sense of desolation these considerations may bring about, should come from the thought that if a mechanism for generating life from inanimate matter exists, this whole picture ceases to be consistent, and a life deprived universe stops becoming the final absorbing point of the evolution of the living beings.

For what concern the present work, this gives us a reason for the use of a constant population size.

1.2 Time-scales

The dynamics of evolution is driven by three major actors, namely genetic drift, mutation, and selection. To understand how a population evolves, we should be able to find some criteria to distinguish if, and in which case, one of these driving forces is the dominant one. To do so, we will estimate the typical time-scale for each one of them, and make some comparison. As usual, we will restrain our analysis to the case of two competing lineages only.

1.2.1 Fixation times

Fixation time in presence of selection In order to provide some intuition about the fixation time in case of selection, let us consider the deterministic case. We will discuss the limit of its application in the following, subsection 1.2.2, and we will see that our final expression for the fixation time (eq. 1.18) will only be slightly modified when drift will be taken into account (eq. 1.31).

Consider the invasion of a mutant a in a population of type b. Let us indicate the relative frequencies with x_a and x_b, with $x_a + x_b = 1$. The deterministic evolution is described by:

$$x_a(t) = e^{(\lambda_a - \langle\lambda\rangle)t} x_a(0) \tag{1.15}$$

$$x_b(t) = e^{(\lambda_b - \langle\lambda\rangle)t} x_b(0) \tag{1.16}$$

Solving for $\langle\lambda\rangle$ in eq. 1.15 and substituting it into eq. 1.16 one gets:

$$x_b(t) = \frac{x_b(0)}{x_a(0)e^{st} + x_b(0)} \qquad x_a(t) = 1 - x_b(t) \tag{1.17}$$

where s is the selection coefficient. The initial conditions are set by $x_a(0) = 1/M$ and $x_b(0) = 1 - x_a(0)$. To get the fixation time, we need to impose $x_b(t) = 1/M$, and solve for t in eq. 1.17. We obtain that the time required for fixation of a mutant, with selection advantage s, following implantation, is

$$t_{fix} = \frac{2\ln(M-1)}{s} \sim \frac{2\ln M}{s} \tag{1.18}$$

As one could expect, the larger the selective advantage, the faster the mutant will overcome the wild-type. Notice however that this description is not consistent, as we are neglecting fluctuations. Even in the case of very large population, indeed, the stochastic effects of the model will be important for the initial dynamics of the invading mutants, while its size is much smaller than M. We will discuss this point later, after considering the opposite case, when selection is absent and the dynamics is driven by genetic drift only.

Fixation time in presence of genetic drift If we wish to study fixation in the case of genetic drift, we have to come back to the Moran model. We start with two lineages in the population, with count number i and $M-i$. We can just focus on the first type, and define t_i as the time necessary to reach fixation starting from an initial number of individuals of the first type equal to i. Of course, $t_0 = t_M = 0$. For $i \neq (0, M)$, we can recover a recursive equation in the same way we did for the Moran fixation probability p_i in subsection 1.1.1, see eq. 1.1. Indeed, the time to fix is given by 1 (the time-scale for a creation/deletion event) plus the time to fix in the next step of evolution. The transition probabilities are the same as in eq. 1.7, and so we can write:

$$t_i = 1 + \frac{i}{M}(1 - \frac{i}{M})(t_{i-1} + t_{i+1}) + (1 - 2\frac{i}{M}(1 - \frac{i}{M}))t_i \tag{1.19}$$

This can be rewritten as:

$$2t_i - t_{i-1} - t_{i+1} = \frac{M^2}{i(M-i)} \tag{1.20}$$

which correspond to a discrete Poisson equation, which general solution is

$$t_i = a + bi - M\sum_{k=1}^{i-1}(i-k)\frac{M}{k(M-k)} \tag{1.21}$$

The form of a and b can be obtained by imposing the boundary conditions $t_0 = 0$ and $t_M = 0$, to get:

$$a = 0 \qquad\qquad b = \sum_{k=1}^{M-1}\frac{M}{k} \tag{1.22}$$

and so the final form of eq. 1.21 will be:

$$t_i = (\sum_{k=1}^{i-1}\frac{M}{k} + \sum_{k=i}^{M-1}\frac{M}{k})i - M\sum_{k=1}^{i-1}(i-k)\frac{M}{k(M-k)} \tag{1.23}$$

$$= M\sum_{k=i}^{M-1}\frac{1}{k} + M\sum_{k=1}^{i-1}\frac{M-i}{M-k} \tag{1.24}$$

One last step, to make eq. 1.24 more intelligible, is to approximate the sums in it with two integrals, namely:

$$\sum_{k=i}^{M-1}\frac{1}{k} \sim \int_{1/M}^{0}\frac{dq}{q} = \ln(M) \tag{1.25}$$

$$\sum_{k=1}^{i-1}\frac{1}{M-k} \sim \int_{0}^{1/M}\frac{dq}{1-q} = -ln(1-\frac{1}{M}) \tag{1.26}$$

In the end, we get the final result, which is given by:

$$t_i = M^2(\frac{i}{M}\ln\frac{i}{M} + (1-\frac{i}{M})\ln(1-\frac{i}{M})) \tag{1.27}$$

We obtain that the time required for fixation of a mutant, with no selection advantage, following implantation, is:

$$t_{fix,drift} \approx 2M \tag{1.28}$$

The result is very similar to the one that can be obtained computing t_i in the case of the Wright Fisher model. The only difference with respect to eq. 1.27 is that the coefficient is not M^2, but $2M$. The reason is explained by the fact that in the Wright-Fisher model time is expressed in unit of generation time, which in the case of the Moran model take M events. So, again, the difference between Moran and Wright Fisher models is given by a factor two.

1.2.2 Comparisons

A first comparison: selection vs drift From the estimates we obtained for the fixation time in case of selection, eq. 1.18, and drift, eq. 1.28, we immediately see that, in the case of large population, selection leads to fixation exponentially faster than drift. When concerned about the fixation time, then, we will consider selection as the major actor.

However, the calculations done so far are not completely satisfying. Indeed, to obtain eq. 1.18, we supposed the dynamics of the invading lineage to be always deterministic. This is surely correct while its size is big enough for fluctuations to be considered negligible when compared to selection, but in the very first phase of the evolution they will definitely play a role. We can give an estimation of the threshold size at which the two effects are comparable.

For what concerns the drift, since we are considering early times and a small mutant population, we do not have to consider saturation effects, and the drift of each individual can be treated independently, as happening in parallel. Thus the mutant lineage size m can be thought of as a random walk, with variance $\langle \Delta m^2 \rangle \sim tm$, where time t is the number of occurred generations, this total variance being the sum of the m independent single variances of the individuals. Thus, in m generations, the population drifts of about m individuals. In the same amount of time, selection has provided a change in the population size of $m^2 s$, given that at every generation ms new individuals are created. So we can say that the effects of drift become negligible as soon as $m^2 s > m$, or the size of the mutant colony m satisfies:

$$m > \frac{1}{s} \tag{1.29}$$

After this moment, the evolution becomes deterministic, and the population grows (at least until it gets close to saturation) in an exponential fashion, $m(t) = (1/s)e^{st}$. Indeed,

let us show why this equation for the dynamics turns out to give us the correct value for the average size of the mutant lineage. From the discussion at the end of subsection 1.1.1, we know that the probability p, for an invading mutant, of surviving and fixing is given by its selective advantage s, see eq. 1.13. Then, if we wish to condition the average growth to the non-extinction of the mutant, we have to pose $\langle m \rangle_{surv} = \langle m \rangle / p$, and then the size of the mutant colony (before saturation effects come into play) is given by:

$$m(t) = \frac{1}{s} e^{st} \tag{1.30}$$

More involved and rigorous calculation can be found in Fisher [16], but the line of reasoning and the results are essentially these ones. Notice that everything works *as if* the mutant colony grew exponentially during all the time, but actually this is not the case. Indeed, during the first time while $m < 1/s$, in order to survive, a mutant should overcome drift, the effect of which is by itself dominant over the exponential growth due to selection. Therefore, we should expect that in these times the mutant grows faster than exponential, and this fact compensates for the loss of mutants not being able to survive the drift phase. Now, if we wish to reconsider our estimation of the fixation time in case of selection, including the effects of drift, we can just redo the calculations leading to eq. 1.18. This time however, as the initial value of $x_a(0)$ we should not consider $1/M$, but $1/sM$. Then (considering $x_b = 1/sM$ at fixation time), substituting this initial and final conditions into eq. 1.17 and solving for t, we get:

$$t_{fix} \sim \frac{2 \ln Ms}{s} \tag{1.31}$$

The expression is very similar to eq. 1.18, the only difference being the presence of the selective advantage s in the logarithm. For very small selective advantage, however, the two expressions might give results that differ significantly.

As a side note, let us stress that relation in eq. 1.29 can be used for determining the leading force at the level of a population, by using $m = M$. The same result can be easily obtained also confronting the two probabilities of fixation, by means of drift or selection, eqs. 1.8 and 1.13. Selection will dominate when

$$sM \gg 1 \tag{1.32}$$

When this relation is not satisfied, the selective advantage is so low that is more probable for a mutant to get fixed by random drift that by selection. Adaptation does not take place in this case, and the population is governed by random fluctuations. In the following, we will suppose that relation in eq. 1.32 is always satisfied.

A second comparison: mutation vs selection For what concerns the time for a mutation to appear and establish, i.e. to overcome drift and start evolving deterministically, the estimation is really simple in the limit of low mutation rate. Indeed, let us suppose that the rate for an individual to mutate is given by U, and that this mutation

gives the individual a selective advantage (we are thus considering only beneficial mutation for the moment). In the population, the total rate for creating such a mutation will be MU. If only one mutation appears and it is able to fixate at a time, we are in the framework of the Moran model of section 1.1.1, and so we know what the probability of its fixation is, as computed it in eq. 1.13. The average time to create such a mutation,t_{est}, i.e. the time required for the establishment of a new successful mutation, will then be:

$$t_{est} = \frac{1}{2MUs} \tag{1.33}$$

Again, this limit is valid as long as the competition against the wild-type is carried on by only one mutation, and no new mutation arises before either one of the two existing lineages has achieved fixation. This condition is satisfied as long as the time for fixation of a mutation is smaller than the one to generate another one, namely $t_{fix} \ll t_{est}$, or in other terms, eqs. 1.31 and 1.33:

$$MU \ln(Ms) \ll 1 \tag{1.34}$$

This condition is used to define the *successional mutations* regime. The dynamics of evolution is then made by long periods of stasis, when the population is essentially monoclonal, and nothing happens for times of the order of t_{est}, interspersed with periods of competition of two lineages, which in a time of order t_{fix} will generally lead to an improvement in the fitness of the population, through the fixation of the invading mutant.

1.3 Speed of adaptation

We will define the speed of adaptation as the rate at which the average fitness is increased, i.e.

$$v = \frac{d\langle\lambda\rangle}{dt} \tag{1.35}$$

If adaptation proceeds uniformly, the population distribution will take the form of a stationary wave, moving towards higher fitness values [17–19]. A common used procedure, from a theoretical perspective, is to forget about the actual structure of the fitness landscape, and visualize the population as living on a single one dimensional axis z, in which every point have a fitness $\lambda \propto z$, so that moving forward will correspond to adaptation. Individuals are placed on the fitness axis according to their fitness, two individuals being in the same point if their fitnesses are the same. Reproduction and genetic drift are responsible for variation in the frequency x_i, while mutation allow mutant from a point i to move to a point j, which correspond to change its fitness from λ_i to λ_j. In the following, when referring to travelling fitness wave, we will consider the shape described by the distribution of the population on the fitness axis, i.e. by its frequencies $x_i(t)$.

The Gaussian shape of the travelling wave As a first result, let us show that the travelling wave has approximately a Gaussian shape [20]. In the center of the wave, and for all the lineages for which the dynamics is deterministic, the evolution of their frequency x_i, characterized by fitness λ_i, will satisfy:

$$\dot{x}_i = (\lambda_i - \langle\lambda\rangle)x_i \tag{1.36}$$

In a stationary state, we expect the average fitness to increase regularly, and therefore $\langle\lambda\rangle = vt$. The general equation $\dot{x} = (b - ct)x$ has as solution $x = A_0 e^{bt - ct^2/2} = A_1 e^{(b-ct)^2/2c}$, which in term of our velocity, gives us

$$x_i(t) \sim e^{\frac{1}{2v}(\lambda_i - vt)^2} \tag{1.37}$$

We can thus see that the stationary distribution of the population frequencies is a Gaussian, which has the property that

$$\sigma^2 = v \tag{1.38}$$

This equivalence is exactly the Fisher fundamental theorem of natural selection [21]. It has been formulated in the 30's, as 'The rate of increase in fitness of any organism at any time is equal to its genetic variance in fitness at that time', which is indeed our result. A more general calculation can be provided by the study of the Price equation, [22, 23], in respect of which the Fisher theorem stems as a particular case, in which fitness is supposed to be constant from parent to offspring. We will not discuss it here.

Such a nice result however is far from being exhaustive in the understanding of evolutionary dynamics. First, the value of the speed of adaptation is not known, as we do not know which form the actual distribution has. Second, the first line of this two lines argument, eq. 1.36, is valid only when the deterministic description holds, and so it can describe only the bulk of the distribution, when frequencies are high enough, but fails completely in describing the properties of the tips of the distribution, where mutants are rare and drift may dominate [24]. We will see that the behaviour at the extremities is fundamental in determining the entire evolution.

1.3.1 Successional mutations

In a general way, in the stationary state, the tip of the wave will advance as fast as the bulk of the distribution. Therefore, by estimating the time of establishment of the fittest mutant τ, and its relative advantage s, at stationarity, one can compute the wave velocity simply as $v = s/\tau$.

The speed of adaptation, then, can be easily obtained in the case of successional mutations regime, when eq. 1.34 is satisfied, since the evolution is ruled by the time needed to establish a mutation. Supposing that every mutation gives a contribution s to the fitness, the velocity is given by:

$$v_{succ} = \frac{s}{t_{est}} = 2MUs^2 \tag{1.39}$$

If mutations do not give a constant advantage, but this is instead drawn from a distribution, it is sufficient to replace s by $\langle s \rangle$. So, in the successional mutations regime, the rate of adaptation is *linear* in M.

However, when eq. 1.34 is not satisfied, and several mutations appear simultaneously, the establishment time cannot be computed in the approximation leading to eq. 1.33. The fittest mutant will have to compete with all the other lineages that are present and also with the possible incoming fitter mutations.

Two kinds of competitions can be distinguished. The first is when, after a beneficial mutation appears, a second one shows up, being slightly fitter than the previous one. The concomitant presence of both will impede one of the two mutations from getting fixed, and will also slow down the process of fixation of the other one, that will have to compete also with a lineage fitter than the wild-type. This situation is called *clonal interference*. The second regime takes place when successive mutations can accumulate one upon the other in a mutant, while it is still not fixated. The second mutation can provide a boost in adaptation for a single mutant, favouring it by means of a greater selective advantage. In turn, this will lead to the loss of other mutations, that might also have been beneficial, before they can reach fixation. We have what is called *concurrent mutations*. It is easy to guess that in nature both situations manifest simultaneously. However, from a theoretical point of view, the intractability of the complete problem has led to two general lines of research, in which in turn one of the two situations is not considered.

We will present here some analysis and results obtained in the two cases [25]. The main result is that, due to the competition between mutants, the speed is strongly reduced with respect to the low mutation case (many beneficial mutations are wasted) and the velocity has only a *logarithmic* dependence on M.

1.3.2 Clonal interference

In this case, we will allow several mutants to coexist at the same instant of time, but no multiple mutations. In other words, the population will be only composed by the wild-type and by single mutants [26–28].

In this setting, it is important to provide an expression for the distribution of mutants, $g(s)$. In literature, it is typically taken to be an exponential. Indeed, considering all the mutations as independent and drawn from an unknown given distribution, one can rank them accordingly to their fitness advantage, and try to find a distribution for them, which will be, in general, dependent on the distribution of mutations. However, beneficial mutations will concentrate around the maximum value of fitness, i.e. on one of the tail of this distribution. Record statistics provide a lot of interesting result in this case, that are valid independently on the actual form of the distribution (as long as we are not considering extremely exotic distribution, like Cauchy ones). In particular, differences in the fitnesses can be shown to be exponentially distributed [29, 30]. To be a little more general, we will use

$$g(s) \sim \exp(s/s_0)^{\beta} \tag{1.40}$$

The key approximation in the following, which makes the model solvable, is assuming that mutations are simultaneously present, but they actually do not influence each other for what concerns their selective advantage. By that, we suppose that they are few enough to maintain the average fitness constant while they are competing. Viewed from another perspective, we are supposing that all mutants compete in parallel with the wild-type, just like in the successional mutations regime, and at the end of the process only one is successful and reaches fixation.

With this assumption, we already know which is the probability $p(s)$ for a mutant of selective advantage s to become fixed in the population, as it is simply given by eq. 1.11, or for small s by eq. 1.13. The probability for a mutation to be created and fix is then simply the product $p(u)g(u)$. Let us define s_{fit} the selective advantage for our pretended successful individual [31]. It will fix in a time $t_{fit}(s_{fit})$, computed according to eq. 1.31. The probability of establishing a mutant with selection coefficient greater than s is given by $\int_{s_{fit}}^{\infty} du\, p(u)g(u)$, and therefore the total number of mutants of selective advantage bigger than s_{max} that are created in a time t_{fit} is given by

$$\chi(s_{fit}) = NUt_{fix}/2 \int_{s_{fit}}^{\infty} dup(u)g(u) \tag{1.41}$$

We will suppose that these interfering mutants are Poisson distributed, with their number K satisfying $Prob(K == k) = \chi^k e^{-\chi}/k!$. The probability that they do not appear during the fixation of the mutant s_{max} is then given by $Prob(K == k) = e^{-\chi}$. So, in the end, the probability that a mutation of advantage s appears and get fixed, without other fitter mutations appearing and fixing, is given by

$$P_{fix}(s) = p(s)g(s)e^{-\chi(s)} \tag{1.42}$$

Integrating this probability over all the possible coefficients s, and multiplying this by the total rate at which mutation are produced, MU, we obtain the rate at which a successful mutations is generated in the population. The advantage provided by it will be $\langle s \rangle$, where the average is taken with respect to P_{fix}. The velocity is then obtained as

$$v = \frac{\langle s \rangle}{MU \int ds P_{fix}(s)} \tag{1.43}$$

Of course, this expression is implicit, has one has first to evaluate the integrals in eqs. 1.41 and 1.43. By means of some approximation, this can be done, but report here the calculation is not worthy, as nothing is learned from their computation. Indeed there is an alternative way to derive the value of velocity, which gives the same result the evaluation of eq. 1.43 gives, but that follows a slightly different path.

One can easily understand that the fitter the mutant, the rarer it will be, and thus the rarer it will survive drift, but at the same time with less probability it will be over-competed by new mutants while it is fixating. The successful mutant will then be the one able to find a balance between two effects, low-frequency against selective advantage. This observation provide us a way to give an estimation for the velocity.

Again, let us define s_{fit} the selective advantage for our pretended fittest individual, and $t_{fit}(s_{fit})$ its fixation time. If we define by m the total number of mutants that appeared in the time t_{fit}, we will have that $m = MUt_{fit}$, relating m to s_{fit}. On the other hand, we can also define implicitly s_{fit} be requiring that only one mutant with this selective advantage is created

$$\int_{s_{fit}}^{\infty} g(s')ds' \sim \frac{1}{m} \tag{1.44}$$

This is equivalent to require that all mutants with selective advantage bigger than s_fit will not manifest themselves (their number will be less than one). Using the explicit form for the mutant distribution $g(s)$, eq. 1.40, we can then solve for s_{fit}, and also compute $t_{fit}(s_{fit})$. Considering $\ln M \gg \ln s_{fit}$, we obtain $s_{fit} \sim s \ln^{1/\beta} M$, and $t_{fit} = (\ln^{1-1/\beta} M)/s$. The velocity is then

$$v = \frac{s_{fit}}{t_{fit}} = s^2 \ln^{2/\beta - 1} M \tag{1.45}$$

1.3.3 Concurrent mutations

In the following let us consider the case in which mutations can be additively cumulated, but do not interfere. In this setting, then, all mutations will have the same beneficial effect s, and a clone carrying k mutation will have a selective advantage equal to ks. The population can be thought as a wave moving through discrete steps of size s, that can be characterized by studying the frequencies $x_t(k)$.

The first approach we will describe has been provided by [32]. Even if it suffers from dramatic approximations, we will present it here since it provides the baseline ideas of more involved calculations, and the final result is not so different from ones obtained from more educated hypothesis.

This method makes two basic assumptions, in order to perform the calculation. First, the Gaussian distribution for the travelling wave is supposed to hold even for the tip of the wave. Second, even the fittest mutant is supposed to evolve deterministically. Since we are working with finite population, these two assumptions are necessarily false.

As a starting point, let us compute the value of the lead, i.e. the difference in the fitness between the fittest mutants and the average of the population. We will define it as $\Delta\lambda = \lambda_{fit} - vt$. Notice that this quantity depends on time. We wish to impose that, when the mutant first appears in the population, its frequency is that of a single individual, i.e. $1/M$. Using the first assumption, we can write:

$$\frac{1}{\sqrt{2\pi v} e^{\Delta\lambda^2/2v}} = \frac{1}{M} \tag{1.46}$$

from which we can extract the lead as

$$\Delta\lambda = \sqrt{2v \ln \frac{M}{\sqrt{2\pi v}}} \sim \sqrt{2v \ln M} \tag{1.47}$$

The second assumption let us make an estimate of the approximate time τ at which the fittest mutant gives rise, by mutation, to a fitter mutant. Let us define $x_{fit}(t)$ the total fraction of fittest mutants generated by selection in a time t. Since the drift is not considered, the mutant grows exponentially according to its selective advantage with respect to the mean fitness, and so

$$x_{fit}(\tau) = \int_0^\tau x_j(t) = \int_0^\tau \frac{1}{N} e^{\lambda_{fit} - vt} \sim \frac{e^{(\Delta\lambda)\tau} - 1}{M(\Delta\lambda_{fit})} \tag{1.48}$$

The result is approximated in the sense that $\Delta\lambda$ is time-dependent, but we considered it here as a constant during the time interval τ. This gives us an estimation of τ, as satisfying $x_{fit}(\tau)U = 1/M$. Upon inverting eq. 1.48, one gets

$$\tau = \frac{1}{\Delta\lambda} \ln(1 + \frac{\Delta\lambda}{U}) \sim \frac{1}{\Delta\lambda} \ln(\frac{\Delta\lambda}{U}) \tag{1.49}$$

This is the average time at which one new fitter mutant establishes. The gain in the fittest mutant fitness is then s in a time interval τ, and the velocity can be estimated as $v = s/\tau$. Since the wave is stationary, this velocity should be the same of the velocity of the bulk, and we can require them to be equal. Substituting eq. 1.47 into eq. 1.49, we can get a closed-form expression for the velocity

$$v = \Delta\lambda \frac{1}{\ln(\frac{\Delta\lambda}{U})} = \frac{s\sqrt{2v \ln M}}{\ln(\sqrt{2v \ln M}) - \ln U} \sim \frac{s\sqrt{2v \ln M}}{\ln \ln M - \ln U} \tag{1.50}$$

We can solve for v, neglecting the double logarithm contribution in M, and finally obtain:

$$v = \frac{2s^2 \ln M}{\ln^2 U} \tag{1.51}$$

Although, as we already remarked, the procedure here suffers from the fallacies in the assumptions, it allows to sketch a simple guideline for a deeper analysis. Firstly, one computes the velocity of the bulk, in terms of some implicit quantities, typically the lead of the fittest mutant. Then one considers the tip of the wave, and is able to compute the velocity of implantation of the fittest mutant. Again, this will depend in general on its lead with respect to the bulk of the population. The system is then closed by the fact that at stationarity the two speeds have to be the same.

More involved calculations A calculation following the line of reasoning just described has been done by Rouzine et al. [33–35]. We will not report their calculations here, since they are extremely involved (another derivation, following the line of [16], is provided in [36]). However, let us say that they relax strongly the two approximations that leads to the results of eq. 1.51. First, the growth of the fitter mutant is not considered to be deterministic. The other mutants are supposed to grow deterministically, but this is not a stringent hypothesis, since from what we already know, i.e. that the shape of the fitness wave is similar to a Gaussian, the next-to-fittest mutant frequency

will be exponentially larger than the fitter mutants one. Secondly, the form of the wave is not given a priori, but it is estimated from the deterministic equations that govern the behaviour of the less fit mutants. The curve describing the wave is shown to have a cut-off, and this cut-off is interpreted as the point at which the deterministic description should break down, i.e. where the fittest mutant is. Matching the frequency at the deterministic cut-off with the frequency obtained from the stochastic treatment of the fittest mutants allows to close the system of equations, and to compute (implicitly) the value of the wave velocity. An explicit expression can be obtained for large M, yielding

$$v \sim \frac{2s \ln(M\sqrt{sU})}{\ln^2[(s/U)\ln(M\sqrt{sU})]} \tag{1.52}$$

Another estimation, following a different approach, has been done by [16], and subsequently by [36]. Without entering in the details of the calculation, we can give an idea of the line of reasoning. The focus is on the evolution of the fittest mutant, treated stochastically, while the other less fit mutants are, as usual, considered evolving deterministically. We have already seen, in subsection 1.2.2, that we could give an estimation of the evolution of the frequency of a mutant of selective advantage s by supposing that, after reaching a size of $1/s$, it will evolve deterministically. Now, this was enough to give an estimation for the time of fixation of the mutant, since most of the fixation time will be spent in the deterministic growth phase, at least for large M (remember that the growth in the stochastic phase is faster than exponential). However, if we are interested in the time of establishment, this description is of course not sufficient. Desai and Fisher propose then to define a stochastic variable τ, encoding the time at which the fittest mutant, with selective advantage sk, would have reached size $1/sk$, supposing that its growth had always being deterministic. In other words, this means that its growth is ruled by

$$m(t) = \frac{1}{sk} e^{sk(t-\tau)} \tag{1.53}$$

Notice that both $m(t)$ and τ are two stochastic variables. One can study the evolution of $m(t)$ with the assumption that we are far from saturation effect, and therefore apply the techniques used in the Galton-Watson process (see subsection 1.1.3) for the growth of an unbounded population. Upon estimating when $\langle m \rangle \sim 1/sk$, one can extract an expression for $\langle \tau \rangle$ in function of the lead k. Now, $\langle \tau \rangle$ is a good estimation for the establishment time, since it is the time that a clone is supposed to spend before becoming deterministic. The velocity can then be computed by $v = s/\langle \tau \rangle$. In order to obtain an explicit expression for $\langle \tau \rangle$ one needs to estimate k, and this can be done by a simple consideration: summing up all the mutants one should get the population size M. After a time $t_q = \langle \tau \rangle$ the fittest mutant has size $1/sk$. The previous mutant, $(k-1)s$, started growing deterministically, and did that when its size was $1/sk$ (before establishing it was the fittest mutant), but after that it becomes the next-to-fittest, and so its deterministic growth is given by $(k-1)s$, making its size at time t_q equal to $(1/sk)e^{k-1}t_q$. For the

second-to-fittest mutant, the size will then be $(1/sk)e^{k-1}t_q e^{k-2}t_q$, and so on. Here we supposed that all the mutants took the same time to establish t_q. Requiring that the sum of the size of all these mutants gives M allows to compute the value of the lead k. With that, one can finally extract the value of the velocity, obtaining

$$v = \frac{2s^2 \ln(Ms) - s^2 \ln(s/U)}{\ln^2(s/U)} \tag{1.54}$$

While being slightly different, the expressions found for the velocity in the approximation of concurrent mutations, eqs. 1.51, 1.52, and 1.54, all show that, compared to the case of successional mutations, eq. 1.39, the increase of v with the population size M and the mutation rate U changes from being linear to be logarithmic. This slowdown can immediately being understood by considering that the distribution is wide in fitness. So most of the mutations will fall in the bulk, therefore not contributing to the tip of the distribution, which determines the rate of adaptation. Desai and Fisher provide an interpretation of the contribution of M and U to the speed of the evolution as an indirect effect. Increasing M, causes the bulk to have more individuals and then to move slower, and this allows the fittest mutants to increase their lead, which in turn make adaptation go faster. Increasing U, on the other hand, reduces the time for fittest mutants to appear, giving them more time to grow before the bulk gets closer, so that their effectiveness is increased and the global speed is larger.

1.3.4 Infinite population size

To conclude, let us show what happens in the case of $M = \infty$, and see why the conclusions we can draw from such a limit are not biologically meaningful. In this setting we can consider simultaneously cloning interference and multiple mutations, and let us define as $x_t(n, k)$ the frequency of mutants which present n mutations, for a total selective advantage of ks_0. In this specific case, let us couple mutation and reproduction, in the sense that every event of reproduction will be followed (with probability U) by a mutation in the offspring. The general equation describing evolution of the $x_t(n, k)$ will then be:

$$x_{t+1}(n,k) = (1-U)\frac{e^{ks_0}}{\langle w \rangle} + U \sum_l \frac{e^{(k-l)s_0}}{\langle w \rangle} x_t(n-1, k-l) g_0(l) \tag{1.55}$$

where the first contribution comes from the offspring of lineage (n, k) that did not mutate after reproduction, while the second term is the sum of individuals generated by the other lineages, and then mutated to (n, k). One can solve this equation recursively, but it is useful to rewrite it in terms of the two generating functions for f and g, namely:

$$F_t(h,z) = \sum_{n,k} h^n z^k x_t(n,k) \qquad\qquad G(z) = \sum_l z^l g_0(l) \tag{1.56}$$

With these definitions, we have that

$$\langle w \rangle = F_t(1, e_0^s) \tag{1.57}$$

Using this relation, we can rewrite eq. 1.55 as

$$F_t(h,z) = (1-U)\frac{F_{t-1}(h,ze_0^s)}{F_{t-1}(1,e_0^s)} + U\frac{hF_{t-1}(h,ze_0^s)}{F_{t-1}(1,e_0^s)}G(z) \tag{1.58}$$

that can be solved iteratively, giving

$$\begin{aligned} F_t(h,z) =& \frac{F_{t-1}(h,ze_0^s)}{F_{t-1}(1,e_0^s)}\frac{1-U+UhG(z)}{1-U+UG(1)} && (1.59)\\ =& \frac{F_{t-2}(h,ze^{2s_0})}{F_{t-2}(1,e^{2s_0})}\frac{1-U+UhG(z)}{1-U+UG(1)}\frac{1-U+UhG(ze_0^s)}{1-U+UG(e_0^s)} = ... && (1.60)\\ =& \frac{F_0(h,ze^{ts_0})}{F_0(1,e^{ts_0})}\prod_{\tau=0}^{\tau=t-1}\frac{1-U+UhG(ze^{\tau s_0})}{1-U+UG(e^{\tau s_0})} && (1.61) \end{aligned}$$

We are interested in $\langle w\rangle$, so using eq. 1.57 we have

$$\langle w\rangle = \frac{F_0(h,e^{(t+1)s_0})}{F_0(1,e^{ts_0})}(1-U+UG(e^{ts_0})) \tag{1.62}$$

or, since we are mostly interested in the fitness, we want $\ln\langle w\rangle$:

$$\ln\langle w\rangle = \ln(\frac{F_0(h,e^{(t+1)s_0})}{F_0(1,e^{ts_0})}) + \ln(1-U+UG(e^{ts_0})) \tag{1.63}$$

Now we are able to show that the limit of infinite population size gives rise to unrealistic behaviours. First, let us consider the case when mutations are absent. In such a setting, naively we will expect the population to fix to the best fit mutant, and in the long time limit the fitness will saturate to this one. The existence of such a best-fit mutant is assured by the finiteness of the population. However, in the case of an infinite population, such best-fit mutant is not assured to exist, and indeed to have one we must require a cut-off k_0 in the initial distribution of individuals, such that $x_0(n,k) = 0$ for every $k > k_0$. Otherwise, all the mutants with fitness bigger than $\ln\langle w\rangle$ will grow exponentially, and since the initial k, i.e. the selective advantages, are not unbounded, there will always be a mutant with fitness higher than the average one, and therefore $\ln\langle w\rangle$ will keep on increasing, even in absence of mutations. Thus, even in the case when we will wish to treat the system as continuous, and the frequencies of individuals being described by a continuous distribution, we will always suppose that an implicit cut-off exist, and the distribution to be identically zero for all frequencies smaller than $1/M$. If we avoid this problem, and we made an extremely conservative choice on the initial distribution, i.e. we consider the population as monoclonal, with $x_0(n,k) = \delta_{n0}\delta_{k0}$, once again our infinite population size approximation will provide us non-biologically feasible results. With this initial condition, $F_0(h,z) = 1$ identically, and eq. 1.63 will reduce to

$$\ln\langle w\rangle = \ln(1-U+UG(e^{ts_0})) \sim \ln(e_{max}^k s_0 t) \tag{1.64}$$

for large time, where $k_{max} = max_k\{k|g_0(k) \neq 0\}$, which determines the most selective advantaged mutant. Indeed, given the exponential growth, this best-fit mutant will dominate the $G(e^{s_0 t})$ contribution, being the largest term of the sum. Since we have no drift, stochastic fluctuations being excluded by the $M = \infty$ limit, the deterministic growth of the best-fit mutant, no matter its original size, will dominate in the long term. So the final prediction for the velocity in this infinite size framework will be:

$$v_\infty = k_{max} s_0 \tag{1.65}$$

Once again, we see that this limit has no sense in the case in which mutation can achieve any selective advantage. Indeed, if we do not impose a cut-off in the mutation distribution, i.e. we perform the limit $k_{max} \to \infty$, the adaptation speed becomes infinite. Again, the explanation is simple. Every time the infinite population mutate, all the possible values of selective advantage are sampled, and in some sense just one step after the initial condition of monoclonal population, we are back to the case of an unbounded population distribution. Even if extremely favoured mutants will be extremely few, the absence of drift will make them grow deterministically and dominate the evolution.

To conclude, this shows us that taking the limit $M \to \infty$ in a simple way is wrong and gives unrealistic results. Even when we will like to do a continuum limit and approximate the population frequency with a continuum distribution, we will always have to be careful and impose ad-hoc cut-offs.

Chapter 2

Population Temperature

> "I don't know - Agnieszka said, shaking her head - It feels like my life is stuck. I am getting older, but the most I could do is already gone."
> "Then you have to leave - Kovacs replied - Go away, go to the south. The climate is warmer there. It'll feel awkward at the beginning, but then things will be going faster than now."
>
> Motos Bartom
> *Farewell to Kaliningrad*

In this chapter, a parallel between populations and thermal systems is drawn and deeply investigated.

Chapter Teaser

- why, in the regime of successional mutations, a population of size M is equivalent to a thermodynamic system at temperature $1/M$, so that small populations are hot, large ones are cold, 2.1.1;
- why this is not true when clonal interference and concurrent mutations are present, but we can prove that the equivalence is still valid in a broader sense, 2.1.3;
- what is a glass, and what does it mean that a glass ages, 2.1.2;
- why boolean expressions have lot in common with glasses, 2.2.1;
- why large populations behave and age just like glasses, and several striking proofs of that, 2.2 and 2.3;
- how one can speed up evolutionary experiments through the smart exploitation of a set of chemostats, 2.3.2;

- how come that population will keep memory of previous periods of stasis, 2.3.1;
- how a fluctuating environment can keep a population young, 2.3.3.

2.1 Population as a thermal system

In this section we will show how, in the successional mutations regime, the monoclonal populations that characterize the evolution in this setting (see end of subsection 1.2.2) follow a dynamics driven by detailed balance. The distribution for the reproduction rates at equilibrium will then have the same form of the canonical Boltzmann distribution. This, and the biological fact that such an equilibrium is usually far from being reached, will lead us to a brief introduction to glasses, justified by our need of out of equilibrium physics. This parenthesis closed, we will prove that a sort of detailed balance holds in a much broader range of evolutionary parameters, and not only in the low mutation rate limit of the successional mutations regime.

2.1.1 Detailed Balance

Let us recall the formula for the probability of fixation of two competing lineages, eq. 1.11. A mutant of fitness λ_B invading a population of wild-type with fitness λ_A will get fixed according to:

$$p_{A\to B} = \frac{1-\frac{\lambda_A}{\lambda_B}}{1-(\frac{\lambda_A}{\lambda_B})^M} = \frac{\lambda_A-\lambda_A}{\lambda_B^M-\lambda_A^M}\lambda_B^{M-1} \tag{2.1}$$

Considering the probability of the opposite event, invasion of B by a single A mutant, $p_{B\to A}$, we can see that eq. 2.1 leads us to

$$\frac{p_{A\to B}}{p_{B\to A}} = \frac{\lambda_B^{M-1}}{\lambda_A^{M-1}} \tag{2.2}$$

and so taking $p_A = \lambda_A^{M-1}$, and an equivalent expression for p_B, one obtains

$$p_A p_{A\to B} = p_B p_{B\to A} \tag{2.3}$$

This is precisely the detailed balance equation. Since every competition between two different lineages is ruled by such an equation, we can claim that as long as we will be in the successional mutations regime, and neglecting the short periods during which fixation of a mutant takes place, the population will be described by monomorphic populations, reaching an equilibrium defined by the probability of having a dominant lineage of fitness λ, given by

$$p_{eq}(\lambda) = \lambda^M \tag{2.4}$$

where we used $M-1 \sim M$, since we will always be in the limit of large M. The particular form of eq. 2.4 suggests us to introduce a fictitious energy, E, defined as

$$\lambda = e^{-E} \tag{2.5}$$

The use of this energy is readily understood by noticing that with this definition we have $p(\lambda) = e^{-ME}$, which is the usual Boltzmann weight, with an inverse temperature equal to the size of the population, or

$$\beta = M \tag{2.6}$$

Let us remark that this result is not a feature of the particular model we used, and it is indeed easy to follow the same line of reasoning in the Wright Fisher model, starting from eq. 1.14, and getting $\beta = 2M$.

Our derivation has been done in the case of symmetric mutations, and without considering properly that, together with the probability of fixation after implantation, one should take into account also the probability of implantation of the invading mutant. Indeed, in a colony of all A type individual, the creation of a single B individual happens with a rate given by M/τ_{AB}, where τ_{AB} is the average time that it takes to a single mutation $A \to B$ to happen. In complete generality, we cannot assume $\tau_{AB} = \tau_{BA}$. The ratio between the transition probabilities will be

$$\frac{p_{A\to B}}{p_{B\to A}} = \frac{\tau_{BA}\ \lambda_B^{M-1}}{\tau_{AB}\ \lambda_A^{M-1}} \tag{2.7}$$

that takes the place of eq. 2.2. The equilibrium probability distribution will not be the one of eq. 2.4 any more. However, it is not difficult to think about redefining the quantities entering the probability distribution so that detailed balance is still guaranteed. In order to make possible to preserve detailed balance, we have to require that our transition probabilities do not generate stationary distribution with limit cycles. In other words, the path $A \to B \to C$ should have the same probability of being followed as the inverse one, $C \to B \to A$. This means that the mutation rates should satisfy

$$\frac{\tau_{ab}\tau_{bc}\tau_{ca}}{\tau_{ac}\tau_{cb}\tau_{ba}} = 1 \tag{2.8}$$

If this is the case, we are assured that detailed balance will be satisfied, and we can introduce $\beta_\tau \hat{E}_B = \ln \tau_{AB}$, and redefine the energy as

$$E_A = \frac{\beta_\tau}{\beta}\hat{E}_A - \ln \lambda_A \tag{2.9}$$

The role that τ plays is the one of a chemical potential. With this definition of the energy, we can reformulate the detailed balance condition, eq. 2.3, with the equilibrium distribution defined by (for $M \gg 1$)

$$p_{asymm}(A) = e^{-\beta E} = \lambda_A^M e^{-\beta_\tau \hat{E}_A} \tag{2.10}$$

In the following, however, we will always consider the transition rates symmetric, $\tau_{AB} = \tau_{BA}$, and eq. 2.10 will reduce to eq. 2.4.

The mapping to equilibrium thermodynamics can be completed by defining a free fitness in the same way one defines a free energy for thermal systems, and deriving all the theorems of statistical physics of equilibrium in the new setting of population dynamics. This has indeed been done in [37], but the detailed balance condition was known to hold even before [38, 39] and was later used by several authors [40–43]. However, this mapping suffers from two limitations: the first one is that it can only work in the regime of successional mutations, i.e. when eq. 1.34 holds. The second limitation is a practical one: although we are assured, by the detailed balance condition, eq. 2.3, that the system will reach equilibrium satisfying eq. 2.4, the dynamics might be slow enough so that in biologically feasible time-scales the equilibrium will never be actually reached. In this sense, the study of populations will rather have to be mapped to statistical physics of non-equilibrium. In the following, we will see that this is actually possible, a notion of temperature as inverse of the population size can be maintained, and several results obtained in out of equilibrium thermodynamics will have a direct application in the context of population dynamics.

Before showing how this mapping can be worked out, it is appropriate to recall some general features of out-of-equilibrium systems. In particular, we will be interested in the presence of emerging time-scale separations.

2.1.2 Glasses

Probably the main object of study in non-equilibrium physics is represented by glasses. The amount of work that have been devoted to their study is impressive (for some reviews see [44–46]). Since we will be dealing with glasses and glassy features in our study of population dynamics, let us give a brief introduction to two of the main classes of glasses, namely structural and spin glasses. While in the former the disorder and the glassiness manifest themselves in the positions and orientation of the molecules, in the latter they are present in the magnetization of atoms. However, both these kinds of systems have many features in common.

Real glasses Structural glasses are, with respect to static properties, almost indistinguishable from liquids [47]. Indeed, it is the dynamics that differentiates the glass from the liquid phase in a material [48]. While in the liquid phase, the system presents fast fluctuations, due to the free movement of single molecules, and equilibrium is normally reached rapidly. By reducing the temperature, however, it may happen that the system develops other, longer, time-scales, due to collective effects in the interactions of molecules [49]. This is a very general behaviour that manifests itself when a liquid is cooled down, below the melting temperature, yet not starting crystallization to become a solid. We are then speaking of a supercooled liquid. The final outcome, either the solid or the supercooled liquid phase, depends on the cooling rate, the presence of impurities in the liquid, and other factors. The relaxation associated to the longer time-scale is

referred to as α relaxation. As the temperature is reduced, α relaxation times become longer and longer. In the supercooled phase, however, one can still speak about equilibrium, in a somehow broader sense (the true equilibrium would be the solid state), since the state of the system can be defined unequivocally by locating it on the PVT plane.

When temperature drops below a certain value T_g, however, this is no longer true. The state of the system depends on the previous history, e.g. on the cooling rate, and the system keeps on relaxing, with a (slow) dynamics whose time-scale depends on the time passed since it has start relaxing. The system is in a out-of-equilibrium condition. Its properties at a given instant t will be different from the same properties measured after having waited until some time $t + t_w$. We say that the system is in the glass phase. Its time- and history-dependent behaviour is defined as *aging* [50].

Spin glasses, as structural glasses, do not present a clear transition in static properties with respect to common para-magnets. The differences, once again, are to be looked for in the dynamics. At high temperature, a magnet typically responds rapidly to an external field, with the internal spins aligning with it in exponentially short time. Below a given temperature, however, this relaxation slows down by different order of magnitude. In a naively way, this slowdown can be explained by means of a simple picture. Magnetic bonds in the material are distributed in a random disordered way, so that some spins will prefer to align with each other, and be in opposition with others. This will cause the system to form domains of aligned spins. The inter-domain orientation is however randomized, and in order to reach higher magnetization values a system should grow and merge domains, trying simultaneously to align with the field, and to overcome frustration. This is of course a slow process, since it involves the reorientation of large numbers of spins. We thus have emergence of new time-scales, given by the movement of domain walls, much slower when compared to the fast single spin dynamics. Thus, while cooling down the system, we will have the emergence of α relaxations, and for very low temperature the system will start to age.

Correlation Numerically, separation of time-scales and aging can be studied and described by defining an auto-correlation function $C(t)$, as a measure of how much the system, e.g. its molecular configurations, at $t = 0$, will be different from itself at a time $t > 0$ [51]. $C(t)$ will be 1 for identical systems, so $C(0) = 1$ by definition, and $C(t) = 0$ when the systems are uncorrelated. The precise functional form will change from case to case, but in general its behaviour will follow the general scheme depicted in fig. 2.1. At high T, the system presents only fast relaxations, and the correlation drops rapidly down to zero. When temperature is lower, slower relaxation start to appear. Then, when $T < T_g$, the correlation does not depend only on the separation time between the states, but also on the time waited t_w. So it is necessary to define a two time auto-correlation, $C(t_w, t_w + t)$, which measures the autocorrelation for the system at a time t_w and at a subsequent time $t_w + t$. As t_w grows, $C(t_w, t_w + t)$ requires longer time to reach zero.

Trap model and ergodicity breaking From a theoretical point of view, the generation of fast and slow time-scales can be interpreted with a simple picture. In a mean field

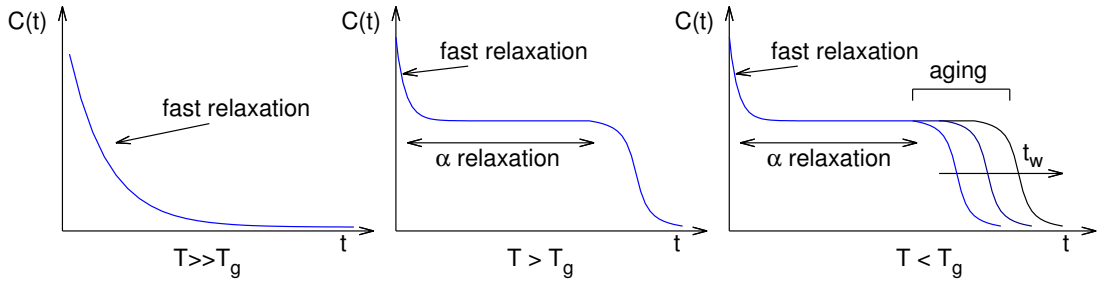

Figure 2.1: A sketch of the behaviour of the correlation in time. From left to right, the temperature T is taken down. In left panel, the system is in the liquid phase, and fast thermal fluctuations dominate the dynamics, causing the correlation to decay rapidly. In the central panel, a new longer time-scale shows up, as the temperature is taken down close to the glass transition T_g. Correlation first decays by means of the thermal fluctuations, but then the presence of slower relaxations causes the system to stay correlated for more time. Finally, in the right panel, temperature is below the glass transition. The time for correlation to disappear is not constant, but grows with the waiting time t_w.

approach, the system state can be supposed to be a point moving in an energy landscape, presenting a huge number of local minima of potential, corresponding to metastable states. The impossibility for a glass to reach equilibrium is due to the difficulty in finding the true equilibrium out of a tremendous large number of local minima [52]. Indeed, this situation is referred to as *weak* ergodicity breaking, as the system is not able to reach all the states not in light of an actual state separation (as in the normal "hard" ergodicity breaking), but as a consequence of the limited time available to move into a configurational space that would instead require an infinitely long exploration.

Each one of these minima is at the bottom of a valley, or a trap, and to move among these, the system should climb the energy barrier surrounding the minimum it is in. At high temperature, this does not constitute a problem, and the system can enter and go out of the trap easily. As the temperature goes down, however, for the system is more and more difficult to exit the trap, and a certain point the temperature is so low that it will exit a trap only to immediately fall into another one.

It is not difficult, within this idealization, to provide a mechanism for the inset of broken ergodicity and aging [53]. Assume that the time τ to exit a trap is proportional to $\exp(E/T)$, where E is the energy of the trap, and T the temperature of the system. This is a common choice for the functional form of relaxation times due to the overcoming of energy barriers, typically referred to as the Arrhenius law. Then, for exponential or power-law distribution of E, one finds that the average of τ is infinite. This is caused by the large tail of the τ distribution, and this fact has strong relevance. Indeed, when one estimates the longest time spent in a trap, t_{max}, after letting the system relax for a time t_w, one finds that $t_{max} \sim t_w$, meaning that the system spends basically all the time in the deepest trap. One can therefore have an interpretation for the growth of the α relaxation time with t_w. As long as the the waiting time augments, the system will

be able to explore deeper and deeper traps, and the time required for going out a trap, i.e. the slow relaxation time-scale, will grow larger and larger, as it is dominated by the maximal value encountered.

The interpretation of the time-scale separation would then proceed as follows. Each trap has its own internal landscape, in which the system is able to relax rapidly. Going out of a trap requires overcoming the energy barrier given by the trap depth, and this of course requires larger time. In this way, e.g. in the context of structural glasses, one can think of the several, small, single molecular vibrations as relaxations inside the trap, and jumps among traps as large and slow collective structural rearrangements, giving rise to α relaxation time-scales.

Canyon model Let us provide another way to model the landscape. Consider the state of the system as enclosed in a narrow valley, with steep borders but a gentle longitudinal slope. Different valleys are connected through bifurcations, each one with several (almost flat) possible directions, just like in a canyon. In the transverse sense, the steep walls cause the system to equilibrate fast, and fluctuations present a fast dynamics. In the longitudinal direction, however, since the valley is only slightly tilted, the movement is slow. Once again, every valley will be connected through some path to the others and ergodicity is not in principle broken, but the high number of valleys and the slowness of the dynamics make the system unable to relax easily.

This last framework has the privilege to have the slow dynamics being constituted by a continuous movement, rather than by rare jumps, happening almost instantaneously. Seen from the point of view of the correlation, the former model will predict then that relaxation of the correlation will happen rather smoothly for a single realization of the system, while in the other case there will be no a priori reasons to suppose different traps to be correlated. In our practical case of interest, studied in section 2.2, we will see that the canyon picture is to be preferred.

This brief introduction will make the reader more familiar with the fact that, considering a single realization of a disordered system, and diminishing the external temperature, we obtain a transition from liquid (or magnetic) to a glass phase. To show how we can extend our parallel size of the population / temperature, we will then show that, taking several realization of a system, increasing the size of a population will cause it to show a glass transition.

2.1.3 Coarse grained population dynamics

We have seen so far that the presence of different time-scales is a typical situation in out of equilibrium systems. We will show how this feature will turn out to be very useful to extend our notion of temperature in the context of population dynamics far from equilibrium.

Let us now study the following situation. Consider a population in which the possible mutations can be grouped into two subsets, say A and B, each one containing several lineages. Mutations between lineages will happen with a certain average rate, $1/\tau$, and

every time an individual will mutate, it will do to a lineage belonging to its current subset with probability p, and to one of the other subset with probability $1-p$. For simplicity, let us assume that the fitness is totally epistatic, and mutations can connect all lineages indifferently. Let us indicate lineages of group A with the label a_i, and those of group B with b_i. In a given state a_i we will have a number m_{a_i} of individuals, with fitness λ_{a_i}. The total number of individual is M, divided in the two subsets containing M_A and $M_B = M - M_A$ individuals respectively.

Such a situation can be thought of as referring to a situation in which a bi-allelic gene is responsible for choosing between two metabolic pathways, A and B, and each one of these can manifests itself in several different ways (the a_i and b_j). Or, and this is the situation in which we will concentrate on, we will consider this separation as originated by time-scale separation, with states in A being temporally far from state in B. Or one can think as A and B being two ecological niches, and individuals in one can mutate or migrate into a different niches, where their fitnesses change due to the different environments. This situation is probably the easier one to understand, and for a moment we will refer to A and B as niches, and a_i and b_j as species.

Suppose that the mutation rate $U = 1/\tau$ is small, so that eq. 1.34 is satisfied for every difference in fitness between any species. Then the dynamics will satisfy detailed balance as described before in subsection 2.1.1, and the population will cluster in one or the other lineage, changing from time to time the niche, all this accordingly to the relative fitnesses of the species. But let us now consider a much higher mutation rate, or smaller τ, with $p \sim 1$. Inside the two niches, we will have that the successive mutations regime does not hold any more, and clonal interference and polymorphism will be present.

However, mutations/migrations between the two niches will keep being rare, with a small rate of mutation $U = (1-p)/\tau$. Then what if we coarse grain our system, and we treat the two niches as two species, with their fitnesses being given by some average on their internal organizations? Let us show that, with proper definitions and caveats, one can get again detailed balance for these coarse grained competing mutants.

The demonstration is very simple. We first need the probability of increasing and decreasing the number of individual in A. They can be obtained by simply summing over the probability of increasing (decreasing) the number of individuals in a given species a_i, provided that a death occurs in a species b_j. In other words, one should exclude from the count the events that consist in a mutation from a_i to a_j, and the birth in a_i followed by a death in a_j. Mutation from a_i to b_j, as we said, can be neglected. Then we easily obtain:

$$\begin{aligned}
\pi_{M_A \to M_A+1} &= \sum_{i\in A} \frac{m_{a_i}\lambda_{a_i}}{M\langle\lambda\rangle} \frac{\sum_l m_{b_l}}{M} = \frac{M_A\langle\lambda\rangle_A}{\langle\lambda\rangle M} \frac{M-M_A}{M} \\
\pi_{M_A \to M_A-1} &= \sum_{i\in A} \frac{\sum_{l\in B} m_{b_l}\lambda_{b_l}}{M\langle\lambda\rangle} \frac{m_{a_i}}{M} = \frac{(M-M_A)\langle\lambda\rangle_B}{\langle\lambda\rangle M} \frac{M_A}{M} \\
\pi_{M_A \to M_A} &= 1 - \pi_{M_A \to M_A+1} - \pi_{M_A \to M_A-1}
\end{aligned} \tag{2.11}$$

We defined $\langle\lambda\rangle_A$ as the average of the fitnesses over the actual distribution of mutants in A, i.e. $\langle\lambda\rangle_A = \sum_{i\in A}\lambda_{a_i}m_{a_i}/M$, same for $\langle\lambda\rangle_B$, and $\langle\lambda\rangle = (M_A\langle\lambda\rangle_A + M_B\langle\lambda\rangle_B)/M$. A quick look at these transition probabilities let us recognize the same expression we obtained in the case of two competing colonies, eq. 1.10. We can then follow the same procedure as before, and find out that the probability of moving all the individuals to the subset B, starting from a situation in which the whole population is in the subset A and only one individual is in one of the b_i states, is given by

$$p_{A\to B} = \frac{1}{1+\sum_{j=1}^{M-1}\gamma^j} = \frac{1-\gamma}{1-\gamma^M} \qquad \gamma = \frac{\langle\lambda\rangle_A}{\langle\lambda\rangle_B} \tag{2.12}$$

The formula is the same as in eq. 2.1, with the only difference consisting in having fitnesses replaced by averages on fitnesses. So, imagine now to have several niches, with individuals able to mutate between them but with a very small rate. The internal dynamics of species needs not to have any constraint, the different lineages can suffer from clonal interference, or be in a successional mutations dynamics, or even be evolving by means of random drift. The only things that we need to know is the final fitness distribution inside a niche J, $\langle\lambda\rangle_J$. Then, we are sure that the dynamics of the subsets will satisfy detailed balance, and that the final probability distribution in equilibrium will be

$$p_J = \langle\lambda\rangle_J^M \tag{2.13}$$

Let us spend some words about the averaged fitness we used. Notice that since m_{a_i} is a priori a time dependent quantity, so is $\langle\lambda\rangle_A$. We will assume in the following that m_{a_i} are in equilibrium inside A, and so $\langle\lambda\rangle_A$ is a constant, determined as a given (unknown) function of the λ_{a_i}.

This might turn out to be a strong assumption, for two reasons. Firstly, M_A is not supposed to be large at all times, so in principle the equilibrium distribution of m_{a_i} may not be adequately sampled. Since we are supposing M very large, however, the time spent by the system at low M_A number will not be significant. Secondly, the time-scale of the competition before fixation of A and B should be larger compared to the time for the mutants inside A and B to reach equilibrium internally to the subset. This is a strong limitation in this two subsets model, as it forces strong constraints on the differences between $\langle\lambda\rangle_A$ and $\langle\lambda\rangle_B$. However, this happens when the two processes, intra- and inter-subset competition verify simultaneously. This issue is automatically solved when studying spatial separated ecological niches: assuming migration times slow compared to intra-niche dynamics is usually not a strong assumption. In this case however, imposing a fixed population size constraint might seem to be artificial. The other possibility of avoiding this inter-intrastate time-scale competition is to take it as a fundamental feature of the model. We will indeed consider a case in which the fitness landscape has the structure of a canyon, like the energy landscape we described for glass in the 2.1.2 subsection. The approach is sketched in fig. 2.2. Here and in the following, for schematic

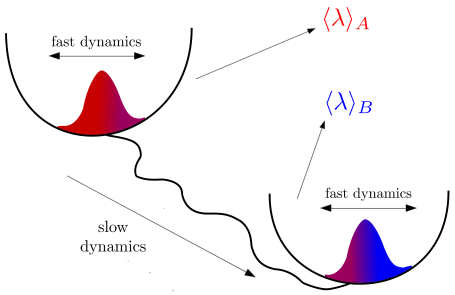

Figure 2.2: An example of time-scale separation, in a canyon-like fitness landscape.

representation we might refer to valleys, while in a fitness landscape one should better look at them as ridges. The reader will overlook this lack of rigour.

Let us stress that if, in principle, this definition of $\langle\lambda\rangle_A$ lets us prove detailed balance, it is in practice not directly applicable. Indeed, to compute it, one has to know the equilibrium clonal distribution inside the subset, which does not satisfy any detailed balance relation, and remains unknown. In general, we will estimate the averaged fitness only a posteriori, computationally.

2.2 Population glass

In order to prove our equivalence between a thermal system and a population, we will consider a system that behaves like a glass, investigate its glassy features in the thermal setting. Then, we will show that these same features manifest, when the several copies of the same system are taken to form a population. In some sense, the role of the thermal reservoir for an individual is played by the rest of the population. Using the knowledge acquired in statistical physics to study population dynamics has provided several interesting results so far [54–58]. A suitable choice for a glass system will be provided in the boolean satisfiability framework [59]. Before giving a definition of our fitness function, it is preferable to take some time to introduce satisfiability problems [60], describe some of their features, and show how they will represent a good choice for our purposes.

2.2.1 Boolean satisfiability

A boolean variable x can assume only two values, TRUE or FALSE (resp. 1 or 0). We have three main binary operations, $and(\wedge)$, $or(\vee)$ or $xor(\veebar)$. They return a TRUE result, for two variables x and y, only if: $(\wedge)$ both x and y are TRUE; $(\vee)$ at least one is TRUE; $(\veebar)$ one and only one variable is TRUE. There is also the $not(\neg)$ operator, that invert the logical value of a variable. We will refer to $\neg x$ as the conjugate of x. A combination of variables and their conjugates by means of these operators is what is called a boolean expression. The problem of finding a given set of variables x_i so that a given expression is solvable, i.e. its final value is TRUE, is referred to as satisfiability problem. In the case

in which it is possible to find such a set of variables, the expression is defined to be SAT (satisfiable), otherwise it is classified as UNSAT.

We will define *clause* of size k an expression that contains k variables, related by means of one kind of operator only. Let us concentrate on disjunctive clauses, that is clauses containing only $\vee$. More general expression can be obtained by relating this disjunctive clauses by means of conjunctive operator, namely $\wedge$. What we have is referred to as the conjunctive normal form, CNF, which takes the general form:

$$\bigwedge_{i=0}^{\alpha N} \bigvee_{j}^{k_i} z_{j_i} \tag{2.14}$$

where z_{j_i} can be x_{j_i} or its conjugate. Here N is the total number of variable, and a single variable can appear more than once in the expression. All boolean expressions can be transformed into such a normal form. As a side note, let us comment that the CNF is not the only conventional normal form, as one can consider clauses made by conjunctive operators, connected via disjunctions. In that case one speaks of DNF (disjunctive normal form). In the DNF form, the satisfiability problem is trivial. Indeed, a DNF expression is automatically satisfied once at least one of the clauses can be satisfied, and this will be the case for every clause that does not contain simultaneously a variable and its conjugate. Passing from a CNF to a DNF expression can be done systematically, but it requires an exponential number of steps. From a computational point of view, then, this does not simplify the problem.

The expression in eq. 2.14 is in general studied with $k_i = K$, i.e. with all the clauses containing the same number of variables. The satisfiability problem is referred then as K-SAT. The interest on K-SAT stems from a striking transition in its behaviour in the large N limit. Indeed, for a given K, there is a threshold in the number of clauses, individuated by a critical value of $\alpha = \alpha_c(K)$, such that, with probability 1, the system is SAT below $\alpha_c(K)$, and UNSAT above. In general, for a given realization of K-SAT, with $\alpha \lesssim \alpha_c(K)$, it is really difficult to find the solution x_i. Indeed it has been shown [61] that, by approaching $\alpha_c(K)$, in the phase space of configurations, the set of solving configurations first starts to shrink, and then at a certain value of α becomes subdivided into several clusters, that grow in number exponentially, shrinking in size. In the end, when the threshold value $\alpha_c(K)$ is reached, the are no more solutions.

Physical interpretation This phase space clustering has an immediate interpretation once one uses the number of errors, i.e. of false clauses, to define an energy for the system, as:

$$E(x_i) = \sum_{i=0}^{\alpha N} \delta(z_{i_1} + z_{i_2} + z_{i_3}) \tag{2.15}$$

We see that finding a solution corresponds to finding a ground state for the energy. From the picture we described above, we can understand that the energy landscape for

a K-SAT with increasing α has the same features that one of a glass when lowering the temperature. The proliferation of minima, divided by energy barrier (the number of false clauses one should pass through to connect one cluster of solutions to another one), is exactly the feature giving rise to slow glassy relaxations. To be sure of dealing with such an entropic dominated landscape, we will put ourselves in the UNSAT phase, $\alpha = 6$. A true ground state will not exist, and the system will try to reach the configuration that minimizes the number of errors, i.e. of FALSE clauses.

In our study we will focus on a slight modification of the 3-SAT problem, in which disjunctive clauses do not contain *or*, but rather *xor*. We speak then of XORSAT, and its general form will be

$$\bigwedge_{i=0}^{\alpha N} (z_{i_1} \veebar z_{i_2} \veebar z_{i_3}) \tag{2.16}$$

All the results we will provide in this chapter are valid also for the K-SAT, as we claim them valid in general for every system with glassy features. From the SAT perspective, XORSAT has the privilege to be always solvable by Gaussian reduction, and its properties, along with its phase diagram, have been worked out in detail [62]. In the case of XORSAT, the energy takes the form

$$E(\{x_i\}) = \sum_{i=0}^{\alpha N} [1 - (z_{i_1} + z_{i_2} + z_{i_3}) \bmod 2] \tag{2.17}$$

Let us stress that similar models are not a novelty in the context of population dynamics. Kauffman [63] in the 80's proposed its NK model to investigate genome evolution. It consists of assigning to an individual a set of N spins $\{x_i\}$, and evaluate its fitness by summing the contribution of the fitness of each spin. For a given spin, its fitness depends on K other spins, so that the total fitness is $\lambda(\{x_i\}) = \sum_i \lambda_i(x_{i_1}, ..., x_{i_K})$. The peculiarity of this model is that the fitness landscape ruggedness can be tuned. For $K = 0$, fitness is simply additive, while for $K \sim N$ the fitness is highly epistatic, and the landscape is extremely rugged. We will not deepen into the results obtained through this model [64–67] nor its biological feasibility. As we already pointed out, we use an energy like eq. 2.17 with the sole purpose of having a rugged landscape, and without any biological immediate interpretation in mind.

To prove the validity of our choice of the XORSAT as a glassy model, we can simulate its behaviour. Given a set of clauses, we take a realization of XORSAT, namely a set of variables $\{x_i\}$, and we make them evolve according to a Metropolis algorithm, with the probability of accepting a move, i.e. changing one variable value, given by $p = \min(1, \exp(\beta(E_{new} - E_{old})))$, where E_{old} and E_{new} are the two energies before and after the switch, computed according to eq. 2.17. For different values of β, one can concentrate on correlation, and compute

$$C(t_w, t_w + t) = \frac{4}{N} \sum_i \left(x_i(t_w) - \frac{1}{2}\right)\left(x_i(t_w + t) - \frac{1}{2}\right) \tag{2.18}$$

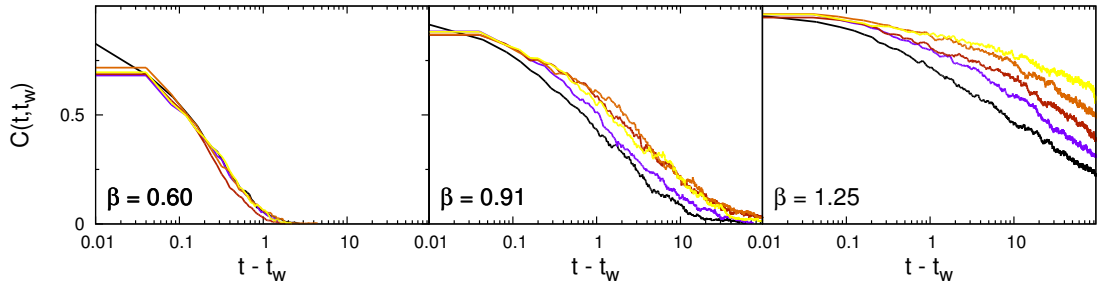

Figure 2.3: The correlation $C(t_w, t_w + t)$ for a single thermal realization of XORSAT, as defined in eq. 2.18, plotted as a function of the time t, for different value of β. Different colours represent different values of t_w, the darker the lower. The behaviour at different temperatures, described in the main text, reproduces the qualitative picture of fig. 2.1.

The correlation will be 1 when $\{x_i(t_w)\}$ is equal to $\{x_i(t_w + t)\}$, and 0 when it is its conjugate. For high temperature we expect $C(t_w, t_w + t)$ to be independent of t_w, and $C(t_w, t_w + t) = C(0, t)$. This is indeed what happens in fig. 2.3(left), where the system is clearly in the liquid phase, and it decorrelates completely on time-scales of the order of the switching time of a variable. For lower temperature, fig. 2.3(center), we see the emergence of slower relaxation, as the correlation vanishes over time-scales higher by some order of magnitude. Finally, in fig. 2.3(right), the system is in the glass phase, and the relaxation of the correlation strongly depends on t_w, and the system is clearly aging.

We have then what we wished for, a system whose evolution can remain for long times far from equilibrium, and that presents a neat time-scale separation. These are exactly the two ingredients that were needed to apply the coarse-grained description of subsection 2.1.3.

2.2.2 M population, $1/M$ temperature

We are now ready to define our population and to show how the thermal-population correspondence can be demonstrated. Our individuals will be identified by a set of boolean variables, $\{x_1, \ldots, x_N\}$, and their fitness is defined by

$$\lambda(\{x_i\}) = e^{\frac{E(\{x_i\})}{N}} \tag{2.19}$$

where $E(\{x_i\})$ is the XORSAT energy defined in eq. 2.17. The factor N is put to have a non-divergent fitness in the limit $N \to \infty$. Every individual will be able to mutate independently, by changing the logical value of one of its internal variables. The average time for such a mutation to happen will be denoted by τ.

The population will evolve as a diffusive process on the N-dimensional hypercube, with individuals able to jump between connected vertices, and population being kept together (localized) by means of the fixed size condition [68] (we will discuss the localization of a diffusing population caused by the fixed size constraint later, in section 4.1). Notice that the dynamics at the level of the individuals is unbiased, and totally random.

Without imposing a constant population size, we will have every individual performing a random walk on the hypercube.

A note of caution is necessary here. In the thermodynamic limit, we can think as our system as performing a motion with continuous diffusion, along one (slow) direction, where the fitness is parametrized by the position $\lambda(x)$. The diffusion coefficient D substitutes τ as the parameter encoding the mutation rate. In this situation, the condition of successional mutations regime as we have derived it loses significance. Indeed, a way of understanding it was to suppose that the population is always condensed in one lineage, and only one mutation can happen at a time, with the number of lineages never exceeding two. If we introduce the concept of diffusion, this condensation is not possible any more, since from the very instant following reproduction two individuals will be differentiated. What can be shown [18] is that in the limit

$$\sqrt{\frac{D}{\lambda}}\nabla_x E \ll \frac{N}{M} \tag{2.20}$$

the evolution of fitness of the system can be described by a diffusion equation, for which a fluctuation dissipation theorem can be shown to hold, with the role of the temperature T being played by our

$$\beta = \frac{M}{N} \tag{2.21}$$

Notwithstanding the individual random diffusive motion, we know that the results of the this dynamics will be selected accordingly to their fitness outcome, with the population trying to maximize its global fitness.

As a first example of this thermal-population similarity, we perform an annealing procedure with two different systems, fig. 2.5. The first one (red line) corresponds to a thermal annealing of a single XORSAT realization. In the complex energy landscape created by eq. 2.17 for a given set of clauses, the system is evolving according to a Metropolis Montecarlo algorithm, with the usual Boltzmann factor $e^{-\beta E}$. The system is created at an high temperature T, and then slowly cooled down, in a way so that it is (at least well above the glass transition) always in equilibrium with respect to the external temperature. The energy of the system decreases, as temperature is lowered, but as T_g is approached the system is less effective in minimizing its energy. At T_g and below the evolution is in practice stuck, and the system is almost insensitive to further decrease in T. One can see this in the change of concavity described by the energy curve.

The second system (blue line) is instead constituted by M realizations of XORSAT $\{x_i\}$, moving on the same energy landscape of the thermal system, but with the individuals dynamics being simply diffusive. In this case the annealing procedure is done by adding an individual at a time (for large populations this is equivalent to continuously lowering the temperature). As the population size grows, higher fitness are reached, but when the size becomes too high, the evolution almost stops. The mutation rate we used here is low enough so that the population is essentially monoclonal, and the system is in the successional mutation regime. The similarity in the behaviour of the thermal and population XORSAT is quite striking, the curves in fig. 2.5 overimpose remarkably well.

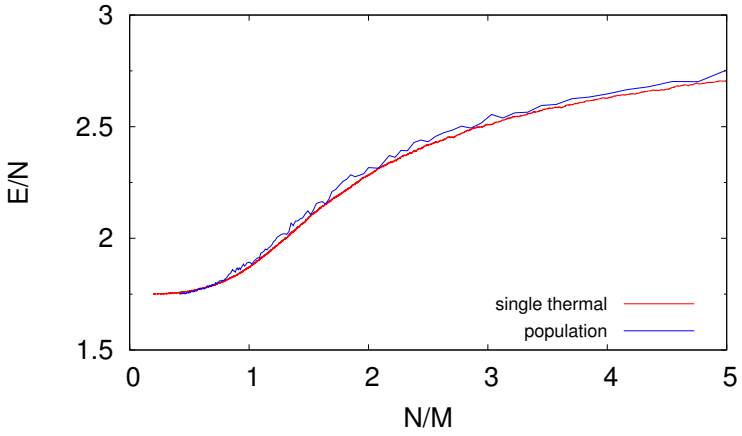

Figure 2.4: A comparison of two annealing procedures. Red line correspond to the energy of a single XORSAT realization, with external temperature $T = N/M$. Blue line shows the behaviour of the energy $E/N = \ln \lambda$, as the (normalized) size of the population M/N is increased.

However, as we already pointed out before, a *pure* monoclonal population is not needed. Indeed, even if this is not the case, we will recover detailed balance, and consequently a thermal dynamics, with the caveat of using not directly the fitness in eq. 2.19, but rather its average, as defined in subsection 2.1.3. The dynamics satisfying eq. 1.34 (or better eq. 2.20), and those that do not, will be automatically separated by their different time-scales, given our choice of the XORSAT error count as the fitness function.

Correlations and the glass-phase transition We will define a correlation in a similar way we did for the thermal XORSAT, eq. 2.18, with an additional averaging over the population:

$$C(t_w, t_w + t) = \frac{4}{N} \sum_i \left\langle x_i(t_w) - \frac{1}{2} \right\rangle \left\langle x_i(t_w + t) - \frac{1}{2} \right\rangle \tag{2.22}$$

where the angle brackets mean average over all the individuals in the population. The single individual diffusion, being landscape independent, is a rapid process, which time-scale is given by the average mutation rate $1/\tau$. On the contrary, the movement of a large population will generally require longer times, especially in the case where beneficial mutations are not immediately available, i.e. are not in the neighbour vertices of the hypercube. This will give rise to α relaxations in the correlation of the system, just as it happened in the case of the thermal XORSAT, subsection 2.2.1. This is exactly what we see in fig. 2.5(top), where we can identify a behaviour similar to that of a liquid-supercooled-glass transition (exemplified in fig. 2.1), but with the varying external parameter being constitute by the population size, rather than the temperature. For small populations (top-left), the dynamics presents no time-scales different from the

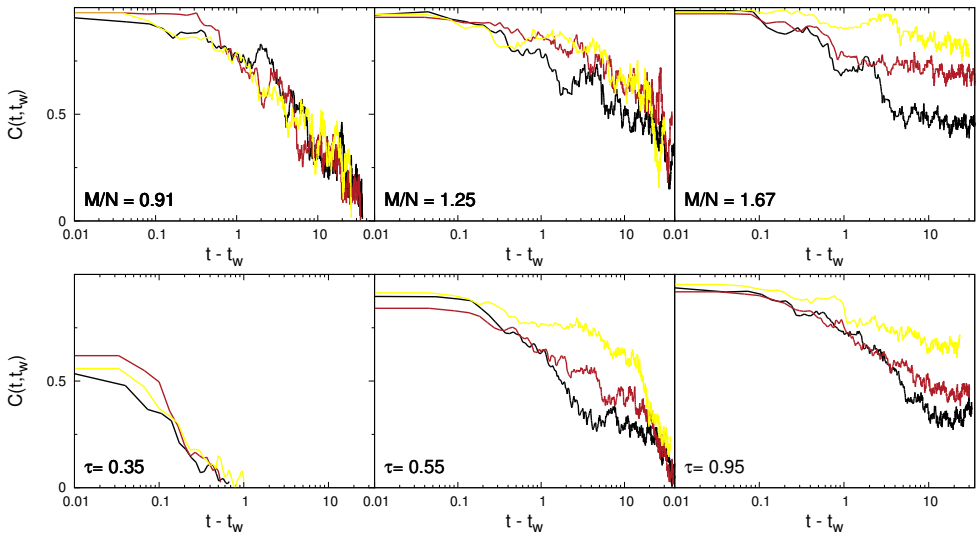

Figure 2.5: The behaviour of the correlation $C(t_w, t_w + t)$, defined in eq. 2.22, for a population of M individuals, as a function of time t. Top panels show the behaviours for different values of M, while bottom panels show the liquid-glass transition in the mutation rate τ^{-1}. The color-code refers to the waiting time t_w, with lighter curves referring to higher values of t_w. The (M, τ) values used here are also indicated in the phase diagram reported in fig. 2.7.

individual one, and correlation decays to zero in times of the order of τ. For larger populations (top-center), a longer relaxation time-scale starts to manifest itself, with a typical time-scale of $t_\alpha \gg \tau$ (notice the log-scale on the time axis). Finally, for large populations (top-right), the system presents aging, as the relaxation time-scale t_α is not a constant, but depends on the evolution time (t_w) of the population, being longer for older population. Notice that the correlations presented here are related to a single population. We see that the curves are relatively smooth, and do not present evident discontinuities. In light of what we said at the end of subsection 2.1.2, the energy landscape that better fits this behaviour is the one of a canyon rather than a collection of traps.

Having described the qualitative nature of this glass transition, we can study it quantitatively. A way to do it is to calculate the fluctuations in the correlation [69], defined as follows:

$$\chi_4(t) = \langle C(t_w, t_w + t)^2 \rangle - \langle C(t_w, t_w + t) \rangle^2 \tag{2.23}$$

where the average is to be intended over several waiting time t_w, and the definition of the correlation is the one given in eq. 2.22. The definition of $\chi_4(t)$ we give here does not depend on the waiting time t_w, as we will be concerned in computing $\chi_4(t)$ in the $T \geq T_g$ regime only.

In the liquid phase, the correlation is equal to one at initial time, and decays rapidly to zero, in a time of the order of τ. Thus, if we look at the fluctuations of the correlation,

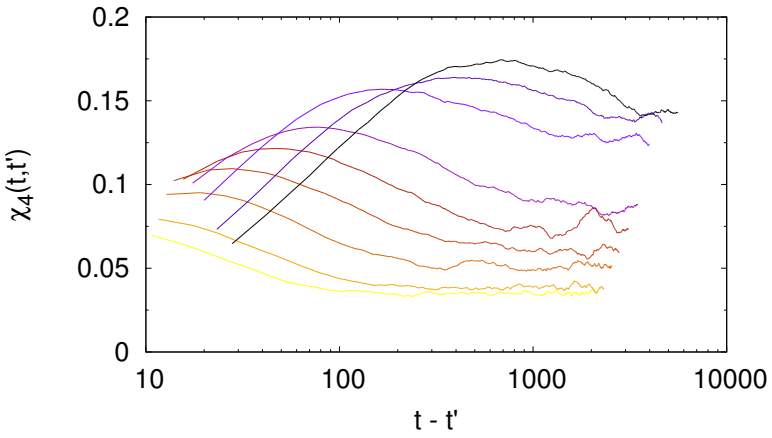

Figure 2.6: χ_4 value approaching transition while varying the mutation rate τ^{-1}, increasing from lighter to darker curves. Note that times are in logarithmic scale. After reaching the glass transition, the curve for χ_4 (not shown here) do not show any maximum.

we expect that for very short (resp. long) times, the fluctuations will be absent, as the correlation will be identically 1 (resp. 0). In between, the correlation goes down, and its value does fluctuate, with a maximum around the point at which correlations are supposed to drop the quickest. Therefore, by studying $\chi_4(t)$ as $T > T_g$, one can think as the value of t at which it reaches its maximum as a good indication for t_α. At $T \leq T_g$ the curve for $\chi_4(t)$ has no definite maximum, as the t_α is not defined for all the times, but instead increases as the time goes by. Indeed, $\chi_4(t)$ is not a well-defined quantity in this setting, as its value will depend on t_w. However, by looking at which temperature, i.e. population size, the time corresponding to the maximum of $\chi_4(t)$ diverges, we can estimate where the glass transition takes place. An example of the evolution of χ_4 when approaching the glass transition is given in fig. 2.6.

Up to now, we completely ignored the role of the mutation rate, $1/\tau$, in our discussion. However, it should be not surprising to suppose that its magnitude plays a role in the evolution of the population. Apart from the trivial effect of speeding up fast relaxation, a higher mutation rates does play a role also for what concerns slower α relaxation. Indeed, the mutation rate is directly related to the localization in the fitness space of the population distribution. For high τ, the population tends to condense and cluster to a single point, while for more moderate values it will be more spread. This in turn will mean that the population will be closer to the base of the peak, thus increasing the possibility that an individual will get away from the peak to start ascending another one, and eventually population might reach fixation there. Then, not being only a function of M, the time needed for slow relaxations t_α will depend also on τ. And indeed, by looking at the correlation $C(t, t_w)$ while varying the mutation rate instead of the population size, what we see, fig. 2.5(bottom), is a transition from liquid to glass, very similar to the one observed in figs. 2.3 and 2.5 (top).

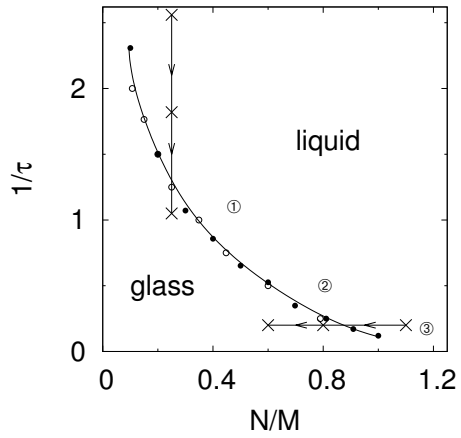

Figure 2.7: Phase diagram showing the liquid-glass transition line in the (M, τ) space, found by looking at the χ_4 divergence, by varying M (filled circles), or τ (empty circles). The agreement is very good. In the figure are also indicated the parameters used in fig. 2.5, by means of the crosses along the arrows. The points marked by circled numbers are the values of (M, τ) corresponding to the populations of fig. 2.9, and for which the crooks relation has been proven to hold, fig. 2.8.

The complete phase diagram is presented in fig. 2.7. For small populations, selection against slightly deleterious mutations is not too strong, and the system can escape local fitness maxima quite easily. For larger populations, the force of selection grows, and moving in the landscape across lowlands of small fitness becomes harder. Of course, a higher mutation rate enables more mutation to be produced, and therefore ease the landscape exploration. With these arguments, one can understand qualitatively the aspect of the transition line.

2.2.3 Test of detailed balance

Crooks relation We have seen that our system decorrelates in time of the order t_α. We can interpret this time as the typical time it takes to the population to escape a metastable state of relative high fitness. Near the glass transition, when $t_\alpha \gg \tau$, we can easily distinguish a *fast* evolution, which corresponds to the competition of simultaneously present lineages, happening close by in the fitness space , and a *slow* evolution, corresponding to the slow motion of the entire population in its different current lineages, all across the fitness landscape. In such a two-fold time-scale evolution, we can apply the coarse-graining mechanism on fast evolution that we have described in subsection 2.1.3, get rid of the fast dynamics, and show that the slow remaining degrees of freedom are in detailed balance. In particular, we will show that there are cases in which detailed balance does not hold between populations separated in time, but holds when the average value of these is considered.

In order to show that, we need first to demonstrate a relation for the fitness of two populations, when their dynamics is ruled by detailed balance, which goes under the name of Crooks Fluctuation Theorem [70–72]. Consider a population in equilibrium. Let us for the moment assume that detailed balance holds, so that the distribution of the fitnesses is given by $p(A) = e^{ME_A/N}$. Let us perturb the system, by switching on an external field h, so that the energy becomes $E_A \to E_A^* = E_A + hNm_A$, where m_A is the equivalent of a magnetization, $m_A = \sum x_i/N$. After the field is switched on, we have detailed balance with $p^*(A)p^*_{A\to B} = p^*(B)p^*_{B\to A}$, where the transition probabilities $p_{A\to B}$ are given by eq. 2.1, calculated with the substitution $E_{A,B} \to E^*_{A,B}$. In particular, we can rewrite this detailed balance relation as:

$$p(A)p^*_{A\to B} = p(B)e^{Mh(m_B-m_A)}p^*_{B\to A} \tag{2.24}$$

Now, suppose the system after some time has reached a state B, with $m_B = m_A+\Delta m$. The probability of increasing the magnetization of such a value is exponentially repressed with respect to the probability of decreasing the magnetization of the same amount. Indeed, using eq. 2.24 and permuting $A \leftrightarrow B$, we have:

$$\begin{aligned}
P(\Delta m) &= \int dA\, dB\ p(A)p^*_{A\to B}\delta((m_B - m_A) - \Delta m) = \\
&= \int dA\, dB\ p(B)e^{Mh(m_B-m_A)}p^*_{B\to A}\delta((m_B - m_A) - \Delta m) = \\
&= \int dB\, dA\ p(A)e^{Mh(m_A-m_B)}p^*_{A\to B}\delta((m_A - m_B) - \Delta m) = \\
&= e^{Mh\Delta m}\int dB\, dA\ p(A)p^*_{A\to B}\delta((m_A - m_B) - \Delta m) = \\
&= e^{Mh\Delta m}P(-\Delta m)
\end{aligned} \tag{2.25}$$

or equivalently

$$\frac{P(\Delta m)}{P(-\Delta m)} = e^{Mh\Delta m} \tag{2.26}$$

This formula is generally referred to as Crooks relation. We have to stress the two main hypothesis we made in order to demonstrate eq. 2.26. First, before activating the external field, the system should be in equilibrium. The Crooks relation is then useful only if applied to liquid or equilibrated supercooled fluid, but is not applicable using an initial state in the glass phase. Notice however that if the glass phase is entered after the switch, only detailed balance is necessary, not equilibrium.

Second, all the derivation in eq. 2.25 leans on the presence of detailed balance. In our population setting, then, eq. 2.26 should be valid only as long as eq. 2.3 holds, and it will allegedly fail otherwise. It is not difficult to prove, however, that a "coarse-grained"

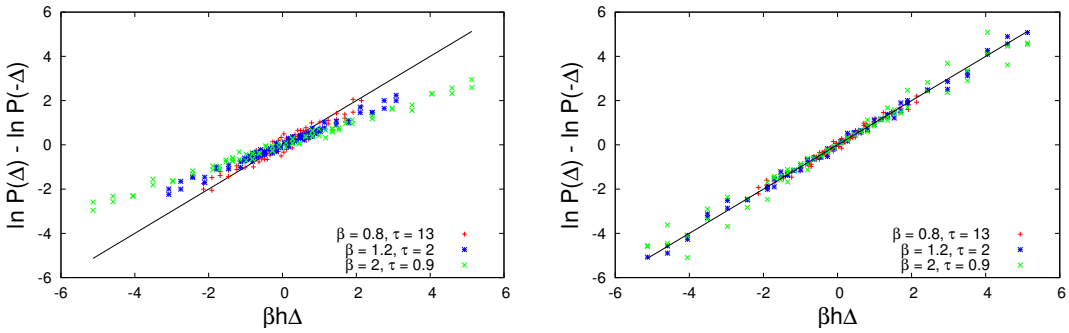

Figure 2.8: Figure showing the test of the crooks relation, eq. 2.26, with energies taken at an instant t (left), or averaged over a time interval $[t, t+\Delta t]$ (right). The choice of the (M, τ) parameters locates the system just above the liquid-glass transition, as shown by the marked point in the phase transition diagram of fig. 2.7.

Crooks relation will hold if we start from the "coarse-grained" detailed balance of eq. 2.12. The formula is the one of eq. 2.26, with Δm substituted by its average over the fast degrees of freedom.

A test of the Crooks relation With eq. 2.26 (and its coarse-grained version), we are ready to show how the averaging over fast dynamics constitutes a possibility to recover detailed balance even when it does not hold in its original form, eq. 2.3. We will let our population of XORSAT individuals evolve and relax for some time, until equilibrium is reached. Then, we switch on a field h, and we average the fitness of the different lineages present in the population, over a given interval of time $\tau \ll \Delta t \ll t_\alpha$. The system is let relax again for some time, namely $3t_\alpha$, so that we are assured that the population will be decorrelated from the original one. After this relaxation, the population fitness is averaged again, over a time interval Δt.

The results are presented in fig. 2.8, for different values of M and τ. The two figures represent the same runs, but in one case, fig. 2.8(left), the quantities of interest are those of the instantaneous populations at time t and $t+3t_\alpha$, while in the other case, fig. 2.8(right), the averages are considered, with averaging over the intervals $[t, t+\Delta t]$ and $[t+3t_\alpha, t+3t_\alpha+\Delta t]$. In fig. 2.8(left), the data strongly deviate from the line representing eq. 2.26, indicating that detailed balance is not satisfied for the chosen (M, τ) parameters. With these values, indeed, the population is highly polymorphic, and clonal interference and concurrent mutations effects are relevant. One can see this clearly by looking at fig. 2.9, that shows a sketch of the lineage-decomposition of the population for the three sets of parameters. Let us notice that detailed balance is strongly violated for the data referring to fig. 2.9(a), where a lot of simultaneous competing mutations are present, while the deviation from the behaviour predicted by eq. 2.26 is weaker for the data corresponding to the population in fig. 2.9(c), that it is almost monoclonal.

The agreement with eq. 2.26 is instead excellent in the case of the averaged data, fig. 2.8(right). The scaling is very good for all the sets of parameters, with no clear

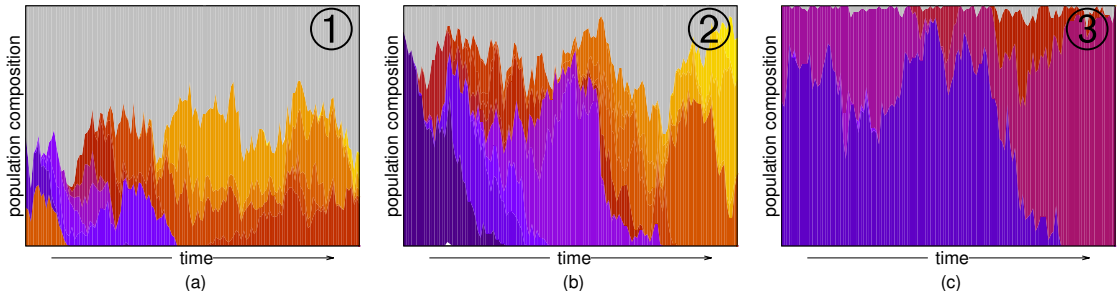

Figure 2.9: The composition of the population for three different values of (M, τ), corresponding to cases of the test of the Crooks relation, fig. 2.8. Every lineage is depicted with a different color, and its vertical width at a given time corresponds to its fraction with respect to the total population. The top grey part represent all the lineages that never reach, during their evolution, a fraction of at least 10% of the total.

distinction between the three behaviours. This should not be surprising, as the differences between populations in fig. 2.9 are mainly due to their instantaneous behaviour, while the landscape they are (slowly) exploring is the same, and for what concerns their slow dynamics (properly coarse-grained), detailed balance is evidently present. We have then show that even in conditions when the presence of multiple mutations disrupts the detailed balance relation in its basic form, we are able to recover its applicability, by focusing on the slow coarse-grained degrees of freedom.

As a side note, let us stress that the introduction of an external field is not the only way to verify detailed balance. Another, similar Crooks relation can be obtained in the case of a jump in temperature, $M \to M + \Delta M$. The equivalent expression for eq. 2.24 is

$$p(E_A)p_{A\to B} = p(E_B)e^{\Delta M(E_B - E_A)}p_{B\to A} \tag{2.27}$$

and following the same steps as in eq. 2.25 one easily finds

$$\frac{P(\Delta E)}{P(-\Delta E)} = e^{\Delta M \Delta E} \tag{2.28}$$

The beauty of this derivation is that we do not need an external field to act on the system, but the population is perturbed from its equilibrium by simply lowering the temperature, or increasing its size. One can also study the validity of detailed balance in the glassy phase, since the system can be let equilibrate at a size M which correspond to a liquid phase, and only after that the glass phase is entered by a jump in the population size. However, the main disadvantage of such an approach is that in the glassy phase the relaxation time t_α is no more time-independent, and the correct time that should be waited in the simulations for two populations to be uncorrelated is not easily estimated.

2.3 Phenomenology of population thermodynamics

In this final part of the chapter, we will exploit the thermal correspondence to give new insights on the evolution of populations. Indeed, now it should be clear, for example, that bottlenecks in a population will give the same consequences as temperature spikes in glasses. Moreover, we can suggest that memory effects can arise, when a population is restrained to a size at which it was constrained for a long period before. Or we can figure out how to engineer sets of chemostats in order to speed up the evolution of bacterial colonies in an experiment. And we can understand how a fluctuating environment can limit the increase of fitness to a given threshold.

2.3.1 Kovacs effect

A two time-scale separation of the kind we saw in section 2.2, is at the basis of the explanation of a phenomenon studied in structural glasses by Kovacs [7] in the 60's, and later reproduced in computer simulations [73]. The experimental protocol is the following. A liquid system is considered, and quenched down to a temperature T_1 close to the glass transition, and let relax (but not equilibrate). A second change in the temperature, $T_2 > T_1$ is then performed, when the system has relaxed to the energy that will correspond to the equilibrium at T_2. Then, if only one time-scale was present, one would expect that the system, by finding itself already at the good energy for equilibrium, will stay still. Instead, what one typically sees is a sudden increase in the energy, followed by a slower relaxation to lower energy values. While surprising at its discovery, this behaviour has a simple explanation in terms of a two (or more) time-scale separation. While a $T = T_1$, the system is in (metastable) equilibrium, for what concerns both the fast thermal time-scale and the slower configurational one. When the system is heated up to $T = T_2$, the fast time-scale immediately equilibrates to the new temperature, and this means that thermal fluctuations will cause the total energy to increase. On the other hand, the slow dynamics has no time to relax in the immediate, and the relaxation at the level of the configurations takes more time, causing the total energy to relax on longer time-scales.

Let us transfer this reasoning in our population dynamics context. A large-size M_1 population, after some relaxation, will get trapped in one maxima of fitness, being strongly localized. If the number of individuals is suddenly decreased to some value M_2, the selective forces will become weaker, and an immediate decrease of the population fitness will take place, as the distribution will become wider around the peak. However, the population will be able to travel away from the peak, and on the long run higher peak will be visited, and the fitness will start to increase again. This behaviour is indeed found when we apply the $M_1 \to M_2$ protocol we just described. It should not also be surprising that the smaller the M_2 value, the more the fitness will initially decrease, since the instantaneous de-localization effect will be stronger, and the instantaneous population distribution wider (and consequently less fit). The Kovacs effect, for a shift in M, is showed in fig. 2.10(left).

We have seen that the relaxation in the correlation presents the emergence of a

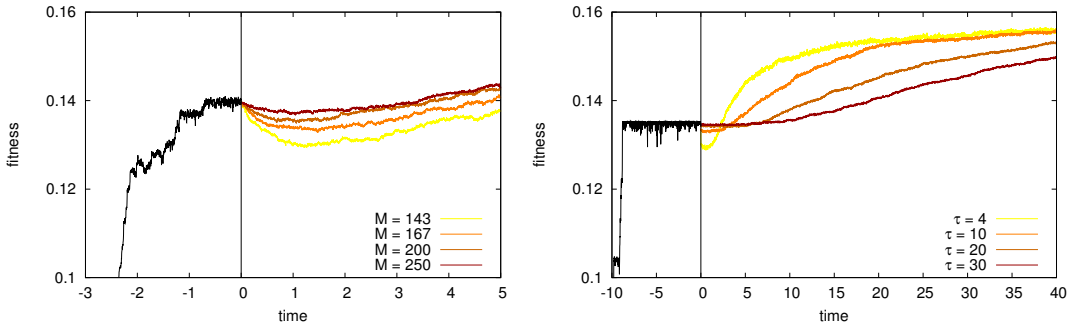

Figure 2.10: An example of the Kovacs effect for a population of XORSAT. In the left panel a population quenched at very low temperature, M_q=1000, undergoes a bottleneck at times $t = 0$, shrinking to $M = \{143, 167, 200, 250\}$. In the right panel is the mutation rate that, starting from a value $\tau = 40$, is increased to $\tau = \{4,10,20,30\}$. In both cases, an immediate decrease in fitness is obtained, followed by a slow increase, that leads the system to be fitter than before the switch.

time-scale separation even in the decrease of the mutation rate. Indeed, one can obtain a similar Kovacs effect even after a transition $\tau_1 \to \tau_2$, with $\tau_1 > \tau_2$. The results of simulations are showed in fig. 2.10(right). Again, a lower value of τ_2 causes, in the immediate, the fitness to decrease more.

Memory effects Along with the Kovacs effect, other glassy features due to the existence of several time-scales can be borrowed in the context of population dynamics. The concomitant presence of different processes, acting on different time- and length-scales, may cause the system to experience and show some memory effects [74]. One can see them experimentally in spin glasses, upon studying their a.c. susceptibility [75], by performing the following temperature protocol. Starting at a temperature T_0, the system is cooled down slowly, to a temperature T_1. Then, the temperature is kept fixed, while the systems optimizes and decreases its susceptibility. After a given time, the process of annealing is started again, and the system is cooled down to a temperature T_2. During this time, the system susceptibility increases to reach the annealing curve it would have followed without the stop at T_1, and then decreases by following the curve. The fact that the dynamics following the equilibration at T_1 is the same as if this equilibration had not taken place, is referred to as *chaos* effect. But then the temperature is taken up again, slowly, from T_2 to T_0, and one even more surprising thing happens. When a temperature $T = T_1$ is reached, even without a stop in the heating procedure, the system somehow "remembers" that it had optimized at that temperature, and there is a drop in the susceptibility, that decreases almost instantaneously to the value it had after the equilibration. The temperature protocol and its effects on the susceptibility are sketched in fig. 2.11.

Since computer simulations are at the moment not able to reproduce these features, we did not try to replicate them with our XORSAT population, but it is not unrealistic

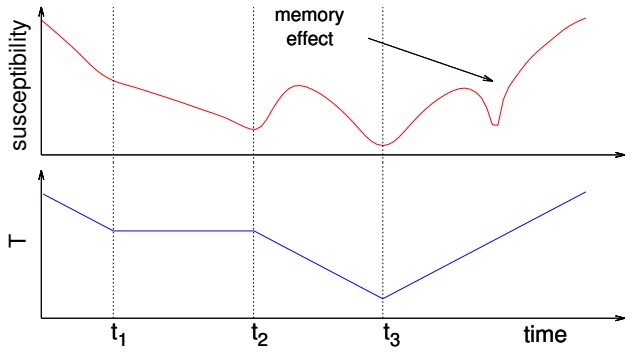

Figure 2.11: Bottom curve shows the temperature protocol. The temperature is cooled down from T_0 to T_1 in a time t_1, then the temperature is kept constant until t_2, and from t_2 to t_3 is lowered down to T_2. After t_3, the system is heated from T_2 back to T_0, without stasis. The behaviour of the susceptibility in correspondence of the temperature changes is sketched just above and described in the text.

to imagine that the thermal protocol described before will produce the same memory effects in case of a population, with the role of T replaced by the population size. Such a behaviour could also provide insight on the history of a population, in the case it has undergo period of stasis in its growth in size. If one varies the size of the present population, one should see a sudden increase in the fitness every time the size is the same of that maintained during a stasis period.

2.3.2 Parallel tempering

The concept of parallel tempering was invented in the context of computer Monte Carlo simulations [76]. A problem of such simulations is that they operate at fixed temperature T, sampling over the space of configurations. The system is made evolve by accepting or discarding its configuration according to some rules (typically the Metropolis algorithm), such that the probabilities of transition from one configuration to another one satisfy detailed balance. This condition, together with the ergodicity of the process (namely all the configurations might be visited in finite time, and not periodically), guarantees that the simulation will eventually sample the equilibrium distribution. However, and at this point this should not result surprising for the reader, it may happen, especially at low temperatures, that the system finds difficulties in sampling, in short time, the whole space of configurations, since it remains stuck for long times in metastable states. This will not be the case for high T simulations, that have a much greater capability of escaping such local minima. The basic idea for parallel tempering can be summarized this way: use systems at high T to create configurations that are then made evolve at low T.

The way this is done in practice is the following. One takes K realization of a physical system, at different temperatures, $T_1 < T_2 < ... < T_K$, make them evolve according to

a standard Monte-Carlo method and, from time to time, operate a switch between two configurations at two different temperatures (or switch the temperatures). The switching probability that one could use is given by the Metropolis algorithm, namely one passes from one old configuration a to a new configuration b with a probability given by $Q = \min(1, p(b)/p(a))$, with $p(a)$ and $p(b)$ given by the usual Boltzmann weight. Now, the different realizations are independent, so the joint probability is just the product of the single ones, and so a switch between configuration i at T_i with configuration j at T_j is given by

$$Q = \min\left(1, \frac{e^{-\beta_i E_j} e^{-\beta_j E_i}}{e^{-\beta_i E_i} e^{-\beta_j E_j}}\right) = \min\left(1, e^{(\beta_i - \beta_j)(E_i - E_j)}\right) \tag{2.29}$$

The choice of this probability is dictated by the request of having detailed balance in the process, in order to guarantee that the final distribution will be the equilibrium one. Since we are dealing with Markov processes, that is processes in which there is no memory of previous configurations, but only the actual one will determine the dynamics, we are assured that a configuration, put in a low temperature T when sampled from an higher temperature T', will behave just as if it was sampled at temperature T. Of course, for the exchange to be accepted with the rule of eq. 2.29, given the exponential factor within, the two energies of the configurations should not be too different, and for that to be possible it must be that the two temperature are not too far away from each other (otherwise the energy distribution will not even overlap). Moreover, one wishes not to have too many temperatures in the system, in order to reduce the computational cost, but on the other hand it is important to span a significant range of temperature. The number of realizations, the value of the temperature to use, and also the frequency at which switches should be attempted is an open issue, and we will not be concerned about it.

Our interest here, after having introduced the rationale of parallel tempering in computer science, is to devise a similar procedure for speeding up the evolution in biological systems. For small populations, a reasonable value of the mutation rate is sufficient for sampling a good amount of evolutionary solutions, and to explore a relevant portion of the fitness landscape in some finite time. However, as the population grows, selection forces constraint the population around local maxima, and evolution can be stuck for long times. We see that we have to deal with the same problem of the difficulty of sampling that a Monte Carlo simulation at low temperature has. But if we recall our interpretation of population dynamics in term of a thermal system, we can imagine that a biological parallel tempering will provide us a solution.

Indeed, let us take K chemostats, containing population of sizes $M_1 > M_2 > ... > M_K$. If the mutation rate is not too high, we know that each one of them will sample fitness according to an equilibrium distribution given by eq. 2.4, since the evolution will satisfy detailed balance. We can thus perform a swap between two populations, with size

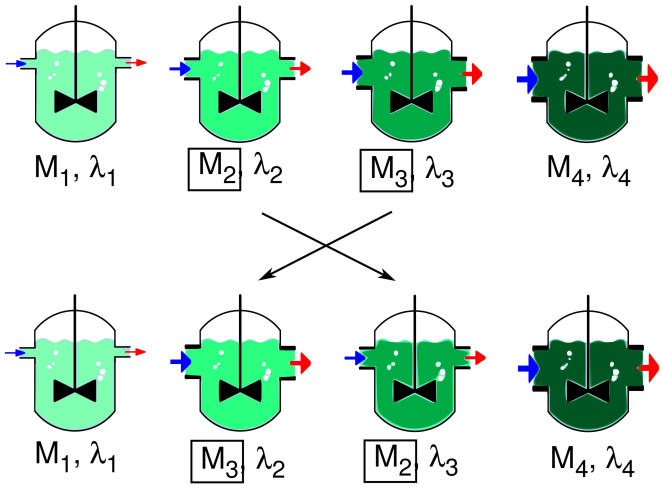

Figure 2.12: Parallel tempering in an experimental setting. Several chemostat are prepared, containing different population sizes M_i, controlled by means of the regulation of the in- and out-fluxes. Every now and then, two population belonging to different chemostats are exchanged, according to the rule of eq. 2.29.

λ_i and λ_j, and sizes respectively M_i and M_j, by accepting it with a probability:

$$Q = \min\left(1, \frac{\lambda_j^{M_i}\lambda_i^{M_j}}{\lambda_i^{M_i}\lambda_j^{M_j}}\right) \tag{2.30}$$

It is clear that in a biology laboratory what will be done is the swap in the population sizes, by changing the in-flux and the out-flux in the chemostat so that the size of one population is reduced and that of the other one is increased. The procedure is sketched in fig. 2.12.

Of course the increase and decrease in population size should be fast enough so that no mutations occur in the meantime, but from our study of the successional mutations regime, eq. 1.2.2 we know that periods of competition will be short compared to the total evolution time. With this choice of the transition probability, as in the previous case, we are assured to reach the equilibrium distribution by detailed balance.

Another way of implementing the parallel tempering mechanism is to make use of the invasion probability, eq. 2.1. For a given population size M, we know, given two types A and B, that the ratio of the two processes, A invading B and the opposite, are provided by eq. 2.2. Now, let us consider two chemostats, i and j, containing two species A and B. We can denote the probability of invading A by B in chemostat i, and invading B by A in chemostat j as $P(i : A \to B \quad \text{and} \quad j : B \to A)$. The probability of such an event, divided by the probability of its opposite, gives us (using eq. 2.2)

$$\frac{P(i : A \to B \quad \text{and} \quad j : B \to A)}{P(i : B \to A \quad \text{and} \quad j : A \to B)} = \frac{\lambda_j^{M_i}\lambda_i^{M_j}}{\lambda_i^{M_i}\lambda_j^{M_j}} \tag{2.31}$$

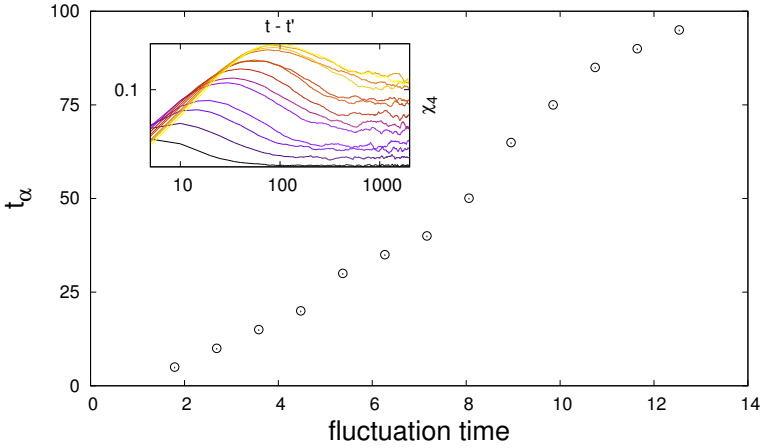

Figure 2.13: The value of the relaxation time t_α in function of the fluctuation time t_{env}. In the inset, χ_4 curves for different t_{env}, lighter curves corresponding to higher values.

which is exactly eq. 2.30. We have then a direct way to implement the parallel tempering. Every time we decide to try a swap, we duplicate the chemostats A and B. Then one insert one individual of A in the new B' population, and one B in A'. If both are fixating, we substitute A with B' and B with A', otherwise we discard the newly created samples. Notice that in this way we do not need to know the fitnesses of λ_A and λ_B, as the system will tune itself to swap with probability given by eq. 2.31 naturally.

2.3.3 Rejuvenation in fluctuating environment

The last aspect we will investigate in this context of thermal populations is the property of rejuvenation. We have seen that dynamics in glasses is dominated by extremely slow relaxations, due to the difficulty of optimizing in an extremely rugged landscape, where the huge number of metastable states gives rise to entropic barriers difficult to overcome. In general, the optimization problem is extremely hard to solve, and equilibration takes place in extremely long, practically infinite, time-scales.

But what will happen if the time available for the system to relax is finite? Indeed, let us consider the case where the energy landscape is not fixed, but it is instead slowly changing. After some time, we can expect that the landscape will be totally different from the original one, and so the configuration acquired by the system when relaxing in the old landscape will result to be totally unoptimized in the new setting [77]. In other words, relaxation has to start again. It is not surprising to see that the system behaves as if it did not age at all during the previous time. This property is called rejuvenation.

If there is a continuous change in the landscape, we expect the t_α necessary for relaxation to be bounded. Indeed, if the landscape decorrelates on a time t_{env}, the configurations of lower energy will typically be decorrelated in that time as well, and thus the system, by trying to optimize and reach the ground states, will decorrelate on time of the order of t_{env}. And since we know that the age of the system t_w is of the

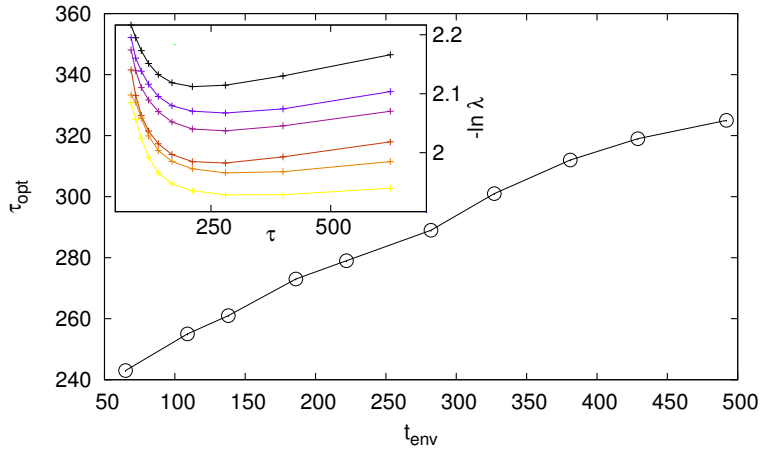

Figure 2.14: Inset: the average fitness acquired during evolution as a function of the mutation rate τ, for different values of t_{env} (darker colors correspond to larger fluctuation rates). Each curve presents a minimum, which indicates the value of $\tau_{opt}(t_{env})$. Main figure: the values of τ_{opt}, as a function of the environment fluctuation rate.

order of the relaxation time, but relaxation is essentially reset every t_{env}, we see that a glass will not be able to be older than $t_w \sim t_{env}$. Let us stress that even if several different glasses will show the same age, their properties will be different. Indeed, a glass that would have aged more in a static environment will have slower dynamics, and its relaxation will be less efficient in reducing the energy. We will come back to this issue in a moment.

We will investigate rejuvenation in our XORSAT population dynamics context. The change of the fitness landscape can be seen as a fluctuating environment, where different external parameters concur in changing the fitness of an individual (climate changes, food resources, incoming diseases, and so forth). We will implement the change in our simulations by modifying the XORSAT statement that provides (the logarithm of) the fitness function for an individual, eq. 2.17. Every time interval Δt, a given number of variables n in the clauses are changed randomly, by inverting their logic value. On average, the fitness landscape will then decorrelate on times of the order of $t_{env} \sim 3\alpha N \Delta t/n$. As a measure of the decorrelation time, we can use the t_α, computed by looking a the fluctuations of the correlation, χ_4, as already described in subsection 2.2.2. From what we said before, we expect $t_\alpha \propto t_{env}$, which is exactly what fig. 2.13 shows. A population in a rapidly fluctuating environment will decorrelate faster than a population in a quasi-static one.

One can also evaluate the effects of rejuvenation by looking at the relaxation of the fitness of a system, while the environment is changing according to different values of t_{env}. Since the time available for optimization is of the order of t_{env}, it should be clear that for slower fluctuations the average fitness will result to be higher with respect to the case of faster changing environments. The system is said to be "surfing" over the

metastable states that require a relaxation time longer than t_{env} to be reached, and therefore the energy will seem to reach a plateau of optimization [78]. The values of such plateau are plotted in the inset of fig. 2.14. Notice that for different values of the mutation rate, the adaptation is different. Indeed, another aspect that one can take into consideration is that having a fluctuating environment can lead to a selection in the size and mutation rates of a population [79]. Let us focus on the latter. We know that, in principle, lower mutation rates $1/\tau$ contribute to have a more localized population, thus more fit, and upon waiting long enough, the system will also be able to climb higher and higher peaks. However it is clear that, if the time available to optimize is not infinite, as in the case of a fluctuation environment, this slowness in improving the fitness will have a cost and will be selected against. One can thus expect to have, for a given t_{env}, an optimal value for the mutation rate, $\tau_{opt}(t_{env})$, that will guarantee that the system will exploit all the timespan it is available to relax, but not more, so to reach the best possible fitness [80]. We can think of this condition loosely by requiring $t_\alpha(\tau_{opt}(t_{env})) \sim t_{env}$. The effect of such a selection can be seen in the fact that the curves in the inset of fig. 2.14 present a minimum, which is different for every given value of t_{env}. The mutation rates for which these minima are reached represent the τ_{opt}, and we can see their evolution with the environmental change rate by looking at fig. 2.14.

Chapter 3

Coupled models

Oh Marilou!
I want you to know I love you
I'd never tried to hide
We're always side by side
Oh Marilou!
I just said that I love you
why don't you understand
you need to take my hand
Oh Marilou!
D'you hear I said I love you
I'll stay in front of you
But I'll help you make it through

A Boom Root
Song for Marilou

In this chapter, we will study the evolution of an adapting population, with particular attention to the case when its fitness is coupled to that of other adapting populations.

Chapter Teaser

- what is the Random Energy Model, and what it has in common with an evolving monomorphic population, 3.1;
- how two interacting populations will see their adaptative time-scales separate drastically, 3.2.1;
- how an hierarchy of adaptation is naturally established in several interacting populations, 3.2.2;
- how one population can evolve faster, exploiting the adaptation of another population, by exchanging and acquiring fitness from it, 3.2;

- how the exploited population, capable of adapting faster, might be forced to undergo selectively disadvantageous changes, even in the infinite population size limit, 3.2.

3.1 Fitness REM

We have seen in chapter 1 the presence of several regimes of evolution of an adapting population. In the successional mutations regime (see subsection 1.3.1), we are able to solve exactly the problem at equilibrium, finding an expression for the probability distribution of the fitness, eq. 2.4, since detailed balance is assured by the transition probabilities. We have seen, however, in chapter 2, that in many cases this equilibrium can be extremely difficult to reach, given the complexity of the optimization process. Therefore, one might wonder what can be said about the behaviour of a system before reaching equilibrium. In this chapter, we will investigate how a system increases its fitness alone, and later the case of several systems that are put in the condition of interacting. As we will see, things will drastically change in the latter case, as an even small coupling will generate a well-defined hierarchy in the interacting systems.

In the following of this chapter we will be concerned only about the successional mutations regime, as it allows us to simplify things enormously. Indeed, we have seen that in this regime the evolution is constituted by a series of long periods of stasis, during which the population is basically monoclonal, interspersed by periods of fast competition between two lineages, lasting until one of the two reaches fixation. This suggests the construction of a meta-model, in which the population is considered as a single entity, and evolution is reduced to a one body problem. We will therefore identify the "state" of the population as the fitness of its dominant lineage, λ, or equivalently its energy $E = -\ln \lambda$ (defined as in eq. 2.5). The population size M will find its significance in playing the role of the external temperature $T = 1/M$. We already know from section 2.1 that the equilibrium probability distribution will be the one in eq. 2.4, namely the one generated by the detailed balance condition satisfied by Moran transition probabilities.

In principle, however, we do not know what λ exactly is. As usual, let us try to make the fewest number of assumptions. Consider an individual, with its genome. For simplicity, let us suppose that its genome is constituted by N genes, each of which can be present in only two allelic variants. The number of possible genomes is then 2^N, and it is rather unlikely that such a huge number of genotypes can be representatively sampled, even by huge population, since for all relevant biological systems $M \ll 2^N$. The treatment that one should use is then stochastic, and this will be indeed our approach. If we consider all the genes as giving a small, independent contribution to the fitness [81], we are assured by the theorem of central limit that the final fitness distribution will have a Gaussian form. Such a system, however, corresponds exactly to a well-renowned model, the Random Energy Model, introduced by Derrida in the 80 [82]. Since it will turn out to be useful in the following of our population oriented analysis, let us open a short parenthesis on pure statistical physics and consider some features of the REM.

3.1.1 REM

The Random Energy Model has been introduced as the first example of disordered model that exhibits a phase transition. Disordered model means that the energy of the system should not be considered as a deterministic function of some parameters, but rather a random variable. A typical example of a disordered system is a spin glass, where the magnetic moments of molecules inside the solid are in random positions and random orientations, so that for every different actual realization of such a glass the configurations are random. If one has to treat statistically a system like this one, such a stochasticity in the configurations cannot be ignored. Even if one could calculate, for a given configuration, the value of the energy of the system, the fact that in general the configuration of a given realization is not known is preventing to use the usual thermodynamic approach. What we can do, in turn, is to make some assumptions about the probability of having a given energy, and treat the energy as a stochastic variable. The evolution of the system will then be that of a classical thermodynamic system, with the equilibrium distribution given by the Boltzmann factor, $\exp(-\beta E)$, with the only (important) difference that E is not a number but a stochastic quantity.

The Random Energy Model works as follows. We consider N spins, each one giving an independent contribution, and therefore, as said before, the probability distribution for the energy will be Gaussian, i.e.

$$p(E) = \frac{1}{\sqrt{2\pi N\sigma^2}} e^{\frac{E^2}{2N\sigma^2}} \tag{3.1}$$

Since the total number of spin configurations is 2^N, the number of states in the infinitesimal interval $[E, E+\delta E]$ will be $S(E) = 2^N p(E)$. A fundamental property of the REM, which is crucial for calculations done on disordered system, is the fact that it is *self-averaging*. This means that the relative variance of the energy, averaged over the samples, $\langle (E - \langle E\rangle)^2\rangle / (\langle E\rangle)^2$, goes to zero as $N \to \infty$. In other words, if large enough, a single realization is representative of all the samples. One will then have that all metallic alloys, no matter their precise microscopic organization, will have the same magnetic properties, provided that the sample are macroscopic. Or, the other way around, we can be confident that make computations about the average properties of the system is enough in order to understand the behaviour of a single sample.

In order to stress the extensive character of E, let us define $u = E/N$, the energy density (the term density will be dropped in the following, but we will remember that we are talking of an intensive quantity). The entropy becomes

$$S(u) \sim e^{N(\ln 2 - u^2/2\sigma^2)} \tag{3.2}$$

The number of configurations for a given energy cannot be smaller than 1, and therefore there exists a value for the energy, which we will call *freezing* energy u_{frz}, below which the number of configurations is less than one. The number of configurations having $u < u_{frz}$ can for all practical purposes be considered zero, as it is exponentially suppressed in N. We can estimate the freezing energy easily, by means of

$$S(u_{frz}) \sim 1 \qquad \Rightarrow u_{frz} \sim -\sqrt{2\ln 2\,\sigma^2} \tag{3.3}$$

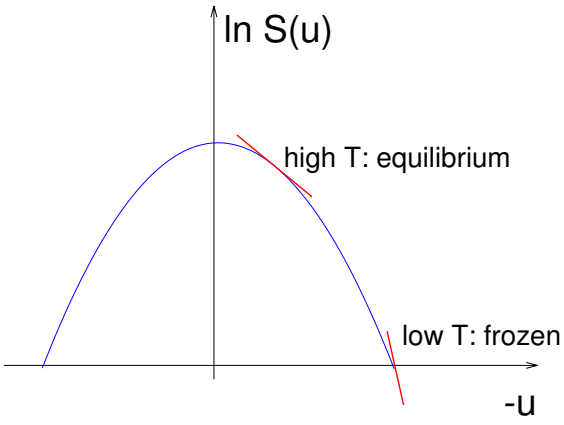

Figure 3.1: A sketch of (the logarithm of) the entropy distribution as a function of (minus) the energy in the REM. The temperature represents the slope of the curve at a given energy.

The energy will decrease, but never below the freezing value of $-\sqrt{2\ln 2\,\sigma^2}$. To compute the actual value of the energy, for a given temperature, we should use the usual Gibbs measure, with the addition of the term related to the entropy of the configurations. In other words, the probability to obtain a given energy will be given by

$$P(u) \sim e^{S(u)} e^{-\beta N u} = e^{N(\ln 2 - u^2/2\sigma^2 - \beta u)} \tag{3.4}$$

Again, since we are facing exponentials in N, we can consider that the actual energy will be the one maximizing the probability $P(u)$, thus satisfying

$$\beta = -S'(u) = -\frac{u^*}{\sigma^2} \tag{3.5}$$

While used to find u^* in this context, eq. 3.5 can in principle be used as a definition for a temperature of a system at energy u^*. For the moment, however, we are more concerned about finding the equilibrium energy u^*. We have two possibility, either $u^* > u_{frz}$, and in this case the system will evolve, reducing its energy, until it reaches the equilibrium value, either $u^* \leq u_{frz}$. In this second case, the system cannot take an energy lower than u_{frz}, no matter the value of its temperature. Therefore, we will say it is frozen, as it is forced to stay in the only configuration available at the lower energy. By computing the free energy density, one can see that a second order transition happens at $\beta_{frz} = -u_{frz}/\sigma^2$, as for $\beta > \beta_{frz}$ the free energy stops decreasing with the temperature, and assumes a constant value.

The definition of β as given in eq. 3.5 has an immediate geometric interpretation, look at fig. 3.1. Since it is the derivative of the entropy, it corresponds to the slope of the tangent of the entropy curve, at the given u value. We can then see graphically that the systems cannot reach zero temperature (a perpendicular tangent), as the slope value cannot be greater than that of the tangent of $S(u)$ at β_{frz}.

3.1.2 A single model

The brief parenthesis on the REM does turn out useful in our case. Indeed, if we consider that fitness arises as a sum of independent contributions of N genes, adding our knowledge on the Moran process and its equilibrium probability, we can easily claim that the probability distribution for the energy density u, will be

$$P(u) \sim e^{S(u)} e^{-\beta N u} = e^{N(\ln 2 - u^2/2\sigma^2 - \beta u)} \tag{3.6}$$

the same as the Random Energy Model [83, 84]. Therefore, we will have a freezing energy given by $u_{frz} = -\sqrt{2 \ln 2\, \sigma^2}$, and the system will try to optimize by reaching the equilibrium energy according to $u_{eq} = \max(u_{frz}, -\beta\sigma^2)$. The equilibrium temperature, of course, needs to be intended in the population dynamics framework, i.e. as the inverse of the population size.

We will suppose that the fitness, as in a disordered system, is totally epistatic. This means that, from every state λ, every other λ' can be reached. We will use primed quantities to indicate the new state reached by an evolutionary jump. One can then wonder whether the equilibrium value will be reached immediately (in a single jump) or not. Before doing some calculations, we can speculate about the relaxation process. Starting from a given λ, we know that the probability of going backward is exponentially suppressed in M, as one can immediately see by recovering the Moran probability of implantation of a colony, eq. 2.1. On the other hand, however, jumping towards higher fitness is proportional to the fitness advantage that will be obtained, eq. 1.13, but the number of states, going to lower λ, decreases exponentially in N. For large populations, then, we will expect that, starting from a moderate value of λ, the system will increase its fitness regularly, but by means of little steps $\delta\lambda$ [85]. In the following, since we will use the analogy with the Random Energy Model, we will be using the energy density u rather than the fitness. Adaptation will then correspond to decreasing the energy of the system.

In order to estimate the average energy change of a jump, $\langle u' - u \rangle$, we need to consider the number of actual configurations with energy u, times the probability of going from u to u', that is

$$\langle u' - u \rangle = \frac{\int du' e^{S(u)} p_{u \to u'} (u' - u)}{\int du' e^{S(u)} p_{u \to u'}} \tag{3.7}$$

and we can approximate the transition probability by $p_{u \to u'} \sim (u' - u) \chi_{[u' < u]}(u')$, where χ is the characteristic function. The jump is then given by

$$\langle u' - u \rangle = \frac{\int_{-\infty}^{u} du' e^{S(u)} (u' - u)^2}{\int_{-\infty}^{u} du' e^{S(u)} (u' - u)} = \frac{2\sigma^2}{Nu} \tag{3.8}$$

Every time a jump happens, this is its average value. In order to obtain the evolution of the fitness, we need to compute the average time elapsed between two successful mutations. The probability that a mutant invades and fixate in a wild-type of energy u,

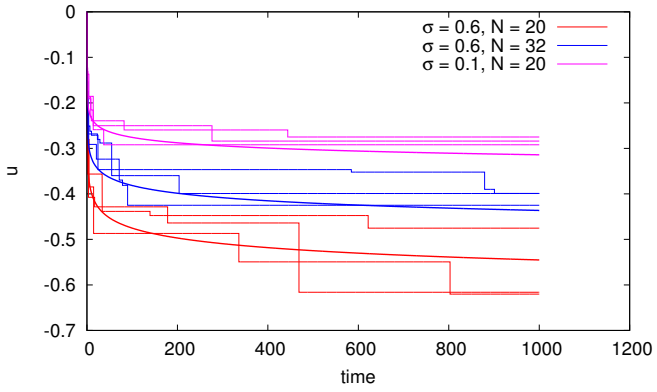

Figure 3.2: The evolution of one population cooling down, for different values of (σ, N). Thick, smooth lines represent solutions of eq. 3.11, while thin, stepped lines are simulations of coarse grained population, evolving through Moran model probabilities. Data are always in agreement with the predicted behaviour, for all the parameters considered.

$p_{inv}(u)$, can be computed for our disordered model as the average of $p_{u\to u'}$ over all the possible new configurations, that is

$$p_{inv}(u) = \frac{\int du' e^{S(u)} p_{u\to u'}}{\int du e^{S(u)}} = \frac{\sigma^3}{\sqrt{2\pi N} u^2} e^{-\frac{Nu^2}{2\sigma^2}} \tag{3.9}$$

For a population of size M, whose individuals mutate every τ, the rate of attempted jump is M/τ. Then, the time elapsing between two successful jumps is given by

$$\tau_{inv} = \frac{\tau}{M} p_{inv} \tag{3.10}$$

From eq. 3.9 we can then see that the time in-between two jumps is exponential in N. This should not be surprising, since as we said before the number of states decreases exponentially in N as we go down in energy. We can finally find an equation for the evolution of the energy (or the fitness), of our simple model of a low-mutating, epistatic fitness population:

$$\frac{d\,u}{dt} = \frac{\langle u' - u \rangle}{\tau_{inv}} = \frac{\sqrt{2}\, M \sigma^5}{\sqrt{\pi} N^{3/2} u^3 \tau} e^{-\frac{Nu^2}{2\sigma^2}} \tag{3.11}$$

The fact that this speed of adaptation is linear in M should not be surprising. We are in the successional mutations regime, and our result is consistent with what we obtained in section 1.3. We can see that eq. 3.11 is in good agreement with simulation data, see fig. 3.2.

3.2 Interacting models

In the following, we will be interested in the evolution of interacting systems. One can consider systems as co-evolving populations, or blocks of genomes contributing almost

independently to the fitness [86, 87]. We will start with the simplest case of two coupled systems, that will show a far from trivial behaviour. We will then show what happens when three systems are put in contact, and make some conjectures about the general situation of several interacting systems.

3.2.1 Two systems

We will treat the fitness as multiplicative. This means that, for two systems with fitness λ_1 and λ_2, the total fitness will be given by $\lambda_{tot} = \lambda_1\lambda_2$. The energies will then be additive, $u_{tot} = u_1 + u_2$. However, such a choice alone is not particularly interesting, as the probability of jumping for a system will be the same as if the other system was not present. The Moran probability for fixation of an invading mutant, eq. 1.11, contains the ratio $\lambda_{tot}/\lambda'_{tot}$ for this double system. If we suppose to try an implantation $u_1 \to u'_1$, jumping with system one only, since $u'_2 = u_2$, we have that $\lambda_{tot}/\lambda'_{tot} = \lambda_1/\lambda'_1$. The probability of fixation is then the same as if system one was uncoupled. To obtain a non trivial behaviour, we have to impose by hand an interaction term. The analogy with physics suggests to introduce it by defining a magnetization, $m = s_1 \cdot s_2$, defined as the product of the spins (i.e. genes) of the two systems, and add to the energy the quantity

$$u_{int} = -\epsilon \sum_{i=1}^{N} s_i^1 s_i^2 = -N\epsilon m \tag{3.12}$$

We are then interested in the number of configurations to which a system can jump to. The total number will be, taking e.g. system one as the jumping one, given by

$$e^{NS(u',s'_1)} = \sum_{\{s'_1\}} e^{-\mu(s'_1 \cdot s_2 - Nm')} e^{-\frac{Nu^2}{2\sigma^2}} \tag{3.13}$$

where μ is introduced as a Lagrange multiplier. A rapid calculation, see appendix A, leads us to a nicer expression for the entropy S, in terms of the magnetization m, instead of the spin configurations $\{s_1, s_2\}$, given by

$$S(u, m) = -\frac{1+m}{2} \ln\left(\frac{1+m}{2}\right) - \frac{1-m}{2} \ln\left(\frac{1-m}{2}\right) - \frac{u^2}{2\sigma^2} \tag{3.14}$$

Since we are interested in the evolution of the population, that is in its out of equilibrium dynamics, we will consider the external temperature to be zero, or the population to have infinite size, so that a jump to a less fit population will be impossible. The forward probability will be of order 1, but it will be exponentially suppressed in N by the entropic contribution. Please note that what has to decrease in a jump is not the energy of a single system, but the total energy, defined as

$$u_{tot} = u_1 + u_2 - \epsilon m \tag{3.15}$$

In a single jump, the energy of the non-jumping system will remain the same, so it will be the sum $u' - m'$ that will be lowered. There might be cases where the single energy

contribution u' is higher than before, being compensated by a larger decrease in the magnetization m'. In any case, we will expect that the two systems will decrease their energy, slowly, until they will freeze, i.e. the number of configurations will be of order one, or $S(u_{frz}, m_{frz}) \simeq 0$.

With a jump, a system will typically go to the values of (u', m') that maximize its entropy. It is useful to parametrize such values by introducing an effective temperature β_{eff} [88], in the same spirit of the REM, eq. 3.5, maximizing the (logarithm of) the probability, $\beta_{eff}(u' - \epsilon m') - S(u, m')$. In other word, β_{eff} satisfies the saddle point equations

$$\beta_{eff} = -\frac{u'}{\sigma^2} \qquad \longrightarrow \qquad u' = -\beta\sigma^2 \tag{3.16}$$

$$\epsilon\,\beta_{eff} = -\frac{1}{2}\ln\left(\frac{1-m'}{1+m'}\right) \qquad \longrightarrow \qquad m' = \tanh(\beta\epsilon) \tag{3.17}$$

In the following, we will drop the suffix, so $\beta_{eff} = \beta$, but we will distinguish between β_1 and β_2, to refer to the two systems. There will be no confusion with the external temperature, that we suppose zero and will not appear in the expressions. With this definition of effective temperature, we will say equivalently that the system will reduce its energy, or cool down in (effective) temperature. Again, this temperature has nothing to do with the population size (that is infinite, as the external temperature is zero), and cooling should not be interpreted in the same sense of increasing the population size, as in chapter 2.

To understand to which state the system will jump to, we can follow a simple reasoning. The entropic contribution will push the new energy u'_{tot} to be the maximum possible, provided that it is not lower than the current one u_{tot}. Now, supposing that we were jumping with system one, we have two possibilities. In the first case, the magnetization is coupled with system two, meaning that $m = m(\beta_2)$. We can then find the new β'_1 by asking that it satisfies the equation

$$u'_{tot} \equiv u_1(\beta'_1) - \epsilon m(\beta'_1) = u_1(\beta_1) - \epsilon m(\beta_2) \tag{3.18}$$

In doing this, we are neglecting the sub-exponential corrections that should be present in this equivalence. The jump in u_1 is macroscopic, of the order of $\epsilon(m(\beta'_1) - m(\beta_2))$, so they are not so relevant. Such an assumption is however incorrect in the second case, when the magnetization is coupled to system one, $m = m(\beta_1)$. In this case, eq. 3.18 will give us $\beta'_1 = \beta_1$, trivially. What we will suppose then is that jumps of system one will be extremely small. Since a jump $(u_1, m(\beta_1)) \to (u'_1, m(\beta'_1))$ does not involve system two, we are considering a dynamics substantially identical to the one presented in subsection 3.1.2, where we found that the jumps in energy were $O(1/N)$, see eq. 3.7. We will not compute here the precise magnitudes of such jumps, since their precise value is not relevant to our analysis, but we will denote them in the following with δ_{11} or δ_{22}, depending on which system is jumping. As we did in subsection 3.1.2, we can provide differential equations for the evolution of the two energies u_1 and u_2, in the same way

we did when we found eq. 3.11. Indeed

$$\frac{du_1}{dt} = \frac{\epsilon}{\tau_{12}+\tau_{21}}(m_2 - m_1) - \frac{1}{\tau_{11}}\delta_{11}\frac{\tau_{21}}{\tau_{12}+\tau_{21}} \tag{3.19}$$

$$\frac{du_2}{dt} = \frac{\epsilon}{\tau_{12}+\tau_{21}}(m_1 - m_2) - \frac{1}{\tau_{22}}\delta_{22}\frac{\tau_{21}}{\tau_{12}+\tau_{21}} \tag{3.20}$$

where $m_a = m(\beta_a)$ and τ_{ab} is the time elapsed between a jump of a and the following jump of b. With this definition, during a time τ_{12} there is the possibility of making several jumps 11. In this sense, $\tau_{21}/(\tau_{12}+\tau_{21})$ computes the ratio of the total time during which the magnetization is coupled to system one, and dividing it by τ_{11} gives the total number of jumps of system one while $m = m_1$. Rather than computing the values of τ_{ab} and solving these equations, it is much more instructive to analyse the nature of the jumps, by simple first principles.

A time-scale separation mechanism In the following, we will, without loss of generality, consider $\sigma_1 < \sigma_2$. In the case of the parallel evolution of two non-interacting systems, this means that the temperature of system one will be smaller, and it will be generally colder. Indeed, if the system is started with the same fraction of configurations below the initial state, and jumps are taken alternatively by one or the other system, the number of configurations below each one will tend to be the same. This implies that at all times the effective temperature of the system with large σ is higher than the one of the system with more narrow distribution. We will suppose this to be true even for the interacting systems, and we will check self-consistently that this is the case.

In the following, a jump will be noted by $(a, \bar{b})$, indicating that system a is jumping, while the magnetization is coupled with b. We have four possible jumps:

- $(1, \bar{1})$. The jump will reduce the energy of system one, and decrease its magnetization. We will have $u_1' < u_1$ and $m_1' > m_1$, since u and m are both monotonic function of β, and the other possibility (u and m increasing) is to be discarded, since they would lead to an increase in u_{tot}. System one will then decrease its temperature, but the jump will be small, given by $\delta_{11} \sim 1/N$;
- $(2, \bar{2})$. For the same reasons as before, we will have $u_2' < u_2$ and $m_2' > m_2$. The temperature T_2 lowers, but only slightly, $\delta_{22} \sim 1/N$;
- $(1, \bar{2})$. The starting energy is $u_{tot} = u_1 + u_2 - m_2$. Since system one is colder, notice that $m(\beta_1) > m(\beta_2)$. We have four possibilities:
  a) $u_1' < u_1$ and $m_1' < m_2$. This is not possible, since $u(\beta)$ and $m(\beta)$ are monotonic, so we would have $m_1' > m_1$, and as we said $m_1 > m_2$;
  b) $u_1' > u_1$ and $m_1' < m_2$. This jump is not allowed, since we will have $u_{tot}' > u_{tot}$;
  c) $u_1' > u_1$ and $m_1' > m_2$. Possible;
  d) $u_1' < u_1$ and $m_1' > m_2$. Possible, but its probability is exponentially lower than that of the previous jump.

We can thus conclude that the jump will increase system one energy, and increase the magnetization. The jump in energy will be $\Delta u \sim \epsilon(m_1' - m_2) > 0$;

- $(2, \bar{1})$. The reasoning is the same as the $(1, \bar{2})$, but this time $m(\beta_1) > m(\beta_2)$ is not constraining, since we are jumping with β_2. The jump then will likely decrease the magnetization, and decrease the energy. Again, the jump in energy will be macroscopic, and of magnitude $\Delta u \sim \epsilon(m_2' - m_1) < 0$

For every couple of energies (u_1, u_2) for the two systems, or equivalently for every couple (T_1, T_2) of temperatures, we wish to know which one will be next to be jumping. This can be achieved simply by looking at the entropies corresponding to the states the systems will be jumping to. Let us denote $S_{a,\bar{b}}$ the entropy corresponding to a jump of system a, with magnetization coupled to b. We have four cases, $S(1\bar{1})$, $S(1\bar{2})$, $S(2\bar{1})$ and $S(2\bar{2})$, and in principle one should check the reciprocal relationship between these four. However, only two comparisons are interesting. Either m is coupled with system one, and then one should compare $S(1, \bar{1})$ with $S(2, \bar{1})$, either the magnetization is coupled with system two, and then one should compare $S(1, \bar{2})$ with $S(2, \bar{2})$. The system that will jump first will simply be the one with the higher entropy.

The entropies are computed, for every couple of values (T_1, T_2), by evaluating eq. 3.14 using the saddle point value of the new energy and the magnetization of the jumping system, provided by eqs. 3.16 and 3.17. When the magnetization is coupled to, say, system two, these new values of u_2' and $m(\beta_2')$ are computed simply by taking $\beta_2' = \beta_2$, since we know that the system will do only small jumps, and the entropy will not change, at leading order. For system two, the new temperature should be computed as the one satisfying eq. 3.18.

In fig. 3.3, we have a simulation of several realizations of the two systems evolution, in the (T_1, T_2) plane, with the indication of the line where $S(1, \bar{1}) = S(2, \bar{1})$ and $S(2, \bar{2}) = S(1, \bar{2})$. The initial magnetization is coupled to system one. In this zone we have $S(1, \bar{1}) > S(2, \bar{1})$, and so the evolution proceeds by means of small $(1, \bar{1})$ jumps, until the line $S(1, \bar{1}) = S(2, \bar{1})$ is reached. The temperature T_1 is accordingly decreased (movement to the left). Then, jumping of system two becomes as probable as jumping of system one. A jump $(2, \bar{1})$ is thus performed, and from what we said before the energy of system two is lowered, and so it is T_2. The jump is extensive, and takes the two systems away from the $S(1, \bar{1}) = S(2, \bar{1})$ line (downward). The next jump then has to be necessary $(1, \bar{2})$, since we are in the zone where $S(2, \bar{2}) < S(1, \bar{2})$. Again, this jump is extensive, but causes the system one to increase its energy, and its temperature T_1 (movement to the right). We are then back to the starting situation, magnetization coupled to system one and $(1, \bar{1})$ favoured on $(2, \bar{1})$.

We see that this process is highly asymmetric. The evolution can cross the $S(1, \bar{1}) = S(2, \bar{1})$ only by a small $(1, \bar{1})$ jump, but immediately the coupled system move away from this line, with two large extensive jumps. The fact that the $S(1, \bar{2}) = S(2, \bar{2})$ line is lying above the $S(1, \bar{1}) = S(2, \bar{1})$ one means, in this condition, that a $(2, \bar{2})$ jump will never happen. Every time system two jumps, indeed, we are in a situation where a jump with system one is favoured against another consecutive system two jump.

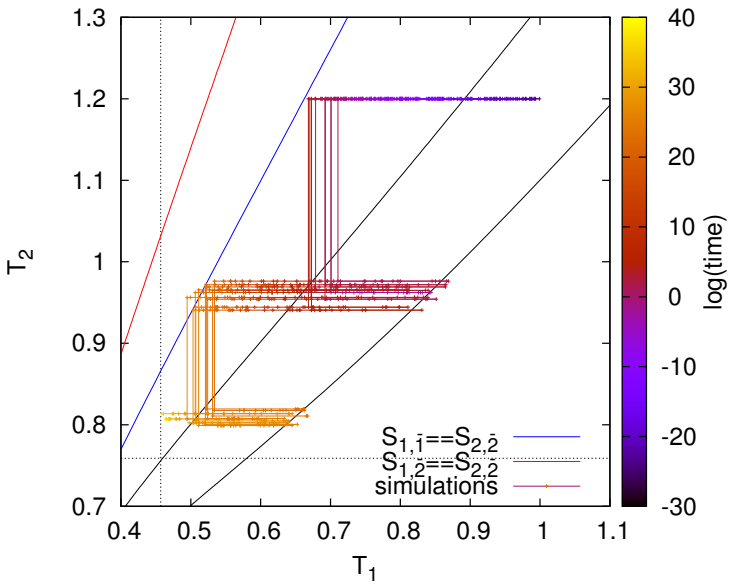

Figure 3.3: Several simulations of the evolution of the temperatures for the two coupled systems. Dashed black lines represent the freezing temperatures. The red and blue lines represent the values of (T_1, T_2) at which jumping with one system or the other becomes equivalent. Below the red (resp. blue) line we have $S(1,\bar{1}) > S(2,\bar{1})$ (resp. $S(1,\bar{2}) > S(2,\bar{2})$). Solid black lines are the expected extensive jumps of the system, $(2,\bar{1})$ and $(1,\bar{2})$. The simulations are in very good agreement with the theory.

It should be evident that this situation does not depend on the initial conditions, and every system of the kind we described, no matter the value of the parameters, provided that $\sigma_1 < \sigma_2$, will converge to this $[(many)left \rightarrow down \rightarrow right \rightarrow (many)left...]$ sequence of jumps. Indeed, even starting from a state where (T_1, T_2) is located into the $S(2,\bar{2}) > S(1,\bar{2})$ zone, the system will start moving downward with $(2,\bar{2})$ jumps, until reaching the $S(2,\bar{2}) = S(1,\bar{2})$ line. There, a $(1,\bar{2})$ jump is performed, but again downward, thus escaping even more from the $S(2,\bar{2}) > S(1,\bar{2})$ zone. After that, either we have crossed the line $S(1,\bar{1}) = S(2,\bar{1})$, and we are back to the previously described situation, either the system will proceed alternating $(1,\bar{2})$ and $(2,\bar{1})$ jumps, until the $S(1,\bar{1}) = S(2,\bar{1})$ line is crossed.

Several comments are needed. First, we can check that system one is systematically colder than system two, as their evolution happens above the $T_1 = T_2$ line. Second, and unexpected, there is a drastic time-scale separation, induced by the coupling. In order to make an $O(1)$ change in its internal energy, system one makes a huge number ($\sim N$) of jumps, each one changing its energy by $O(1/N)$, while system two makes a single, large jump. If a jump consists in an internal rearrangement of spins, we see that system one autocorrelation will decrease much faster than that of system two. Notice that this would have not be the case if the two systems were not coupled. Instead, in that case

they would have been jumping more or less with the same frequency, their temperatures being related by the requirement that the number of configurations below T_1 for system one is the same of those below T_2 for system two.

Finally, it is interesting to study the energy exchanges. In absence of the coupling term, the two systems will perform, alone, several small jumps in order to decrease their temperatures and equilibrate with the external temperature, which we set to zero. By doing so, they will decrease their internal energy, which we can think as being absorbed by an external bath. By switching on the coupling, the behaviour of the two systems change dramatically. System two does not communicate any more with the bath, since as we have seen $(2, \bar{2})$ jumps are not performed. Only system one communicates with the bath, by decreasing slowly its internal energy and the increasing the shared magnetization. This is crucial: when the magnetization reaches a certain threshold, system two can decrease its internal energy, by 'discharging' it into the magnetization. For system two is easier (in entropic terms, $S(2, \bar{2}) < S(1, \bar{2})$) to decrease its energy in this way than exchanging it with the bath. This additional energy temporarily 'stored' in the magnetic field is transferred, with the successive jump, to the internal energy of system one, that is forced to increase its temperature. It will then slowly start to cool down again, by transferring energy to the bath, until a new discharge will happen from system two to system one. We see then that a hierarchy has been established, and a net energy flow follows [system two $\rightarrow$ system one $\rightarrow$ bath], with the direct energy transfer going from system two to the bath not being performed any more.

The beauty of such a model is that all its features were almost unexpected. Nothing was put in by hand, the systems when decoupled followed a simple dynamics, but the introduction of a small interaction sees the generation of a time-scale separation and a drastic change in the energy flows. We have control only over three parameters, i.e. the two σ_1 and σ_2, and the strength of the coupling ϵ. The latter specifies the magnitude of the extensive jumps $(1, \bar{2})$ and $(2, \bar{1})$. When this is reduced, the effect is the one of forcing the evolution to happen closer to the $S(1, \bar{1}) = S(2, \bar{1})$ line. In the limit of $\epsilon \rightarrow 0$, the two lines $S(1, \bar{1}) = S(2, \bar{1})$ and $S(1, \bar{2}) = S(2, \bar{2})$ get close to each other, to collapse when there is no coupling, and the two systems evolve as independent.

Concerning the variation of the σ, we know that it is the system with the smaller σ that will be the cooler one, and therefore the one that jumps more frequently and communicates with the bath. Rather than their actual value, which can give rise only to quantitative differences, what is important is their relative magnitude, since it tells how the asymmetry of the process is realized. At the extreme case of $\sigma_1 = \sigma_2$ we will have no distinction between the systems, and evolution will proceed on the $T_1 = T_2$ line. By increasing σ_2, the line $S(1, \bar{1}) = S(2, \bar{1})$ will get tilted from the $T_1 = T_2$ line, and evolution will not be isothermal any more.

Limited jumps At this point one could argue that, in a realistic system, the magnetization might not in principle vary freely. Large spins rearrangements may not be possible, and a cut-off should be introduced. We will implement this requirement, by asking that if a system jumps from a configuration s to a configuration s', the two are

not too different, and satisfy

$$s \cdot s' > NC \tag{3.21}$$

where C is a parameter that controls the correlation between configurations of spins of one system before and after one jump. For $C = -1$, we are back to the previous situation of unconstrained jumps, while for $C = 1$ we would have that $s' = s$.

The total number of configurations is given by eq. 3.27, to which we add another Lagrange multiplier, $\tilde{\mu}$, in order to enforce our new constraint. We have

$$e^{NS(u',s'_1)} = \sum_{\{s'_1\}} e^{-\tilde{\mu}(s'_1 \cdot s_1 - NC)} e^{-\mu(s'_1 \cdot s_2 - Nm')} e^{-\frac{Nu^2}{2\sigma^2}} \tag{3.22}$$

Again, some algebra is needed to obtain an expression in which the spins do not appear explicitly, see appendix A. We have

$$2^N e^{-\frac{Nu^2}{2\sigma^2}} e^{\mu N m'} e^{\tilde{\mu} NC} e^{N/2[(1+m_o)\ln(\cosh(\mu+\tilde{\mu}))+(1-m_o)\ln(\cosh(\mu-\tilde{\mu}))]} \tag{3.23}$$

where m_o, the value of the magnetization before the jump, is defined as $m_o = s_1 \cdot s_2$. Once again, it is useful to introduce an effective temperature β, in order to parametrize our jump, as in eqs. 3.16 and 3.17, and find the saddle point equations

$$\begin{aligned}
\partial_{u'} \rightarrow \quad & \beta + \frac{u'}{\sigma^2} = 0 \qquad\qquad \partial_{m'} \rightarrow \quad \epsilon\beta - \mu = 0 \\
\partial_{\mu} \rightarrow \quad & 2\,m' + (1+m_o)\tanh(\mu+\tilde{\mu}) + (1-m_o)\tanh(\mu-\tilde{\mu}) = 0 \\
\partial_{\tilde{\mu}} \rightarrow \quad & 2\,C + (1+m_o)\tanh(\mu+\tilde{\mu}) - (1-m_o)\tanh(\mu-\tilde{\mu}) = 0
\end{aligned} \tag{3.24}$$

Here we are not considering C as a variable. By doing so, we would be in the unconstrained case. The saddle point equation for C would read $\tilde{\mu} = 0$, and so eq. 3.23 would be reduced simply to eq. 3.14. The expression for C takes the form $C = m'm$. In our case, instead, we can solve the saddle point equations and find a parametrization in terms of β for all the fields, leading to

$$\begin{aligned}
u' =& \beta\sigma^2, \qquad \mu = -\epsilon\beta \\
m' =& \coth(2\epsilon\beta) - \sqrt{\coth^2(2\epsilon\beta) - 2C_0 m_o \coth(2\epsilon\beta) + C_0^2 + m_o^2 - 1} \\
\tilde{\mu} =& \frac{1}{4}\ln\left[\frac{(1-C_0)^2 - (m_o - m')^2}{(1+C_0)^2 - (m_o + m')^2}\right]
\end{aligned} \tag{3.25}$$

Notice that, with respect to the case before, here also the previous value of the magnetization before the jump is needed to compute where the jump will go, and the values of the current temperatures are not sufficient alone. A unique representation for the lines $S(1,\bar{1}) = S(2,\bar{1})$ and $S(1,\bar{2}) = S(2,\bar{2})$ is not possible any more on the (T_1, T_2) plane.

The expression in eq. 3.23 implements the condition $s' \cdot s = NC$, rather than $s' \cdot s \geq NC$. What we will do in practice, is to consider a limit C_0, and require that $s' \cdot s \geq NC_0$.

To do that, we will consider the unconstrained system, and compute the magnetization with the saddle point formulas of eq. 3.17. The value of C will be obtained by $C = m'm$, as if it was a free variable. Then, if this C satisfies $C > C_0$, we accept the jump, and update the system. Otherwise, we discard this jump, since it will decorrelate the spins too much, and compute the magnetization and the other quantities with the constrained saddle point equations in eq. 3.25.

It should not be difficult to see that, after all this effort, the mechanism for the evolution will be the same as before. The second system is not able to transfer energy to the bath, since it is more convenient to pass through system one. The only difference that we have, compared to the unconstrained case, is that the discharge of system two to system one is not 'complete' but it is limited by the total number of spins that can be flipped in a single jump, i.e. the parameter C_0. By increasing this one, extensive jumps become smaller. However, with the exception of a $C_0 = 1 - O(1/N)$, these jumps remains extensive, and qualitatively distinct from the $O(1/N)$ jumps performed by system one when losing energy to the bath. Therefore, we maintain the time-scale separation, and this key feature of the model remains unaffected.

3.2.2 More systems

After all this training on two coupled populations, we might be able to study what happens in the case in which more systems are coupled together. We will consider the case of three coupled systems, and then try to draw some conclusions for a higher number of coupled systems.

Let us consider three systems with $\sigma_1 < \sigma_2 < \sigma_3$. The coupling constants will be ϵ_{12}, ϵ_{13} and ϵ_{23}, since we will have to introduce three magnetizations. The total energy will be

$$u_{tot} = u_1 + u_2 + u_3 - \epsilon_{12} m_{12} - \epsilon_{13} m_{13} - \epsilon_{23} m_{23} \tag{3.26}$$

Notice that each magnetization can couple with two systems, and not with the third one. Therefore, every time a system jumps, there will be one magnetization (and two energies) that will remain unchanged. Let us suppose that we attempt a jump with system one. We need to find the number of possible configurations, given by

$$\sum_{s_1'} e^{-\frac{N u^2}{2\sigma^2}} e^{-\mu_{12}(s_1' \cdot s_2 - N m_{12}')} e^{-\mu_{13}(s_1' \cdot s_3 - N m_{13}')} \tag{3.27}$$

and the condition that the new values (u_1', m_{12}', m_{13}') will not augment the total energy, $u_{tot}' \leq u_{tot}$. The entropic contribution in eq. 3.27 can be rewritten as (see appendix A)

$$2^N e^{-\frac{N u^2}{2\sigma^2}} e^{N(\mu_{12} m_{12}' + \mu_{13} m_{13}')} e^{\frac{N}{2}[(1+m_{23}) \ln(\cosh(\mu_{12}+\mu_{13})) + (1-m_{23}) \ln(\cosh(\mu_{12}-\mu_{13}))]} \tag{3.28}$$

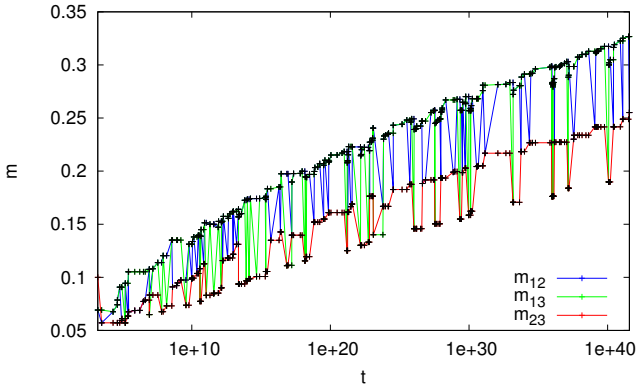

Figure 3.4: The evolution of the three magnetizations m_{12} (blue), m_{13} (green) and m_{23} (red), in the case when $\epsilon_{12} = \epsilon_{13} = \epsilon_{23} = 0.1$. We can see how at every jump two of the magnetizations equilibrate with β_1 (top), β_2 (central) and β_3 (bottom). The black points are used to guide the eye over these three fictitious line. By looking at the number of jumps at every temperature, we can recognized the hierarchy established among the systems.

The saddle point equations are easily obtained, and read

$$\begin{aligned}
\partial_{u'} \to \quad & \beta + \frac{u'}{\sigma^2} = 0 \qquad \partial_{m'_{12}} \to \quad \epsilon_{12}\beta - \mu = 0 \qquad \partial_{m'_{13}} \to \quad \epsilon_{13}\beta - \mu = 0 \\
\partial_{\mu_{12}} \to \quad & 2\,m'_{12} + (1 + m_{23}) \tanh(\mu_{12} + \mu_{13}) + (1 - m_{23}) \tanh(\mu_{12} - \mu_{13}) = 0 \\
\partial_{\mu_{13}} \to \quad & 2\,m'_{13} + (1 + m_{23}) \tanh(\mu_{12} + \mu_{13}) - (1 - m_{23}) \tanh(\mu_{12} - \mu_{13}) = 0
\end{aligned} \tag{3.29}$$

So the values of the new energy and new magnetizations can be expressed in term of the new temperature β_1 and the (unchanged) magnetization m_{23}, as

$$\begin{aligned}
u'_1 &= \beta_1 \sigma^2 \\
m'_{12} &= \frac{1 + m_{23}}{2} \tanh(\beta_1\epsilon_{12} + \beta_1\epsilon_{13}) + \frac{1 - m_{23}}{2} \tanh(\beta_1\epsilon_{12} - \beta_1\epsilon_{13}) \\
m'_{13} &= \frac{1 + m_{23}}{2} \tanh(\beta_1\epsilon_{12} + \beta_1\epsilon_{13}) + \frac{1 - m_{23}}{2} \tanh(\beta_1\epsilon_{13} - \beta_1\epsilon_{12})
\end{aligned} \tag{3.30}$$

As in the constrained case, the values of the new quantities after the jump depend on the current value of the non-changing magnetization. Moreover, the complete system has three temperatures. A two dimensional representation for the entropies and the evolution, as we did in fig. 3.3, will not help in understanding the mechanisms underlying the dynamics. Looking at the evolution of the magnetizations, fig. 3.4, gives us some hints. We can see that m_{12} and m_{13} are most of the time coupled to system one, that seems to be the one jumping more frequently. However, understanding the phenomenology of the energy exchanges just from this figure seems difficult.

Let us try again to use logic instead of brute force. First, we have to set a notation. We will indicate the current coupling fields by a three digit number, where each digit will refer to the coupling of magnetization m_{12}, m_{13}, and m_{23}, in this order. For example, by 112 we will mean that we have $m_{12}(\beta_1)$, $m_{13}(\beta_1)$, and $m_{23}(\beta_2)$. Notice that not all the combinations are possible. After a jump of system one, for example, we will end up having only 112 or 113. There is no way to have at a certain point a coupling 123, for example. Notice also that not all of the couplings are directly connected. Being in 112, one can jump with system one (112), two (212), or three (133). It will not be possible, e.g, to go from 112 to 232, even though both are allowed configurations. All this jump framework is encoded in fig. 3.5, where we condensed data and results of our analysis. Each layer corresponds to a particular choice of the parameters. Left panels present a sketch of the energy fluxes, while center and right figures represent the total number of jumps and the total amount of energy exchanged for each jump. In order to interpret correctly the figure, we have to notice that three kinds of jumps are possible:

- intensive, same coupling jumps: these are the jumps that do not change the coupling, and make a system exchange energy with the bath only. E.g. $112 \to 1'1'2$. The change in energy is of order $O(1/N)$, and such a jump simultaneously reduces the energy of the system and increases the two magnetization coupled to it. In the figures, these jumps are indicated by circles around the coupling;

- extensive, single coupling jumps: these jumps change the coupling of only one magnetization, and therefore are reversible. E.g. $112 \to 2'12'$. The change in energy is extensive, and is ruled by only one coupling coefficient, the one corresponding to the changing magnetization. The other coupling is already in equilibrium with the jumping system, so the corresponding magnetization does not change. In the figures, these jumps correspond to the horizontal ones, where the two directions of jump are possible;

- extensive, double coupling jumps: these jumps change the coupling of both the magnetizations connected to the jumping system. E.g. $112 \to 13'3'$. Therefore, they are irreversible (in this case, the coupling 112 is connected to itself only through the cycle $112 \to 13'3' \to 2'32' \to 1'1'2$). The change in energy is extensive, and is controlled by the interplay of two coupling coefficients. In the figures, irreversible jumps are represented by the vertical lines.

With the expertise acquired in the two systems interacting section, we can understand the behaviour of the three systems by simple reasoning. When the coupling are more or less equivalent, $\epsilon_{12} \sim \epsilon_{13} \sim \epsilon_{23}$, system one, having the smaller σ, is the one that more likely will jump, exchanging energy with the bath. Indeed, for the same Δu, a jump of system one will have much more configurations to jump to, than system two or system three will have. For what concerns system two, it will be more or less in the situation of the two coupled systems, and it will prefer to exchange energy with system one rather than with the bath. The other possibility for it is to exchange energy with system three. However, such an exchange will have the effect of discharging the energy of system

three into the mutual magnetization m_{23}, but this is not possible, since system two is colder than system one, and $m_{23}(\beta_2) > m_{23}(\beta_3)$. Finally, the third system has three possibilities: either it exchanges with the bath, but this will be even less convenient than for system two, either it exchanges energy with one of the other two systems. However, in one case it will have a gain in energy given by $\epsilon_{13}(m_1 3(\beta_3') - m_1 3(\beta_1))$, while in the other $\epsilon_{23}(m_2 3(\beta_3') - m_2 3(\beta_2))$. Now, for $\epsilon_{13} \sim \epsilon_{23}$, we have that $m_{23}(\beta) \sim m_{13}(\beta)$ for the same β value, and this means that the first jump will decrease the energy of system three more, since $\beta_1 > \beta_2$, and will be preferred.

In this case then, with $\epsilon_{12} \sim \epsilon_{13} \sim \epsilon_{23}$, we have that the typical situation will be the one depicted in fig. 3.5 (top-left panel), where system one is the only one giving energy to the bath, and both system two and system three discharge themselves through system one. It is not difficult to understand that the situation will be this one even when ϵ_{23} will be much smaller than the other two coupling. What will happen is that we will reduce the already small amount of exchanged energy between system two and three. In the end, we obtain time-scale separation, but only between system one, performing a large number of small jumps, and the other two systems, that will jump only rarely, exchanging a large amount of energy. The time-scales of system two and three will be separated, but only by order $\sim \epsilon_{13}/\epsilon_{12}$, and thus not diverging for large N.

We have two other limiting cases to explore, with respect to the relationship between the coupling coefficients. First, is the case where we limit the flux between system one and three, $\epsilon_{13} \ll \epsilon_{12} \sim \epsilon_{23}$. From what we said before, we understand that the preferred target of the energy of system three will be system two. If we compared this case, see fig. 3.5 (middle-left panel), with the previous one, the only change we will see is that the flux of energy from system three, rather than going directly to system one, passes through system two. However, once again, the time-scale separation is the same as before: system one will jump extremely frequently, while the jump frequency ratio between system two and three will depend on the relation between ϵ_{23} and ϵ_{12}. No extensive time-scale separation will distinguish these two systems.

Second, we can reduce the interaction between system one and two, $\epsilon_{12} \ll \epsilon_{13} \sim \epsilon_{23}$. In this case, see fig. 3.5 (bottom-left panel), system two will not be favoured in interacting with system one, and will prefer to transfer energy to the bath. Notice however that, being jumps towards the bath being of order $1/N$, in the limit of $N \to \infty$, the coupling coefficient ϵ_{12} must go to zero in order to maintain this situation. We will have then two systems communicating to the bath (they will basically cool down independently), and the third one will exchange energy with both, discharging through the mutual magnetization, with the ratio of the two related by $\epsilon_{13}/\epsilon_{23}$. We have again the incomplete time-scale separation. System three is infinitely slower than system one and two, for $N \to \infty$, but the latter ones will move on comparable time-scales, exchanging energy with the bath a the same (fast) rate.

All our reasoning is confirmed by data presented in the central and right panels of fig. 3.5. System one always jumps a large amount of times, by exchanging with the bath, and this can be seen by looking at the number of jumps with respect to the other two systems. Circles around 112 and 113 are always much thicker than all the other lines.

The only exception is when $\epsilon_{12} \ll \epsilon_{13} \sim \epsilon_{23}$, since in that case, as we said, even system two is exchanging with the bath, and this makes its number of jumps of the same order of that of system one, see fig. 3.5 (bottom - center). In this latter case, by looking at the energy flows, fig. 3.5(bottom-right), we see that system two cools down almost only with the bath, and system three gives its energy in equal parts to system one and system two. Also in the other cases, the study of the energy fluxes leads to the individuation of the pattern of energy exchanges depicted by the sketches on the left. The reader might be puzzled by looking at the energy flows in fig. 3.5(center-right), and in particular to the jumps $112 \to 133 \to 232$. The second jump seems to show that system two is giving energy to system one, while the first one is even more surprising, since it looks like system three is giving energy to system one, while the coupling $\epsilon_{13} \sim 0$. The fact is that in these two jumps is the 'collateral' magnetization that provides the energy exchange. By that, we mean that in the $112 \to 133$ jump, the energy does not pass through m_{13}, but rather through m_{23}. In some sense, the system was charged before, by jumps of system two, but went back to coupling with system one before attempting the jump with system three. Analogous situation for the jump $133 \to 232$, where is system two jumping after system three, but the exchange happens with system one, through m_{12}.

From all this discussion, we might try to draw a conclusion for the case when many systems are interacting. Even though there is an emergence of a separation in the time-scales, these will be only two. On one side we will have systems communicating with the bath, and on the other side systems cooling down by exploiting other systems. The first ones will do an infinite number of infinitely small jumps, while the others will exchange energy by few, large jumps. Even though a hierarchy can be established, organised according to the respective temperatures, and with one system discharging only to the system immediately below it in temperature, it will not be possible to reproduce such an organisation in time-scales, if we are also requiring that their ratio is divergent in the thermodynamic limit.

As a conclusion, let us spend some words about the biological relevance of our findings. Coupling two populations will force one of them to be always more optimized than the other. However, the latter in turn will profit of the more optimized population, by exploiting the fitness advantage that the interaction gives it. For this reason, the well adapted population will be forced, from time to time, to take some steps backward in evolution, performing selectively disadvantageous jumps and reducing its fitness. In other words, the less adapted population will 'steal' fitness from the more adapted one, acting in some sense as an evolutionary parasite. In terms of its internal structure, the first population will undergo a continuous evolution, decorrelating its genomic content in a very short time. The second population, instead, will perform only few jumps (though extremely relevant for its adaptation), and its internal structure will take much more time to differentiate significantly. This time-scale separation will diverge in the infinite genome limit.

In a several interacting populations system, this temporal decorrelation will not take place at all the levels, but only between one group of population (those evolving by themselves), and the other (those acquiring fitness from the more adapted ones). How-

ever, it is possible to establish a sort of adaptative hierarchy, where every population is taking fitness from one, more adapted, population, but losing it in favour of another one, less adapted. The actual organisation of this exploiting-exploited structure will depend on the relative strength of the interactions that couple the different populations.

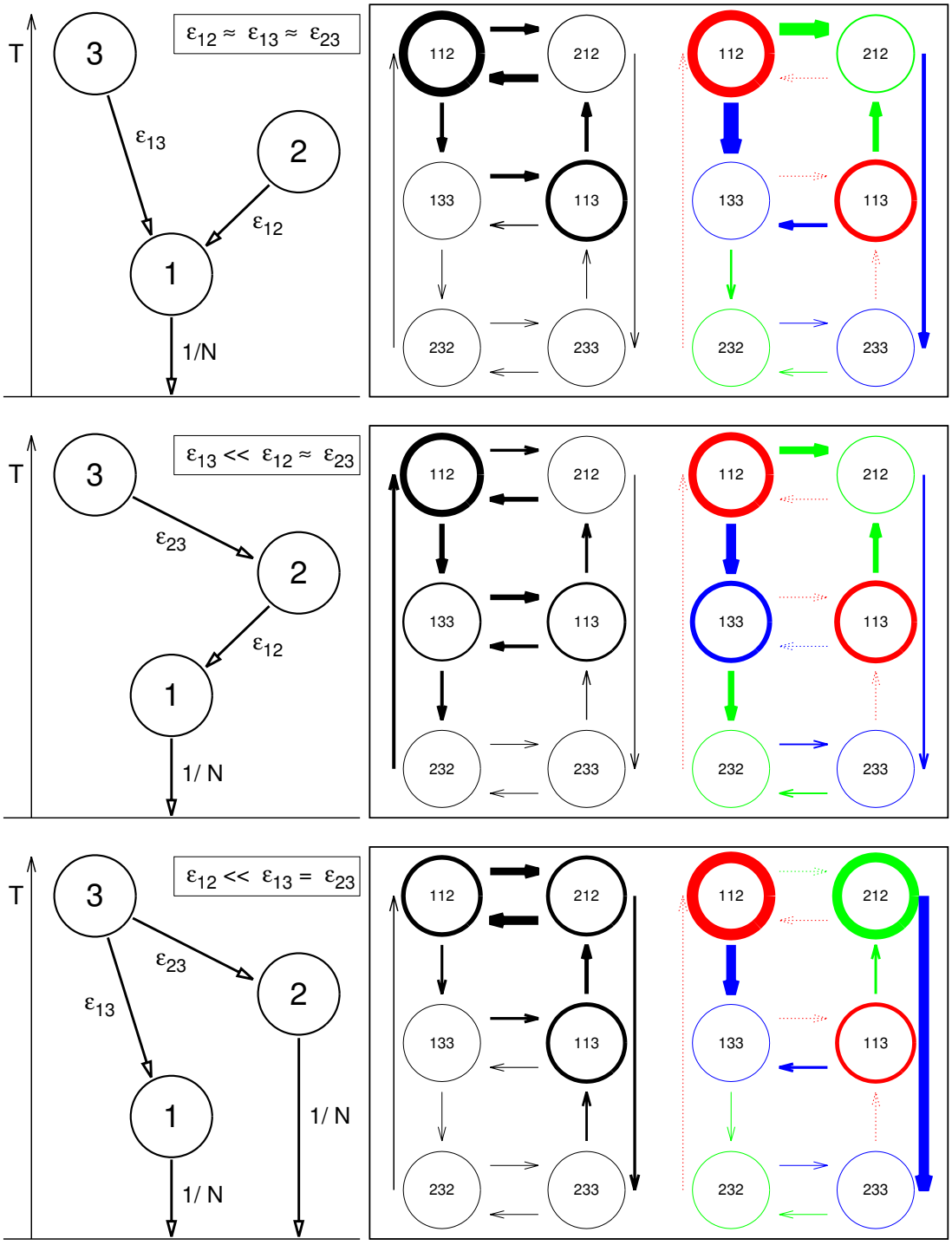

Figure 3.5: The evolution of the three systems, in the three cases described in the main text, from bottom to top. Left: a sketch, showing how each systems loses energy in order to cool down. Center and right: actual simulations. Arrows are in the direction of the jumps. Circles represent jumps for which the coupling does not change. The thickness of each line refers to the total number of jumps (center), or to the total energy lost (right). In the latter case, the color indicates to which system we are referring to (red=1, green=2, blue=3). Dashed line indicate that the contribution is zero, or negative.

Part II

Space and Mutation

Chapter 4

Space as a limiting resource

Death is over us.
She will come and exact its toll,
no matter where you are,
no matter who you are.
Even so, we come together as one,
as we wander,
with no direction,
in this flat desert of our existence.

Rab't Osmot
Chants of the Island

In this chapter, we will introduce a notion of space: individuals will be living and reproducing on a surface.

Chapter Teaser

- why a fixed number of individuals causes the population to localize in the real space, and this localization is stronger the higher the reproduction rate is, 4.1;
- why the trajectory of a population in these conditions is identical to the one of an individual, 4.1;
- how the outcome of evolution can be resumed in *survival of the faster*, 4.2;
- why polymorphism is much more conserved in space that in well-mixed, and how in some situations reaching a monoclonal state can become impossible, 4.2.1;
- why an unfit mutant should prefer to compete with its fitter wild-type on a Petri dish rather than in a chemostat, 4.2.2.

4.1 Constant population size in space

In this first section, let us focus on the behaviour of a monoclonal population that moves only via diffusion, with fixed size M. Such a fixed size constraint is not feasible for a real growth on a Petri Dish, and therefore will be abandoned later. However, its effects are quite striking, and deserve some attention.

All individuals will be supposed to have the same fitness, and reproduction will happen by creation of an individual in the same position of its ancestor, and concomitant removal of a random individual in the population, to keep the size constant. Individuals will also be able to diffuse, all with the same diffusive constant Δ. A possible interpretation of such a situation is that of individuals living on a completely flat fitness landscape, with mutation provided by diffusion. The main difference with fitness landscape dynamics as described in the previous chapters is that in the present case the mutation is infinitesimal and continuous, i.e. the offspring is identical to the parent only at the instant of birth. Therefore in such an interpretation population will always be polymorphic, with typically M different lineages, and the definition of monoclonal population must be substituted by the more blurred one of localized population.

In the well-mixed setting, in case of low mutation rates, population is monomorphic, for large intervals of time. In our space setting, low mutations are mimicked with weak diffusion. What we will have then is that the population generated by a common ancestor will typically spread in its neighbourhood. We will have a sort of localization effect, in the sense that the population will form a sort of island, but this latter will move in space, rather that being fixed. We are able to give an estimation of both its size and its mean displacement.

The wandering island of individuals As for the size, we can immediately indicate a reason for the island to be (softly) bounded in space [89]. Two individuals drift away from each other starting from the moment of their creation. We have seen in subsection 1.2.2 that in a population the number of individuals of a lineages take a time m to drift by a number of m. Therefore, we can estimate in our spatial case what is the time Δt required for a population to be originated by a single ancestor, and that will be $\Delta t \sim M/\lambda$. This means that, if we trace back the movements of the individuals forming the present population by a time Δt in the past, all their trajectories will converge to a single point, i.e. the position at that time of (the individual that will become) the ancestor of the present population. Therefore, two individuals will have been drifting apart for not more than Δt, and their separation will be $\Delta x = 2\sqrt{2D\Delta t}$. We can then conclude that the island radius will be

$$\Delta x \sim \sqrt{\frac{MD}{\lambda}} \tag{4.1}$$

For what concerns the movement of the island, we can again understand its behaviour without doing any calculation. Every $\Delta t \sim M\lambda$ the population is regenerated starting from an individual. Now suppose that we follow the evolution in coarse grained steps

of $t_1 = t$, $t_2 = t + \Delta t$, $t_3 = t + 2\Delta t$, and so forth. During every single time step Δt, we can follow the evolution of the only surviving individual. Since, e.g. the individual generating the population at t_3 will be the offspring of the common ancestor at t_2, and that at reproduction an individual is created in the same exact position of its parent, the dynamics of the last common ancestor will follow a continuous line in space. This line will be a sort of cut and paste over the single dynamics of the individuals that from time to time become ancestors of the population. Two examples of these curves are shown in fig. 4.1(right). This means that the global dynamics will be, on the coarse grained scale, that of a single individual. Now, since we know that the population will be localized in space, it is not a too crude approximation to consider the whole population as a particle of size R wandering with diffusion constant D, the same as the individual one. This is a strong effect given by the combination of the local reproduction and non-local death processes. Indeed, if we consider individuals that are simply diffusing, the variance of the center of the island can be computed by summing up the contributions of the independent variances of the position of the particles, and this leads to a suppressed diffusion constant of $D/\sqrt{M}$.

The behaviour of the island of individuals described here is exemplified in fig. 4.1. The first three figures on the left for each layer represent the instantaneous populations, taken at different times, evolving from left to right panels. Both the populations have the same size M and the same diffusion constant D, but the top one has a four times lower reproduction rate. The starting condition is a random uniform distribution of individuals in a square. After some time, the population localizes, and then starts wandering. By looking at the size of the population, it is easy to distinguish for which one localization effects due to reproduction are stronger. Faster reproduction cause the island to shrink, following eq. 4.1. The rightmost panel in each layer shows the trajectory described by the ancestors of the population. As said before, the two populations undergo a diffusion dynamics, with the same coefficient D, and it is not possible to distinguish which one has the larger reproduction rate.

A complete calculation for the mean displacement of the center of mass of the population $x_{cm}(t)$ can be found in [90]. The dynamics of the population is studied also before the inset of the diffusive behaviour, and it is found that there are three regimes for the movement of the center of mass. Starting with all the individuals located in the origin, on a very short time, $t \ll 1/\lambda$, we have $\langle x_{cm}^2(t)\rangle = 2dDt/M$, where d is the dimensionality of the space. The movement is a normal diffusion of independent particles. This should not be surprising, since the time-scale is the one needed for the onset of reproduction. For long time, $t \gg M/(2\lambda)$, we recover the diffusive behaviour,

$$\langle x_{cm}^2(t)\rangle = 2dDt \tag{4.2}$$

but without the factor $1/M$, meaning that the population diffuses just like a single individual. The time-scale in this case is the one needed for the condensation of the population into a single ancestor. During the intermediate regime, $1/\lambda \ll t \ll M/(2\lambda)$, one has a ballistic motion, $\langle x_{cm}^2(t)\rangle \propto t^2$.

The behaviour of a population in space, as we have seen, depends strongly on the

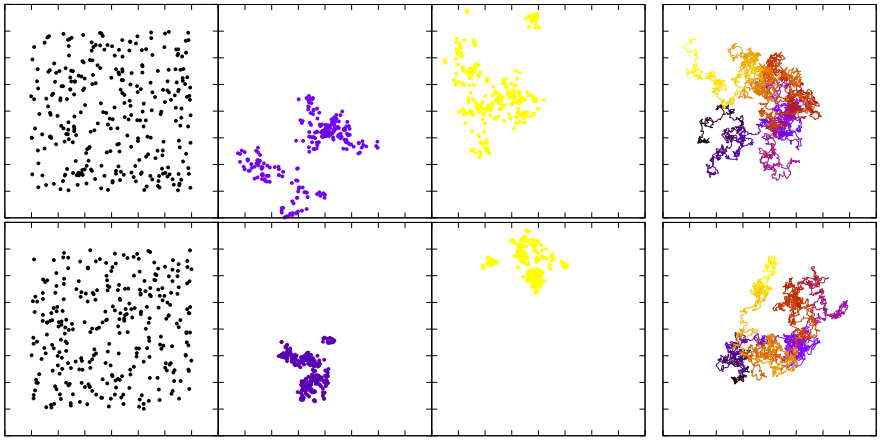

Figure 4.1: An example of diffusing constant size population, $M = 300$ and $D = 0.05$. Top $\lambda = 0.25$, bottom $\lambda = 1$. First six panels on the left: instantaneous populations, at different times, from left to right. Two panels on the right: trajectories of the ancestor of the population, the color-code referring to the time, earlier times being darker.

constraint of constant population size, which is totally non-local. This is fairly justified in a well-mixed environment like a chemostat, where cells are always in competition with each other, the resources available being shared throughout the medium, and the number of individuals being kept fixed by the regulation of the in- and out-fluxes. However, in a spatial environment, e.g. on a Petri Dish, such a constraint is very unlikely to reproduce the actual behaviour of the growth of a colony of cells. What normally happens is indeed the opposite: cells are implanted in a given location on the Petri Dish, and from there they start reproducing. The colony expands as long as there is free space (and nutrients), and the number of individuals keeps growing. In the following, then, while referring to spatial growth, we will generally drop the fixed population constraint.

4.2 Freely growing population

From now on, populations will grow freely, i.e. with no constraints on their size. However, we will suppose, in turn, that an individual can reproduce only if it has some space available surrounding it, and the offspring will be generated in contact with the parent cell, but not in the same exact position. Moreover, we will work with individuals incapable of moving. For these reasons, in the following we will have to distinguish individuals being at the frontier of the population, that will be able to reproduce, and individuals in the bulk, whose ability to reproduce will be inhibited. We will see that the behaviour and properties of the two sets, frontier and bulk, are completely different.

Two main types of growth will be analysed in this work, i.e. the case of a linear front or that of a circular one. The former can be thought as the case in which a colony must grow when confined between two walls. While poorly used in experiments, it is easier to

analyse theoretically, and to simulate. The latter instead is the typical case of growth in a Petri Dish, where individuals start spreading in all directions uniformly from a given point (normally cells are put on a Petri Dish by deposing a drop of solution on the substrate, and surface tension of the drop assures a circular form from the implant).

In line with the rest of the work, we will not be concerned with microscopical or biological details. Although the term cell will be used as a synonym for individual, its characterization remains as simple as described at the beginning of this section. Adhesion forces, biochemical signalling, substrate defects, and other realistic features, all potentially present and significant in an experiment, will be ignored. Also, in experiments, the growth on a Petri Dish is not entirely two dimensional, as after the colony has reached some size there is the appearance of superimposed cell layers, and growth may start also in the third dimension, though strongly suppressed by the difficulty of having access to nutrients, which are located on the substrate. In the following, we will always assume that the growth is simply two-dimensional.

4.2.1 Drift in space

As in the case of the well-mixed setting, it is important to distinguish and analyse the major driving forces determining the evolution. We will study the effects of mutation in the next chapter, and the role of selection in the next subsection. For the moment, let us focus on the effects of random drift. Consider a front of individuals, all with the same reproduction rate, i.e. with the same velocity in occupying space. Since they have no advantage with respect to each other, the competition will be completely stochastic. We will define *domain* the contiguous region of space occupied by individuals of the same lineage. A domain will be typically composed by a part at the front, and a part in the bulk, made up by individuals that were at the front in the past. When it loses contact with the front, a domain closes on itself, and will not grow any more. As long as it touches the front, a domain will be referred as active. A lineage achieves fixation when it manages to be the only one present at the front.

Linear front In order to study a domain, it is sufficient to study the dynamics of its border at the front during the growth [91]. The distance separating the two borders will be noted by X, and it is of course a stochastic variable. Since we will suppose that the population reproduces with a constant velocity, we can study the evolution of $\Delta X = X(t) - X(t_0)$ by parametrizing it with the time t or with the perpendicular growth r, the latter being our choice. Since the competition between individual is ruled only by drift, the borders of the domain are following a purely stochastic dynamics, each one performing a simple random walk, with a given diffusion coefficient D. In this case, we know that each one of the point of the border, advancing from r_0 to $r = r_0 + \Delta r$, will have a movement on the transverse direction of zero average and variance equal to $2D\Delta r$. If we treat them as independent, we have that

$$\langle \Delta X_{ind} \rangle = 0 \qquad \langle \Delta X_{ind}^2 \rangle = 4D\Delta r = \sigma^2 \tag{4.3}$$

or, equivalently, that the probability of having a domain of width x at the front at distance r, which started with width x_0 at r_0, is given by a Gaussian distribution

$$G(x, r|x_0, r_0) = \frac{1}{\sqrt{2\pi\sigma^2}} e^{\frac{(x-x_0)^2}{2\sigma^2}} \tag{4.4}$$

The two random walks made by the borders, however, are not independent, since once they meet they annihilate, closing the domain. The correct probability distribution for the width of the domain, $P(x, r|x_0, r_0)$, should then be zero for all values of $x \leq 0$. In particular, we can set identically $P(x, r|x_0, r_0) = 0$ for every $x < 0$, but we have to require that its limit for $x \to 0^+$ is zero. This can be achieved by defining $P(x, r|x_0, r_0) = G(x, r|x_0, r_0) - G(-x, r|x_0, r_0)$, with G defined by eq. 4.4.

We are now able to investigate the dynamics of drifting lineages, and study the evolution of the population. Since for the moment we have supposed to have no mutations, when a domain closes the corresponding lineage is extinct, and we can then wonder how long does it take to a population to lose all its polymorphism. We will start from the case in which all the individuals are different, and try to find the time it takes for a population with a front of width L to reach fixation. Since the starting point of our domain expansion will be an individual, x_0 should be close to zero, as the borders (almost) coincide. For simplicity, let us take $r_0 = 0$. The limit of the probability distribution of the width (correctly normalized) becomes

$$\lim_{x_0 \to \infty} P(x, r|x_0, 0) = \frac{x}{\sigma^2} e^{-\frac{x^2}{2\sigma^2}} \tag{4.5}$$

valid in the interval $x \in [0 : \infty]$.

The mean of ΔX is then easily computed, and gives

$$\langle \Delta X(r) \rangle = \sqrt{2\pi D r} \tag{4.6}$$

The average number $N(r)$ of active domains at the front of the population after a time r is then simply computed by dividing the front width by the average domain size, and thus

$$N(r) = \frac{L}{\langle \Delta X(r) \rangle} = \frac{L}{\sqrt{2\pi D r}} \tag{4.7}$$

This means that the number of clusters diminishes with the square root of time, and we have a direct estimation of the fixation time by asking $N(r_{fix}) \sim 1$, finding

$$r_{fix} \sim \frac{L^2}{2\pi D} \tag{4.8}$$

We have a first estimation that we can compare to the well-mixed case. Indeed, the number of individuals at the front remains more or less constant during all the evolution, and their number is proportional to the width of the advancing front. In some sense, the population of the front can be considered as an effective population, as its individuals

are the only ones able to reproduce. For M individuals at the front, we have that the time for fixation is $t_{fix} \sim M^2$. Compared to the well-mixed case, then, fixation takes longer time, as in the case of drift we found, eq. 1.28, that the relation was simply linear, $t_{fix} \sim M$. We will see that this resilience to fixation is a characteristic of the introduction of a space setting, and even in the case of selection, studied in subsection 4.2.2, we will find that the fixation time is longer with respect to the well-mixed case.

As a side note, let us say that considering all the individuals as different at the beginning of the evolution might sound as a too stringent hypothesis. However, in the other extreme case in which individuals are of two types only, the presence of spatial separation causes the situation not to change much. Indeed, in this case we will have a probability 1/2 for two individual to be identical, thus making two domains one. All in all, the numbers of starting domains will be reduced only by one half, and the average value of $N(r)$ will be that of eq. 4.7 , only divided by a factor two. All the qualitative considerations still hold.

Circular front Let us consider the other expansion possibility, i.e. when the front is circular. In this case, the same approach can be taken, with the expedient of changing the variable of interest from the width of the domain ΔX to its angle $\Delta\Phi = \Delta X/r$. Proceeding this way, we avoid the problem of the constant increase of ΔX due to the colony expansion in r, and the dynamics of the borders can again be treated as a pure diffusion. The angular diffusion coefficient D_Φ can be expressed in term of the linear diffusion D, by using its definition $\langle \Delta\Phi_{ind} \rangle = 4D\Phi\Delta r$, for independent random walkers, and the equation on the right in eq. 4.3. We have then

$$D_\Phi = \frac{D}{r^2} \tag{4.9}$$

The presence of the r^{-2} is extremely relevant. Indeed, one can redo the same computations as before and find the average angular width of a domain, and then compute the number of active domains after a time r, finding (the role of the total lenght L is played by the total radial angle 2π)

$$N(r|r_0) = \frac{2\pi}{\sqrt{2\pi D(1/r_0 - 1/r)}} = \sqrt{\frac{2\pi}{D(1/r_0 - 1/r)}} \tag{4.10}$$

We have then that the average number of active domains decreases with time, but saturates to a finite value

$$N_\infty(r_0) = \sqrt{\frac{2\pi r_0}{D}} \tag{4.11}$$

Depending on the initial distribution of states at r_0, then, the system might be in the condition of never reaching fixation. The growth in the tangent direction at the front of the colony becomes so fast that border diffusion is not able to compete with it alone. The situation is dramatically different from the linear case. We will see that in case of

difference in fitness between the individual, and therefore with the presence of a drift, fixation will eventually happen even in the circular case, but in an extremely slower fashion that in the linear case.

4.2.2 Deterministic growth

In this subsection, we will study the behaviour of a growing population when lineages do actually differ in their fitness, i.e. in their velocity to occupy space. For the moment, let us neglect stochastic effects, as they can be considered irrelevant for the large-scale behaviour of the system. Indeed, we can obtain good results just by means of geometric arguments.

Linear growth Consider two competing lineages, with different reproduction rates λ_a and λ_b [92]. Supposing $\lambda_a > \lambda_b$, the domain of a cells will advance faster, and will have then the possibility to increase its width at the front, having free space available to reproduce even in the direction transversal to the main growth axis. The a domain will have borders tilted towards the b cells, see fig. 4.2(right). The border must satisfy a principle of minimum path, in the sense that the growth of the a individuals along the border (dashed line in the figure) must equal the frontal growth of the b ones (solid arrow). If ϕ is the opening angle of the a domain, the travelled distances should be equal, $\lambda_a \cos(\phi/2)\delta t = \lambda_b \delta t$, and this gives us an angle

$$\phi = 2 \arccos\left(\frac{\lambda_b}{\lambda_a}\right) \tag{4.12}$$

The border will move laterally at the front with a velocity $\lambda_\perp = \tan(\phi/2)\lambda_b = \sqrt{\lambda_a^2 - \lambda_b^2}$. Therefore, the time required for fixation of lineage a over a lineage b, for a colony with a front of width L, can be estimated from

$$t_{fix,lin} = \frac{L}{\lambda_\perp} = \frac{L}{\sqrt{\lambda_a^2 - \lambda_b^2}} \sim \frac{L}{\sqrt{2\Delta\lambda}} \tag{4.13}$$

for $\Delta\lambda = \lambda_a - \lambda_b << 1$, and λ_a set to 1. As we could have expected, the bigger the difference of fitness $\Delta\lambda$, the shorter the time it takes fixation to happen. If we compare this result with the one obtained in case of spatial expansion with no selection, eq. 4.8, we see that fixation is much more rapid here, depending linearly and not quadratically on the colony front size L. We can also compare this result to the fixation time in the case of a competition between two lineages in a well-mixed environment, eq. 1.18. If we consider that the effective population M_{eff} in the spatial case is made up by individuals at the front, and $M_{eff} \sim L$, we can understand that fixation is much slower in this setting that in the well-mixed space, where t_{fix} scales only logarithmically with $M = M_{eff}$, eq. 1.18. The reason for this slow-down is easily understood, and is due to the local nature of the competition. Indeed, individuals that are far from the borders do not participate to

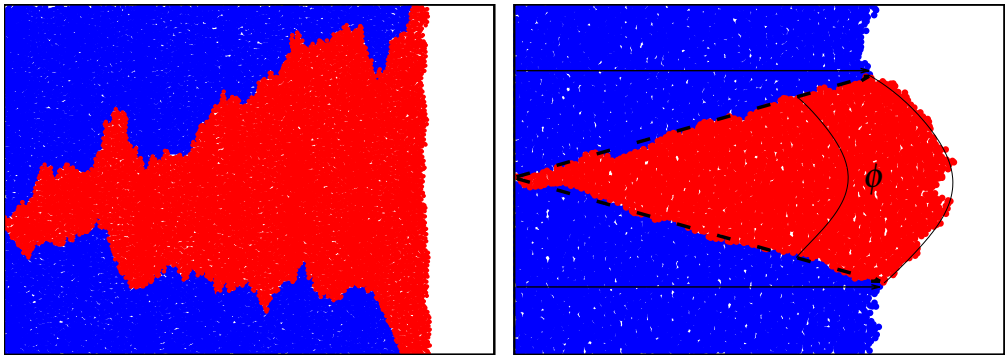

Figure 4.2: Left: two colonies with same fitness, competing for fixation. Right: two colonies with different fitnesses λ_a (red), and $\lambda_b = 0.8\lambda_a$. Solid lines are covered by blue cells in the same time in which dashed lines are by red ones. The opening angle ϕ remains the same during evolution. The two figures are scaled in the growth direction (left to right), so that evolution time in the left figure is roughly three times longer than in the right one.

the competition, and therefore a fitter lineage cannot exploit all its selective advantage simultaneously for all individuals as it would do in a well-mixed setting.

Comparing the different behaviours of the competition of two populations in case of diffusion or selection, fig. 4.2, we can notice a few things. First, when a lineage has a fitness advantage, competition happens in a quasi-deterministic fashion, with borders that are almost straight lines, contrarily to what happens when no mutant is fitter, in which case the line separating the domains is much more ragged. Second, the front itself shows some differences. In the diffusion case, fig. 4.2(left), the two lineages reproduce with the same rate, and from the point of view of the growth they act as a uniform population, the only difference between them being a label. The front, then, is more or less uniform and flat. On the contrary, it is clear from fig. 4.2(right) that in the case of selection the front presents a bump in correspondence of the fastest lineage. We can guess from now that, in the case of several types of particles, with different reproduction rates, the front profile will be much more wavy. We will be studying more deeply the front properties in subsection 5.1.2.

Circular growth The case of a colony expanding with no physical constraint, when the front takes a circular form, can be studied with the same minimum path approach. If we consider the front at the point of contact of the two domains, growing with $\lambda_a > \lambda_b$, we expect that during an increment dr of the b domain, perpendicular to the front, the domain of a cells will grow of $\sqrt{dr^2 + (rd\phi)^2}$, where $rd\phi$ is the lateral gain of domain a over domain b. Therefore

$$\frac{dr}{\lambda_b} = \frac{\sqrt{dr^2 + (rd\phi)^2}}{\lambda_a} \tag{4.14}$$

which leads, upon integration, to

$$\phi(t) = \ln\left(\frac{r(t)}{r_0}\right)\sqrt{1-\frac{\lambda_b^2}{\lambda_a^2}} \tag{4.15}$$

with r_0 the radius of the colony when the first mutant a appeared, when we can consider $\phi = 0$. The other border will evolve with an angle given by $-\phi$. If we wish to give an estimate for the fixation time in this setting, it is sufficient to require that $2\phi = 2\pi$, and this leads, upon inverting eq. 4.15, to

$$t_{fix,cir} = \frac{r_{fix}}{\lambda_b} = \frac{r_0}{\lambda_b}\exp\left(\frac{\pi\lambda_a}{\sqrt{\lambda_a^2-\lambda_b^2}}\right) \sim r_0 e^{\frac{\pi}{\Delta\lambda}} \tag{4.16}$$

where, as before, we have defined $\Delta\lambda = \lambda_a - \lambda_b \ll 1$, and we have taken $\lambda = 1$.

Let us make some comments. First, contrarily to what happens in the absence of selection, eq. 4.11, fixation is always reached when a lineage has some selective advantage. However, compare this expression with the fixation time of the linear case, eq. 4.13. The time for fixation is linear in the initial front size, r_0 (times 2π), as it was in the linear case, with L. The dependence on the fitness difference $\Delta\lambda$, on the contrary, is totally different. While for the linear front the time grew linearly with the inverse of $\Delta\lambda$, in this case the increment is exponential. We can understand the origin of this difference in this way. One can compute the velocity tangent to the front, by $\lambda_\perp = r(t)d\phi/dt$, which leads, by deriving eq. 4.15, to $\lambda_\perp = \sqrt{\lambda_a^2 - \lambda_b^2}$, the same tangent velocity of the linear front. Indeed, this should not be surprising, since the competition takes place only at the local level, and locally the circular front can be considered flat. Since in both cases, linear and circular, the fitter domain advances with the same speed, it is clear that the exponential slowdown in the latter case is entirely due to the fact that the front is expanding.

To resume, let us report here our results for the fixation time in case of the competition of two lineages with selection coefficient $\Delta\lambda = s$:

well-mixed	linear	circular
$2\frac{\ln(Ms)}{s}$	$\frac{M}{\sqrt{2s}}$	$M\exp(\frac{\pi}{s})$

These are the results obtained in eq. 1.31, eq. 4.13 and eq. 4.16. To uniform notation, we took $L = M$ for the linear case, and $r_0 = M$ for the circular one, so that M should be considered as the number of the individuals in the starting, effective, population. We can see that there is a neat hierarchy [well-mixed $\rightarrow$ linear $\rightarrow$ circular] for what concerns the time needed for fixation of a lineage. The times are exponentially longer, in the population size and in the selection coefficient, going from a well-mixed to a circular 2-dimensional expansion. Polymorphism has many more chances to be observed in a circular setting, as deleterious mutations are much more resilient to fluctuations. Experimental estimations of the selection coefficient, especially when this is small, should be conducted for competitions set in such an environment, where the exponentially longer time required to reach fixation allows for more precise measurements [93].

Chapter 5

The selective effects of mutation

> "We need two things in this country: economic growth, and stability. Only these two. And let me say it: my government will not waste a single dollar by investing in academic research! Read my lips: we just don't need it!"
>
> *Sam Rott*
> *off-air at "Meet your Representative" talk-show on CBS, 21st June 2015*

In this chapter, we investigate how the mutation rate, in a well-mixed and in a spatial environment, can constitute a criteria for selection to act in favour or against a given lineage.

Chapter Teaser

- what is an Eden model with mutations, and how does it work, 5.1;
- how, without the need for extremely high mutation rates, deleterious mutation can easily overcome a fitter wild-type, 5.1.1;
- how the properties of the front of an advancing population are strongly dependent on its degree of polymorphism, 5.1.2;
- what is a cloud of deleterious mutations, 5.2;
- how can we maintain the thermodynamical interpretation of population dynamics of chapter 2, when considering also stability as an evolutionary advantage, 5.2
- why selection favours, in space, a population with highly deleterious mutations over a population that generates only slightly less fit mutants, 5.3.1;

- why, in well-mixed and in space, a higher stability is sufficient for a population to acquire a selective advantage, 5.2 and 5.3.2;
- why, in well-mixed and in space, selection correlates high fitness and low mutation rate, 5.2 and 5.3.2.

5.1 Mutational Eden Model

Later in this chapter, we will be interested in the effects of a variable mutation rate, but first we will have to understand how a fixed mutation rate can affect the evolution in space. Even more specifically, we need to know how a specific mutation, that happens with a given rate, can influence the dynamics of a population. We will focus for the moment on the growth of a colony confined by two walls.

A model to address such an issue is a modification of the Eden model [94], when mutation are introduced. The Eden model is defined on a lattice, but the same (qualitative) results can be obtained working off-lattice. In the following, we will consider cells as circles of finite size. The offspring of a cell will be generated in contact with its parent. For geometric reasons this means that a cell can have at most six individuals around itself, and will be able to generate at most five offspring (the sixth cell being its own ancestor). For the moment let us restrict to a very specific case, yet phenomenologically rich, of two types of cells only. Cells of the first type, with reproduction rate λ_f, are able to mutate, into a second type of cells, with fitness λ_s. These second type cells, however, are not able to perform the backward mutation. The case in which all the cells are of the second type, then, correspond to an absorbing state.

We have two forces driving the dynamics. On one hand, we have the competition in the reproduction rates, favouring the fastest one. On the other side, the asymmetry in the mutation process gives a clear advantage to cells of the non-mutating lineage. For every finite size system, fixation of second type state cells will eventually happen. The way in which it happens, however, strongly varies upon the fitness respective magnitudes, and the value of the mutation rate. In particular, it is clear that if non-mutating cells have also an advantage in reproduction, the competition is totally biased towards them, and their success is undisputed. In the following, then, we will suppose that $\lambda_s < \lambda_f$. Labels indeed are for slow, s, and fast, f. In the following, when not specified otherwise, we will take $\lambda_f = 1$.

We provide some examples of the growth of populations in this model, for several values of fitness and mutation rates, in fig. 5.1. For small values λ_s, and large τ, slow particles appear in the front and are almost immediately overtaken, not having the time to reproduce. If their fitness is larger, they might have a chance to reproduce and stay at the front a little longer, giving rise to isolated cluster of λ_s particles, the bigger the greater their fitness. Upon increasing the mutation rate, what can happen is that the borders of these domains can start touching at the front, this fact resulting in a merging of the two domains. This enhances the chance of survival of both the domains significantly, and therefore leads to a great increase in the velocity of fixation of slow particles. Looking

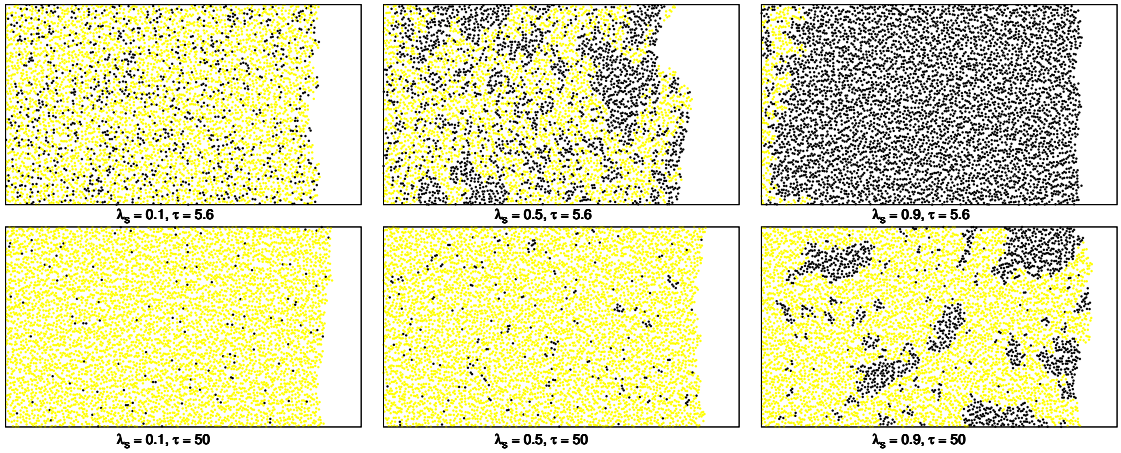

Figure 5.1: Examples of population growing (from left to right) between two walls, for several values of (λ_s, τ). The parameters used here are located on the phase diagram in fig. 5.2. Black particles are the slow ones. It is clear how, going from active to inactive phase (bottom-left to top-right), the number and size of the domains of slow particles grow and cause faster fixation.

at fig. 5.1, notice how the presence of lineages with different fitnesses causes the front to roughen, while this remains rather smooth in the case of a monomorphic population. We will talk more about the front properties in subsection 5.1.2.

5.1.1 Active and inactive phases

The behaviour of the fixation time in such a two lineages model has been studied extensively by [95]. It was found that a phase transition can be identified, while looking at the time required to reach fixation, in the (τ, λ_s) space. In the case of low fitness, low mutation rate, fixation is extremely hard to achieve, and it takes times that are exponentially large in the front size. In the opposite case of high mutation, high fitness, fixation happens instead extremely rapid, as it takes times that are logarithmic in the front size. Thus, the scaling of such a time reminds more the one of a well-mixed system, eq. 1.18, rather than a spatial environment competition, eq. 4.13.

The reason of this drastic change of behaviour is to be seen in the non-locality of mutations and in the clustering of domains. Firstly, mutation is non-local, in the sense that it can happen everywhere in the front, so that more domains are scattered around, and the possibility of having two of them merging is enhanced. Secondly, the merging of domains is not at all a trivial process. If we considered domains as simply growing independently, we would have obtained that the time for fixation is at best, even if we supposed that $\lambda_s > \lambda_f$, linear with the front width. Indeed, we would have that the time is given by eq. 4.13, divided by the number of λ_s domains. This means that the merging of domain borders gives rise to strong non-linear effects, capable of accelerating the dynamics exponentially. Upon studying the scaling of the fixation time, one can

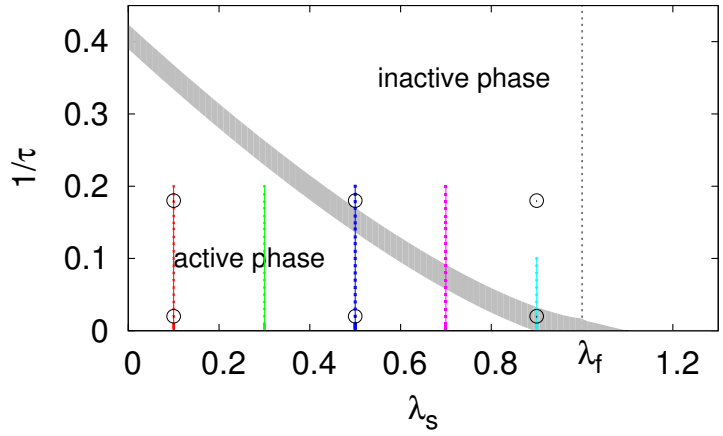

Figure 5.2: The phase diagram in the $(\lambda_s, 1/\tau)$ space. The grey zone indicates the zone where the transition happens. When $\lambda_s > \lambda_f$, we are never in the active phase, no matter the value of the mutation rate. Black circles are the points corresponding to the populations in fig. 5.1. Coloured points correspond to the set of parameters used in the various simulations in figs. 5.3, 5.4 and 5.5, with the same color scheme.

identify these two regimes, and provide a phase diagram similar to the one in fig. 5.2. In accordance with [95], we will refer to active phase when the fixation time scales exponentially with the front size, and inactive phase in the other case.

A further inspection of fig. 5.1 let us see how active and inactive phases look like. While in the active phase, i.e. the three panels close to the left bottom corner, we cannot notice any evolution of domains of slow particles with time, as they seem to remain small in size and number during the growth. The bulk distribution of slow particles is more or less invariant for translations along the growth axis. For the inactive phase, this is not the case. In the rightmost top panel, fixation happens immediately, and the growth is the one of an homogeneous population of slow particles only. In the remaining two panels, the domain distribution is no more homogeneous during the growth, since as time goes by, domain start to merge, and this results in larger portions of space occupied by slow particles. Just by looking at the figure, one can see that the previous translation invariance is lost.

Let us make some remarks about the phase transition. First, there is no sharp transition line, but rather a blurred zone, in which the fixation time assumes a power law scaling. In fig. 5.2, this is indicated loosely by the grey stripe. Second, one can look at the two extremes of this transition zone. When $\lambda_s \geq \lambda_f(=1)$, for every value of the mutation rate the system is in the inactive phase. The reason for this should be clear from what we said before: asymmetry in mutations and fitness differences cooperate in favour of slow cells. On the other hand, also for $\lambda_s = 0$ there is a threshold value for the mutation rate that causes the system to enter the inactive phase. Our two-lineages competition can be mapped to an isotropic site percolation model, in which the non-reproducing

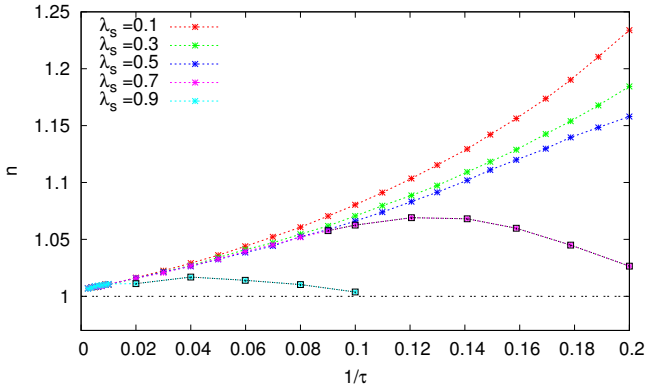

Figure 5.3: Total number of particles at the front, n, as a function of the mutation rate $1/\tau$, for several values of λ_s. The points representing mutation rates in the inactive phase are marked by black squares.

mutant cells play the role of empty sites (through which percolation cannot happen). The critical mutation rate is equal to the threshold probability of empty sites, $p \sim 0.407$.

5.1.2 Front properties

For an homogeneous population, the growth is almost uniform, and the front remains more or less flat. Its actual behaviour is well described in term of the Kardar-Parisi-Zhang equation [96], which accounts for the field theory of a large variety of models, from growth models like the (non-mutating) Eden model [97], to interacting particles models like the ASEP [98]. However, in the presence of mutations, the front stops being uniform and starts to roughen. The reason, as we already explained, is given by the fact that slow particles tend to trail behind the advancing front. The total number of particles at the front augments consequently, see fig. 5.3. One can study the scaling with the front size, and see that this Eden model, with mutations, behaves differently from KPZ, as the critical exponents describing the front roughness are markedly different.

To understand the microscopical behaviour of cells at the front we will take another approach. In order to individuate the mechanism responsible for roughness, we can look at the average time spent by a particle at the front, whether it is fast, t_f, or slow, t_s. For every particle, we have two ways in which it can be surrounded and get passed by the front. Either it reproduces, and it is surrounded by its own offspring, either is encircled by the offspring of its neighbours. For brevity, we will refer to these situations with the terms own-overtaking, and hetero-overtaking. The importance and relative magnitude of the two effects can be estimated by looking at t_f and t_s. Confronting values for different λ_s, at the same mutation rate, one can see the importance of own-overtaking. By comparing the time spent at front for different mutation rates, on the other hand, the behaviour of hetero-overtaking should be clear. With low $1/\tau$ value, a particle is mostly surrounded by fast particles, while for high $1/\tau$ the neighbours are mostly slow

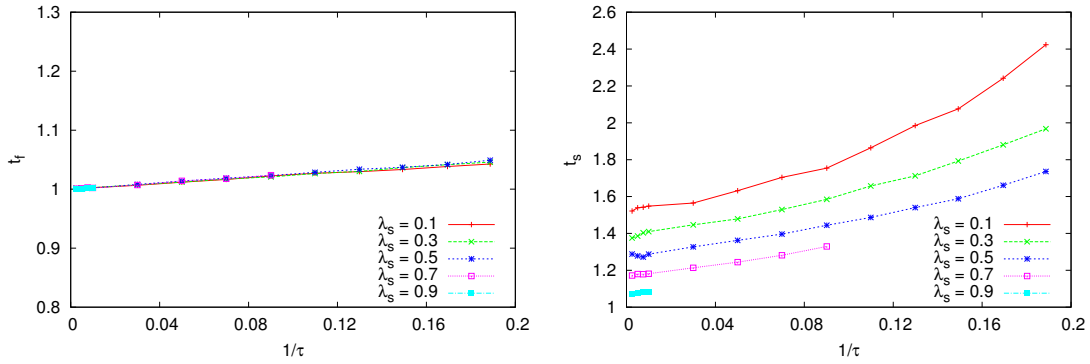

Figure 5.4: The average time spent at the front by fast (left) and slow (right) particles, for several values of τ, λ_s. Fast cells mutating while at the front are not considered here.

ones. By inspecting the actual data, presented in fig. 5.4, one can see that:

- for fast particles, the own-overtaking is the dominant effect. Indeed, as shown in fig. 5.4(left), the time spent at the front is almost constant even for very high values of $1/\tau$, and it is substantially independent from λ_s. Also, in good approximation, we can say that $t_f \sim 1/\lambda_f$, as one could have expected;

- for slow particles, hetero-overtaking is much more significant. Own-overtaking is still present and relevant, as one can see from fig. 5.4(right), since for low $1/\tau$ the t_s are markedly different for the various λ_s. However, as the mutation rate starts to increase, the time spent at the front becomes longer, and for each curve it tends to the asymptotic value of $1/\lambda_s$, as the front becomes more and more rich (and eventually homogeneous) in slow particles.

As a side note, let us say that these data refer to particles that have not mutated during their permanence at the front. Anyway, for particles that are generated as fast ones, but then mutate into slow ones, the situation does not change dramatically, as the time spent on the front is the result of the combination of the two behaviours just described. Computing the time they spend at front in the first phase, while they are fast, the curves are identical to those for fast particles, fig. 5.4(left), except for the fact that the value of the constant plateau is slightly inferior to $1/\lambda_f$. This should not be surprising: in a time $\sim 1/\lambda_f$ fast particles are blocked since they are own-overtaken, and so cannot mutate. Here we are considering particles conditioned to mutate before that happens. After mutation, the curves for t_f reproduce those for slow particles, fig. 5.4(right).

5.2 Selective advantage of stability in well-mixed

Before focusing on the selective effects of the mutation rate in space, we should see how a greater stability can provide a selective advantage in the well-mixed case. In

other words, adaptation will require optimization in both the fitness and the mutational landscape [99]. In the previous chapters, indeed, we always treated mutation just as a source for fitness variability, and never as an element for selection to act on. As usual, we will treat the problem in a very abstract way, limiting the details to the fewest possible.

We start with a population constituted by M (fixed) individuals having two inheritable features, their fitness λ and their mutation rate $1/\tau$. An individual will have its new values of fitness and mutation rate extracted from two probability distributions, $p(\lambda)$ and $q(\tau)$. We will consider the case of strong epistasis, and therefore after a mutation the two new values for (λ, τ) are sampled in a completely random way. We will see that, even in this extreme case of completely independent and decorrelated rates of reproduction and mutation in a single individual, at the level of the population a correlation between fitness and stability will emerge, enforced by selection.

From all what we have learned in this work about evolution, we can confidently expect that, after waiting long enough, a population starting with random reproduction and mutation rates will have adapted, typically fixating into one lineage, characterized by values of (λ, τ) that are significantly higher than the average ones extracted from $p(\lambda)$ and $q(\tau)$. This means that the majority of new mutations will create individuals that are much less fit than the present population, and only a few of them will present a selective advantage. We will have then that the beneficial mutations rate, U, will be much lower than the total mutation rate $1/\tau$. Moreover, for adapted enough population, the probability of finding a mutant with a large selective advantage depends on the explicit form of $p(\lambda)$, but we showed in subsection 1.3.2 that an exponentially decreasing distribution of fitness advantages is reasonable for most cases, and can be assumed to be very low. For this reason, we can suppose to be in the successional mutations regime, eq. 1.34, even for reasonably high value of the mutation rate $1/\tau$.

We know then (subsection 1.2.2 and 1.3.1) that evolution will be characterized by a sequence of periods of monoclonality of the population, separated by rapid competitions following the appearance of a mutant with a fitness similar to the one of the wild-type. In the following, we will analyse how these monomorphic and competition phases are modified in the presence of a non-negligible mutation rate.

First, let us consider the case of a single dominant lineage in the population. For high mutation rate, this wild-type will generate a lot of deleterious mutants, with very low fitnesses. We will refer to this set of unfit mutants with the name of cloud. By definition, individuals belonging to it are not able to compete with the dominant population, and will become extinct. Their number is however continuously replenished by the constant feeding of mutations coming from the dominant population. This flux is one-way only: mutants in the cloud will not mutate back to the wild-type, since the values of (λ, τ) of cells of the latter are in the tails of the distributions $p(\lambda)$ and $q(\tau)$. By mutating, individuals in the cloud will simply remain in the cloud. A similar situation has been encountered in the modified Eden model described in section 5.1, where this asymmetry in the competition was introduced by hand. In the following, we will make the assumption of considering this cloud as non-mutating, and with fitness $\lambda_c \sim 0$. Its overall effect, then, is to reduce the actual population size M to an effective population size M_{eff}, since

only the individuals belonging to the wild-type will be able to reproduce. The number of individuals in the cloud can be estimated as $M/(\tau\lambda)$, and the effective population size is given by

$$M_{eff} = M\left(1 - \frac{1}{\lambda\tau}\right) \tag{5.1}$$

The pattern [monoclonality $\rightarrow$ competition $\rightarrow$ monoclonality $\rightarrow$...] will then be carried out by a sequence of lineages in a size-reduced population.

However, the effects of a non-negligible mutation rate show off also in changing the nature of the computation of two lineages. We have described the cloud of unfit mutants as an inert object, thus not able to participate in the competition, so that the fight for fixation (to M_{eff}) can be considered to take place between two fit lineages only. These will have (λ_a, τ_a) and (λ_b, τ_b) respectively. Since we can restrict the competition to two colonies only, we might be tempted to use the same approach we did in the study of the Moran process, subsection 1.1.1. If the two couples of values (λ_a, τ_a) and (λ_b, τ_b) are not too different from each other, we can consider that the cloud will remain more or less of the same size, and a fixed size constraint can be imposed, at M_{eff}. Since we are in the successional mutations regime, this is not a too stringent assumption. All we need to compute is the transition probabilities $\pi_{i\rightarrow i+1}$ and $\pi_{i\rightarrow i-1}$ for, say, lineage a, and then the fixation probability is recovered in the form of eq. 1.11. In the case of simple selection, neglecting mutations, we easily computed the probabilities for the transition in eq. 1.1. The way to compute them was understanding that the process of an increase of one individual in a is the composition of a birth for a, followed by a death in b. Here, we can indeed operate in the same way. The key idea is that a mutation of a lineage into the cloud can be considered exactly as a death. Indeed, a particle of a cannot mutate back into a nor generate an a individual, but only wait until it is replaced by an offspring of a or b. We have the same structure as in eq. 1.1, with the caveat of using the effective population size M_{eff} instead of the total M. The transition probabilities are

$$\pi_{i\rightarrow i+1} = \frac{\lambda_a i}{M\langle\lambda\rangle}\left(\frac{M-i}{M} + \frac{M-i}{M}\frac{1}{\lambda_b\tau_b}\right) \tag{5.2}$$

$$\pi_{i\rightarrow i-1} = \frac{\lambda_b (M-i)}{M\langle\lambda\rangle}\left(\frac{i}{M} + \frac{i}{M}\frac{1}{\lambda_a\tau_a}\right) \tag{5.3}$$

where the second term in the parenthesis corresponds to the individuals in the cloud coming from mutations of lineage b (top equation) or a (bottom equation). Notice that, e.g. in the top equation, we did not include mutations coming from a into the cloud. This should be understood as follows: the process of mutation of a into the cloud, followed by a reproduction of a, has exactly the same no effect as a reproduction of a, followed by the death of a. In this sense, we can say that mutation is like a pre-announced death (indeed, the mutated individual is automatically excluded from the competition for survival, given that $\lambda_c \sim 0$).

The ratio $\gamma_i = \pi_{i\rightarrow i-1}/\pi_{i\rightarrow i+1}$, needed for computing the fixation probability, has a

nice expression, since it does not depend on i, the number of a individuals

$$\gamma = \frac{\lambda_b \left(1 + \frac{1}{\lambda_a \tau_a}\right)}{\lambda_a \left(1 + \frac{1}{\lambda_b \tau_b}\right)} \sim \frac{\lambda_b \left(1 - \frac{1}{\lambda_b \tau_b}\right)}{\lambda_a \left(1 - \frac{1}{\lambda_a \tau_a}\right)} = \frac{\lambda_b - \frac{1}{\tau_b}}{\lambda_a - \frac{1}{\tau_a}} \tag{5.4}$$

We have here an interesting result. Let us define a quantity that we will call the effective reproduction rate, L, by

$$L_a = \lambda_a - \frac{1}{\tau_a} \tag{5.5}$$

The name of effective fitness for L is chosen because the mutation rate plays here the role of a death rate, and its solely effect is to redefine, reducing it, the actual reproduction rate. This effective fitness will play the exact role that the usual fitness used to play in the absence of mutations. Indeed, $\gamma = L_b/L_a$, and the Moran probability of fixation will be the same as in eq. 2.1, with L substituting λ. We exactly know what the evolution will look like. We will have long periods of time during which the population is essentially monoclonal, with the exception of a non-interacting cloud of $M - M_{eff}$ individuals. Every now and then, a new mutant with an effective fitness comparable with the one of the wild-type will appear, and a competition between the two lineages will take place, as if the total population size where of M_{eff}. Selection will favour the lineage with the higher effective fitness, that will fix with probability ~ 1, and whose probability of becoming extinct is exponentially suppressed in M_{eff}.

We can follow all the steps of subsection 2.1.1, and find out that detailed balance is assured, and that an equilibrium distribution is reached, weighted on the effective, rather than the usual, fitnesses, and with a temperature given by the (inverse of) the effective, rather than the total, population size. It will read

$$p_{eq}(L) = L^{M_{eff}} \tag{5.6}$$

What we can learn from all this discussion can be summarized as follows. First, a high mutation rate is selected against just as a low fitness is. Stability gives an advantage, in the fight for survival, that is non-negligible. In the competition between two populations with the exact same fitnesses, the one with the lower mutation rate is exponentially more likely to out-compete the other. Second, even in this case of independent sampling of fitness and mutation rate, selection forces these two to correlate, and to a well-adapted population the optimization of both the rates is required on the same level.

As a side note, let us say that, in the real world, there exist an optimal, higher than zero, mutation rate, below which population start to lose competitiveness. Indeed external conditions may change, and some degrees of variability should be provided (and this can be achieved through mutations only) in order for a population to be able to face the changing environment. A population incapable of adapting rapidly to the new environment will be clearly disadvantaged. Moreover, at a certain point the selective advantage of a smaller mutation rate will be of the same order of the random genetic drift, and this will likely cause this stability optimization to stop before reaching a zero mutation rate [100].

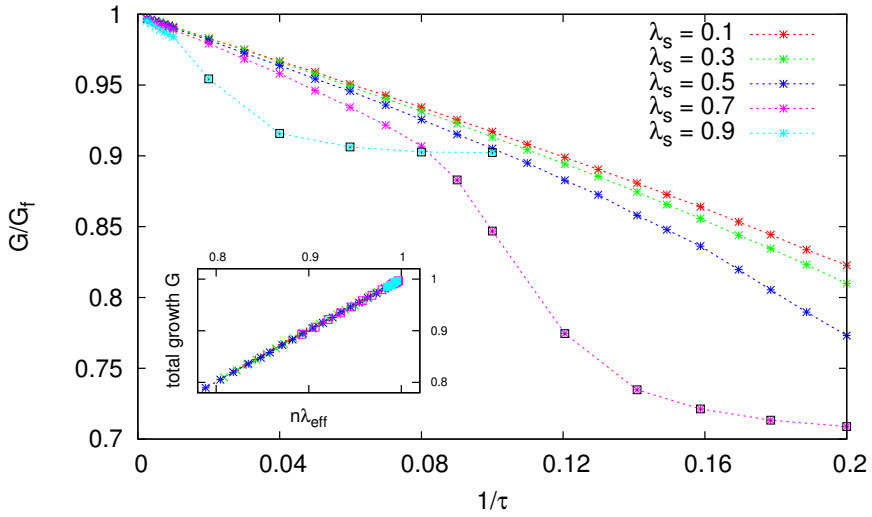

Figure 5.5: Main figure: the normalised distance travelled by the front G/G_f, as a function of the mutation rate $1/\tau$, for several values of λ_s. Black squared points are located in the inactive phase. Inset: the scaling of G with the effective fitness, λ_{eff}, as defined in eq. 5.7. Values of (λ_s, τ) and colors are the same as in the main figure, which correspond in turn to those indicated in the phase diagram of fig. 5.2.

5.3 Selective advantage of stability in space

Let us come back to the spatial setting. It should be clear, at this point of the discussion, that in a spatial environment the fittest lineage is the one that is the fastest in occupying the free available space. The selective advantage is then all enclosed in its velocity to advance. Since we wish to understand how the mutation rate can constitute an element for selection to act on, this section will be dedicated to the study of how the speed of the advancing population is influenced by its mutation rate.

5.3.1 Speed of growth

If in the well-mixed case the presence of a high mutation rate could be easily identified to be deleterious for evolution, being recognized as equivalent to a death rate, it is not clear to what extent it should turn out to be disadvantaging for a growing population. Therefore, before providing any interpretation, let us go directly to the results of simulations. Fig. 5.5 shows the distance G covered by the advancing front in a fixed given time, for several values of λ_s, as the mutation rate $1/\tau$ is varied. The value of the growth G is normalized by the value of growth G_f of a monoclonal population of fast cells only. Black squared points represent values for the growth in the inactive phase, so let us not consider them for the moment. In the limit $\tau \to 0$, $\lambda_s \to \lambda_f$, the value of the front advance converges to the one of a population composed of solely λ_f, as it should. While the value of the mutation rate is increased, as one would have expected, the speed of

growth is reduced, and the front is able to cover a shorter distance in the same time. Indeed, the presence of slower mutants at the front causes the system to slow down, as they act as obstacles for faster particles, that have to reproduce more in order to bypass them, following necessarily a longer path. What is, instead, counter-intuitive, is the behaviour in varying λ_s. Naively, one would expect that, for faster λ_s particles, the front would advance faster than for slower ones. What happens is exactly the opposite. This means that a population having slightly worse mutations, with $\lambda_s \sim \lambda_f$, is evolutionary disadvantaged with respect to a population having extremely unfit mutants, $\lambda_s \ll \lambda_f$.

The explanation for this fact can be found by looking at the composition of the front. For the same mutation rate value, faster slow particles are much more abundant at the front than slow ones, since they reproduce faster and their domains can extend much more. Even if they are only slightly less rapid than fast particles, their higher number enables them to be more effective in slowing down the population growth with respect to the slower, but fewer, slow (slow) particles. The growth can be parametrized by defining an effective growth rate,

$$\lambda_{eff} = \frac{\lambda_s n_s + \lambda_f n_f}{n} \tag{5.7}$$

where $n = n_s + n_f$ and n_f (resp. n_s) is the average number of fast (resp. slow) particles at the front. Please notice that the total number of particles at the front, n, is not a priori equal for all the (λ_s, τ), but will indeed vary as the front roughens up. The scaling of the distance travelled by the front with the effective growth rate of eq. 5.7 is shown in the inset of fig. 5.5.

It is important to notice that, while the speed of the growth can be directly related to the properties of the front of the advancing colony, we cannot say the same for what concerns the properties of the bulk. Indeed, bulk and front have two different behaviours, for a polymorphic population. Consider a slow (black) particle appearing at the front, as sketched in the figure below, surrounded by fast (white) ones.

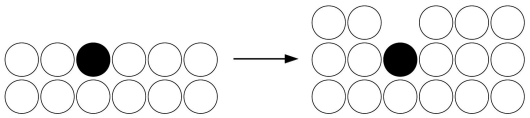

For two different instants of time, separated by $\sim 1/\lambda_f$, the particle may not be able to reproduce, yet not being overtaken by other particles. Then we will have that the slow cell is over-counted at the front, while it will be considered only once for the bulk average. One can see indeed (data not shown here) that, the smaller the value of λ_s considered, the more pronounced this over-counting is, i.e. the ratio of slow particles at the front increases with respect to the same ratio in the bulk when mutants are slower.

Saturation effects As a final observation on our two-lineages model of growth we will provide some comments on the phase transition, from the active to the inactive phase. We have seen that, for a given value of λ_s, by increasing the mutation rate one can

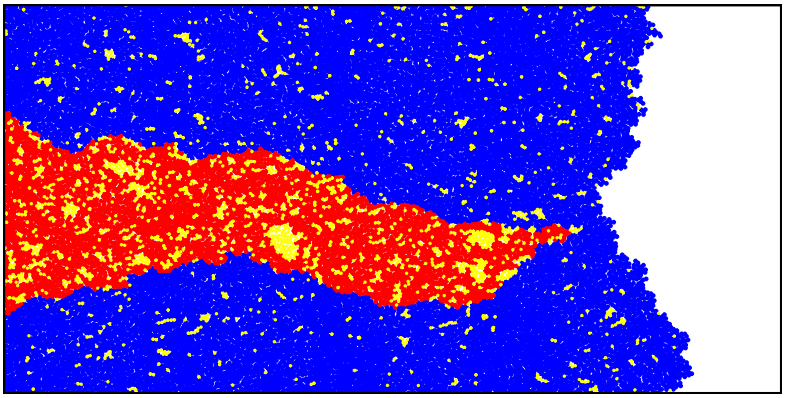

Figure 5.6: The competition between two populations, with equal fitness $\lambda_f = \lambda_1 = \lambda_2$, mutating in the same type of individual with fitness $\lambda_s = 0.3\lambda_f$, but with two different mutation rates, $\tau_1 = 5\,\tau_2$. The fast mutating population (in red), is easily overcome by the more stable population (blue), since it is slowed down by the presence of a larger number of slow particles (in yellow).

cause the system to have a rapid fixation of the less fit lineage. This interval of values is crossed by the squared points in fig. 5.5. We can note at least two things from the curves described by the average growth of the front. First, the curves present a steep drop in the growth, while crossing the zone of phase transition. We can see here a mark of the non-linearity of the cluster merging, main cause of the transition in the fixation time. Second, the curves reach a plateau. The reason is simple: when the fixation is very fast, as it is in the inactive phase, the population grows as a uniform one, composed by slow cells. The value of the travelled distance will simply be $G/G_f = \lambda_s/\lambda_f$ times smaller.

Such saturation effects can be seen also by looking at fig. 5.3, showing the number of particles at the front. For low $1/\tau$ values, an increase in the mutation rate causes a rise in the number of particles at front, since slow particles trail behind, and the front roughens. However, for high $1/\tau$ values, the inhomogeneity of the front starts reducing, as the front becomes populated mostly by slow particles, and an increase of the mutation rate lowers the number of fast particles. For very high mutation rates, fixation happens immediately, and the front is completely homogeneous, and consists of slow particles only.

5.3.2 Mutation rate evolution

With all the results obtained in the previous analysis, we are able to say something about the evolutionary advantage conferred by a given mutation rate. We have seen, fig. 5.5, that a well adapted population, while mutating into less-fit individuals, grows less if the mutation rate is higher. We can then interpret stability as a selective advantage. Indeed, look at fig. 5.6, where two almost identical populations are competing. Both of them are composed of the same (fast) individuals, $\lambda_1 = \lambda_2$, and mutate into the same (slow) individuals, with λ_s, back mutations not being allowed. Their only difference is

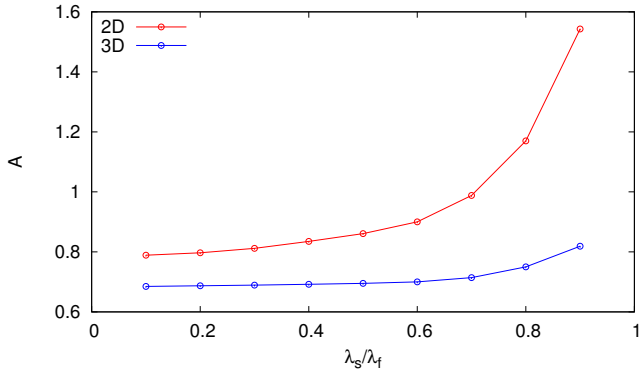

Figure 5.7: The value of the function $A(\lambda_s/\lambda_f)$, computed from the growth retardation factor R as defined in eq. 5.9, for different λ_s values, in two and three dimensions.

in their mutation rates, with the first wild-type population having a mutation rate five times higher. Its lower stability is the only thing that differentiate it from the second population, but still it is sufficient for making it selectively disadvantaged. The fact that the growth of one lineage is slowed down can be seen by looking at the hollow present in the front of the population, in concomitance with the out-competed lineage, right after its extinction. Compared to a competition in fitness, fig. 4.2(right), one can notice that the borders oscillate much more, and the overtaking, though being deterministic, does not proceed as linearly as before. The reason for this is that the slowdown due to the slow particles in the faster mutating population is more a global effect than a localized effect present at the frontiers, where instead most of the times the two particles competing are the fast ones, which are equal. In some sense, then, the dynamics of the border has some element of pure diffusion in it, and indeed it resembles the behaviour in fig. 4.2(left).

Finally, one can look at the general case. Individuals can mutate by changing their fitness and their mutation rate, both λ and τ being chosen from some given distributions, $p(\lambda)$ and $q(\tau)$. The situation is similar to the one of subsection 5.2. Selection will favour individuals with high values of both λ and τ, and the fitness will not be the only selected feature. The evolution will then (in the successional mutations regime) proceed with a sequence of monoclonal populations, selected according to their reproduction rate and their resilience to mutation. When mutations are not too frequent, we expect domains not to merge. For given (λ_s, τ), domains will have an average size and slow down the growth of the wild-type by an average factor. Since they are not merging, their contributions should add up linearly. The number of total domains will be proportional to the mutation rate. In such a linear regime, one can provide a parameter ruling the evolution, like the effective fitness in eq. 5.5 in the well-mixed setting. A population will be successful if it has a larger value of L, defined as

$$L = \lambda - A_p(\lambda)\frac{1}{\tau} \tag{5.8}$$

where $A_p(\lambda)$ is a multiplicative factor that depends on the probability distribution $p(\lambda)$

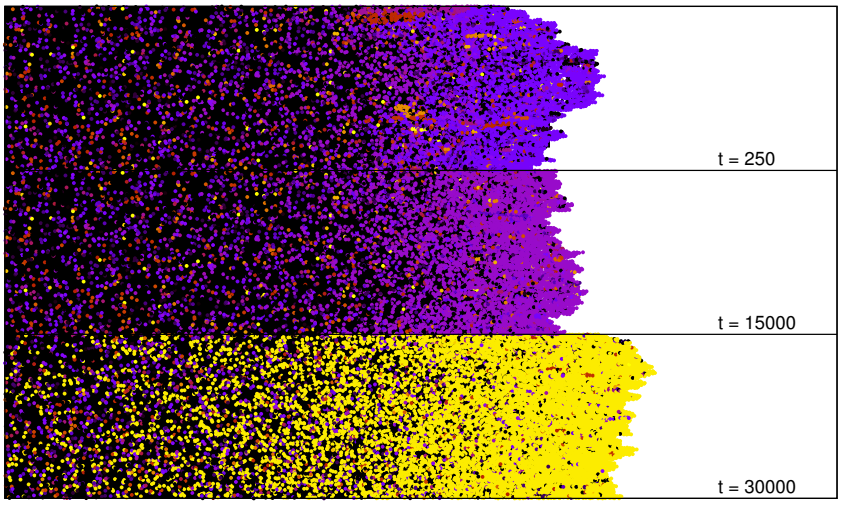

Figure 5.8: A growing population at three instants of time. Lineages are sampled at mutation by two probability distribution $p(\lambda)$ and $q(\tau)$. For longer times, the bulk is not shown entirely, and only the part of the population close to the front is plotted. The color code refers to the mutation rate of the population, from $\tau = 10$ (black) to $\tau = 40$ (yellow). One can see how the penetration of the front in the bulk grows with time, as a combined effect of both increased fitness and decreased mutation rate.

of the mutants, i.e. their fitness relatively to the dominant population (in the well-mixed case, A was simply equal to one). The analytical form of $A_p(\lambda)$ is not known, but in can be computed for the two competing populations model considered before, where it only depends on the λ_s/λ_f ratio. We can estimate the growth retardation factor R defined as

$$R \equiv \frac{G_f - G}{G_f} = A(\lambda_s/\lambda_f)\frac{1}{\tau\lambda_f} \tag{5.9}$$

where G is the distance travelled by the front, and G_f is the distance it would have travelled if it was constituted by fast particles only. In fig. 5.7 the value of A is estimated for different values of λ_s, and in 2 and 3 dimensions. The behaviour, upon varying λ_s, is the one already described, with the growth slowed down more by higher values of λ_s. Moreover, the slowdown is more effective in 2D than in 3D. This should not be surprising: in higher dimensions, the fast particles have more ways to overtake slow particles, and on the other hand for every single slow particles there are more fast particle that can compensate for its slower growth. It is not unreasonable to expect that the higher the dimension, the lower the retardation factor will be.

In general, we can conclude that selection in space will favour both high fitness and stability. If we allow mutations to happen in the bulk, we can see how such a selection is maintained only as long as reproduction is present. Cells in the bulk, indeed, will mutate and choose a random value of (λ, τ) extracted from $p(\lambda)$ and $q(\tau)$, so that

their distributions inside the bulk will just reproduce the two probabilities. Both λ and τ are then completely epistatic. Only in the front, the selection pressure granted by reproduction is able to maintain the dominant (λ, τ) far away from the averages of the distributions, and populations will evolve by sampling successful mutants from the optimized tails of $p(\lambda)$ and $q(\tau)$. We can see these selective effects in action in fig. 5.8. Black cells are those that have mutated in the bulk, and are not significant for evolution. We can see how fitness and stability are selected simultaneously, as the layer of fit particles thickens with time. This is due both to higher fitness, as cells reproduce faster and can cover a larger span in the same time, and to higher stability, as cells conserve their phenomenological state for a longer time after being created at the front, thus being able to enter deeper in the bulk.

As a final comment, let us note that the actual form of the distribution of mutants is important. We have seen indeed, in subsection 5.3.1, that slightly deleterious mutations are more disadvantageous for a population than really unfit one. Then, let us consider two well-adapted populations, with the same mutation rate, but one with a strongly epistatic fitness, while the other one has a fitness which is much more additive-like. Contrarily to what one could have expected, epistasis favours the first one in a spatial competition, as its mutants are not able to compete with it, and are easily overtaken. In other words, Muller ratchet in space is much more efficient if deleterious mutations are really small.

We will not present here results for free, circular growth. From what we have seen in section 4.2, by comparing linear and circular growth, we know that in a circular front the time needed for fixation is higher than in the linear case, and fitness differences are less relevant. Let us remember, however, that the differences found in the linear-circular comparison were due to the fact that the front is expanding. For large enough radius, the circular front can be approximated as linear, and the microscopic behaviour is the same. Then, probably, the magnitude of the retardation coefficient A will be more or less the same, but selection for stability will act less efficiently. Due to the global geometry, and distances from lineages scaling with the increasing radius, higher mutating, less fit lineages, although disadvantaged, will survive for a longer time than in a front setting. In the Eden model with mutations presented in section 5.1, we have seen that in the inactive phase the scaling of time for fixation is logarithmic with the front width, while it is exponential in the case of the active phase. Since the growth of the length of the front is linear with time in the circular case, we can suppose that fixation will happen in the inactive phase only, while the front expansion will be sufficient in the active phase to keep mutant domains apart and avoid the extinction of the fast wild-type.

Conclusions

Even in our extremely simplified description of a population, we have been facing a plethora of different evolutionary situations, testified by the variability of the approaches necessary for their study. The phenomenology has turned out to be extremely rich, especially when one considers that the main subject of study can be resumed in the three words of the title of this work, *Dynamics with selection*. Notwithstanding our aim at homogeneity and self-consistence, and the numerous connections linking the different parts of the manuscript, the reader might be puzzled by the constant change of perspectives in this work. Let us resume here the main conclusions that should be retained, after this long lecture.

Firstly, in chapter 2, we showed that populations can be considered as thermal systems. Small populations have the same behaviour as hot systems, and increasing their number of individuals results in cooling them down. This was known to be the case long before, in the regime of infrequent mutations, and at equilibrium. However, we showed how this analogy can be extended to the case where the population is out of equilibrium, which will be often the case in real life, and even when the usual detailed balance condition, needed to prove the thermal equivalence, does not hold any more, provided that a definite time-scale separation manifests itself. We proved that a generalized version of the detailed balance condition holds, and that the dynamics of an adapting population is for several aspects phenomenologically identical to that of out of equilibrium physical systems. In particular, we showed how a liquid-glass transition can be crossed, by increasing the population size over a certain threshold. The thermal analogy led us to suggest several applications, motivated by results obtained in non equilibrium physics, that would have seemed rather exotic if considered from a biological perspective only. In particular, we showed how evolution can be speeded up in chemostat experiments, with a procedure in all aspects similar to the parallel tempering used in Monte Carlo simulations. We also provided a direct interpretation of the presence of a fluctuating environment as a source of rejuvenation for the system, with the consequence of preventing its adaptation above a given threshold. External changing conditions are shown to supply additional selective pressure to the system, privileging populations that are able to adapt on the time-scale of the fluctuating environment.

We addressed then, in chapter 3, the issue of interacting evolving populations. We restricted ourselves to the case of monoclonal populations, where the analogy with the physics of disordered systems helped us in understanding the main features of adaptative

evolution. We showed how, by coupling two populations, their evolutionary time-scales diverge. Between the two populations, a net fitness flux is exchanged, with the faster adapting population being exploited, and allowing the other one to increase its fitness through their interaction. This mechanism is very robust to quantitative changes, and was by no means introduced by hand, but arises as a necessary consequence from the asymmetry in the two population fitness variances. In case of more than two coupled populations, the time-scale separation exists, but it is not diverging. A net flux of fitness can be established, with faster adapting populations supplying fitness to slower ones.

The attention has finally turned to spatial settings, chapters 4 and 5. We saw that, with respect to the well-mixed case, competition is slowed down, since fitness differences are less effective in leading to fixation, and the net result is a stronger persistence of polymorphism. Different geometries are shown to give rise to different behaviours. In all cases, however, it turns out that the faster lineage in occupying space is also the fitter. That being the case, the evolutionary importance in the reproduction rate is rather trivial, and so we have been concerned about the selective advantage given by the mutation rate, in chapter 5. In the well-mixed case the effect of the mutation rate can be interpreted as a redefinition of the actual reproduction rate. Indeed, a similar relation can be shown to hold in the spatial case, for not to high mutation rates. Deleterious mutants act like obstacles in the growth of the wild-type, and therefore a lower mutation rate guarantees a faster advance. Adaptation will consequently require the optimization of both reproduction and mutation rates.

Appendix A

Computations of the entropy

In this appendix we report some short calculations needed to obtain nicer expressions for the entropy associated with jumps in fitness, presented in chapter 3.

First, let us derive the expression for the entropy in the case of the two coupled models, with constrained jumps, eq. 3.23. The entropy formula, with the spins appearing explicitely, was (we will note s_1 with s, and s_2 with σ)

$$e^{NS(u',s')} = \sum_{\{s'\}} e^{-\tilde{\mu}(s'\cdot s - NC)} e^{-\mu(s'\cdot\sigma - Nm')} e^{-\frac{Nu^2}{2\sigma_1^2}} \tag{A.1}$$

We can then consider only the spin part, and using the fact that the hyperbolic cosine is an even function, we write

$$\sum_{\{s'\}} e^{-\tilde{\mu}s'\cdot s} e^{-\mu s'\cdot\sigma} \tag{A.2}$$

$$= \sum_{\{s'\}} \prod_i e^{-(\tilde{\mu}s_i + \mu\cdot\sigma_i)s'_i} \tag{A.3}$$

$$= 2^{N-1} \prod_i \left[e^{-(\tilde{\mu}s_i + \mu\sigma_i)} + e^{(\tilde{\mu}s_i + \mu\sigma_i)} \right] \tag{A.4}$$

$$= 2^N \prod_i \cosh(\tilde{\mu} + \mu\sigma_i s_i) = 2^N \prod_i e^{\ln[\cosh(\tilde{\mu} + \mu\sigma_i s_i)]} \tag{A.5}$$

$$= 2^N \prod_i e^{\frac{1}{2}[\ln[\cosh(\mu+\tilde{\mu})] + \ln[\cosh(\mu-\tilde{\mu})] + \sigma_i s_i \ln[\cosh(\mu+\tilde{\mu})] + \ln[\cosh(\mu-\tilde{\mu})]]} \tag{A.6}$$

$$= 2^N e^{\frac{N}{2}[\ln[\cosh(\mu+\tilde{\mu})] + \ln[\cosh(\mu-\tilde{\mu})] + m_o \ln[\cosh(\mu+\tilde{\mu})] + \ln[\cosh(\mu-\tilde{\mu})]]} \tag{A.7}$$

$$= 2^N e^{N/2[(1+m_o)\ln(\cosh(\mu+\tilde{\mu})) + (1-m_o)\ln(\cosh(\mu-\tilde{\mu}))]} \tag{A.8}$$

Inserting this last expression into eq. A.1, we recover the expression presented in eq. 3.23.

Let us consider the unconstrained case, i.e. let us derive the expression for eq. 3.14. The starting point is the same entropy as the constrained case, eq. A.1, but without the constraint on the jumps, namely the Lagrange multiplier $\tilde{\mu}$ should be considered zero. By following the same calculations as before, we easily get

$$\sum_{\{s'\}} e^{\mu s' \cdot s - Nm} \rightarrow e^{N \ln 2 + N \ln(\cosh(\mu)) - \mu N m} \tag{A.9}$$

This expression, however, can be further simplified, by considering that the saddle point equation for the field μ gives us $\mu = \tanh^{-1}(m)$. In order to proceed, it is useful to consider the following identities:

$$\cosh(\tan^{-1}(x)) = \frac{1}{\sqrt{1-x^2}} \qquad \tanh^{-1}(x) = \frac{1}{2} \ln \frac{1+x}{1-x} \tag{A.10}$$

By using eq. A.10, we can simplify the exponent in eq. A.9, as

$$\ln 2 + \ln(\cosh(\mu)) - \mu m \tag{A.11}$$
$$= \ln 2 + \ln(\cosh(\tan^{-1}(m))) - m \tanh^{-1}(m) \tag{A.12}$$
$$= \ln 2 + \ln \frac{1}{\sqrt{1-m^2}} - \frac{m}{2} \ln \frac{1+m}{1-m} \tag{A.13}$$
$$= \ln \frac{2}{\sqrt{1-m}\sqrt{1+m}} - \frac{m}{2} \ln \frac{1+m}{1-m} \tag{A.14}$$
$$= \ln \sqrt{\frac{2}{1-m}} + \ln \sqrt{\frac{2}{1+m}} - \frac{m}{2} \ln \frac{1+m}{2} + \frac{m}{2} \ln \frac{1-m}{2} \tag{A.15}$$
$$= \frac{1+m}{2} \ln \left(\frac{1+m}{2} \right) + \frac{1-m}{2} \ln \left(\frac{1-m}{2} \right) \tag{A.16}$$

The final expression, when inserted in eq. A.9, let us obtain the entropy formula of eq. 3.14.

Finally, for what concerns the case of three interacting systems, we can see that the expression for the entropy,

$$\sum_{s'} e^{-\frac{Nu^2}{2\sigma^2}} e^{-\mu_{12}(s'_1 \cdot s_2 - N m'_{12})} e^{-\mu_{13}(s'_1 \cdot s_3 - N m'_{13})} \tag{A.17}$$

is identical to the one presented in the unconstrained case, eq. A.1, with the second magnetization term $\mu_{13}(s'_1 \cdot s_3 - N m'_{13})$ playing the role of $\tilde{\mu}(s' \cdot s - NC)$. One can follow then exactly the same computations, and find that

$$\sum_{s'_1} e^{-\mu_{12}(s'_1 \cdot s_2 - N m'_{12})} e^{-\mu_{13}(s'_1 \cdot s_3 - N m'_{13})} \tag{A.18}$$
$$= 2^N e^{N/2[(1+m_{23}) \ln(\cosh(\mu_{12}+\mu_{13})) + (1-m_{23}) \ln(\cosh(\mu_{12}-\mu_{13}))]} \tag{A.19}$$

which is the expression presented in eq. 3.28.

Bibliography

[1] P. Molander, "The Optimal Level of Generosity in a Selfish, Uncertain Environment," *The Journal of Conflict Resolution*, vol. 29, pp. 611–618, Dec. 1985.

[2] M. Nowak and K. Sigmund, "A strategy of win-stay, lose-shift that outperforms tit-for-tat in the Prisoner's Dilemma game," *Nature*, vol. 364, pp. 56–58, July 1993.

[3] S. F. Elena and R. E. Lenski, "Microbial genetics: Evolution experiments with microorganisms: the dynamics and genetic bases of adaptation," *Nature Reviews Genetics*, vol. 4, pp. 457–469, June 2003.

[4] J. W. Fox and R. E. Lenski, "From Here to Eternity—The Theory and Practice of a Really Long Experiment," *PLOS Biology*, vol. 13, p. e1002185, June 2015.

[5] T. Brotto, G. Bunin, and J. Kurchan, "Population aging through survival of the fit and stable," *arXiv:1407.4669 [physics, q-bio]*, July 2014. arXiv: 1407.4669.

[6] T. Brotto, G. Bunin, and J. Kurchan, "Extending the applicability of Thermal Dynamics to Evolutionary Biology," *arXiv preprint arXiv:1507.07453*, 2015.

[7] A. J. Kovacs, "Transition vitreuse dans les polymères amorphes.," in *Fortschritte Der Hochpolymeren-Forschung*, no. 3/3 in Advances in Polymer Science, pp. 394–507, Springer Berlin Heidelberg, 1964.

[8] S. Wright, "Evolution in Mendelian populations," *Genetics*, vol. 16, no. 2, p. 97, 1931.

[9] M. Eigen, J. McCaskill, and P. Schuster, "Molecular quasi-species," *J. Phys. Chem.*, vol. 92, no. 24, pp. 6881–6891, 1988.

[10] L. Peliti, "Introduction to the statistical theory of Darwinian evolution," *arXiv:cond-mat/9712027*, Dec. 1997. arXiv: cond-mat/9712027.

[11] S. Franz and L. Peliti, "Error threshold in simple landscapes," *J. Phys. A: Math. Gen.*, vol. 30, p. 4481, July 1997.

[12] P. A. P. Moran, *The Statistical Processes of Evolutionary Theory*. Clarendon Press, 1962.

[13] P. A. P. Moran, "Random processes in genetics," *Math. Proceed. Cambridge Phil. Soc.*, vol. 54, 1958.

[14] L. Pauling and E. Zuckerlandl, "Molecules as documents of evolutionary history," *J. Theor. Biol.*, vol. 8, pp. 357–366, 1965.

[15] J. F. Crow and M. Kimura, "An introduction to population genetics theory.," 1970.

[16] M. M. Desai and D. S. Fisher, "Beneficial Mutation–Selection Balance and the Effect of Linkage on Positive Selection," *Genetics*, vol. 176, pp. 1759–1798, July 2007.

[17] L. S. Tsimring, H. Levine, and D. A. Kessler, "RNA virus evolution via a fitness-space model," *Physical review letters*, vol. 76, no. 23, p. 4440, 1996.

[18] D. A. Kessler, H. Levine, D. Ridgway, and L. Tsimring, "Evolution on a smooth landscape," *J Stat Phys*, vol. 87, pp. 519–544, May 1997.

[19] D. Ridgway, H. Levine, and D. A. Kessler, "Evolution on a Smooth Landscape: The Role of Bias," *Journal of Statistical Physics*, vol. 90, pp. 191–210, Jan. 1998.

[20] N. Beerenwinkel, T. Antal, D. Dingli, A. Traulsen, K. W. Kinzler, V. E. Velculescu, B. Vogelstein, and M. A. Nowak, "Genetic Progression and the Waiting Time to Cancer," *PLoS Comput Biol*, vol. 3, p. e225, Nov. 2007.

[21] R. Fisher, *The Genetical Theory of Natural Selection.* Oxford: Clarendon Press, 1930.

[22] G. Price, "Selection and Covariance," *Nature*, vol. 227, pp. 520–521, 1970.

[23] G. R. Price, "Extension of covariance selection mathematics," *Annals of human genetics*, vol. 35, no. 4, pp. 485–490, 1972.

[24] O. Hallatschek, "The noisy edge of traveling waves," *PNAS*, vol. 108, pp. 1783–1787, Feb. 2011.

[25] S.-C. Park, D. Simon, and J. Krug, "The Speed of Evolution in Large Asexual Populations," *Journal of Statistical Physics*, vol. 138, pp. 381–410, Feb. 2010.

[26] P. J. Gerrish and R. E. Lenski, "The fate of competing beneficial mutations in an asexual population," *Genetica*, vol. 102, pp. 127–144, 1998.

[27] H. A. Orr, "The rate of adaptation in asexuals," *Genetics*, vol. 155, no. 2, pp. 961–968, 2000.

[28] C. O. Wilke, "The Speed of Adaptation in Large Asexual Populations," *Genetics*, vol. 167, pp. 2045–2053, Aug. 2004.

[29] J. H. Gillespie, "Molecular Evolution Over the Mutational Landscape," *Evolution*, vol. 38, p. 1116, Sept. 1984.

[30] H. A. Orr, "The distribution of fitness effects among beneficial mutations," *Genetics*, vol. 163, no. 4, pp. 1519–1526, 2003.

[31] B. H. Good, I. M. Rouzine, D. J. Balick, O. Hallatschek, and M. M. Desai, "Distribution of fixed beneficial mutations and the rate of adaptation in asexual populations," *PNAS*, vol. 109, pp. 4950–4955, Mar. 2012.

[32] J. Felsenstein, "The evolutionary advantage of recombination," *Genetics*, vol. 78, no. 2, pp. 737–756, 1974.

[33] I. M. Rouzine, J. Wakeley, and J. M. Coffin, "The solitary wave of asexual evolution," *PNAS*, vol. 100, pp. 587–592, Jan. 2003.

[34] I. M. Rouzine, "Evolution of Human Immunodeficiency Virus Under Selection and Weak Recombination," *Genetics*, vol. 170, pp. 7–18, Feb. 2005.

[35] I. M. Rouzine, E. Brunet, and C. O. Wilke, "The traveling-wave approach to asexual evolution: Muller's ratchet and speed of adaptation," *Theoretical Population Biology*, vol. 73, pp. 24–46, Feb. 2008.

[36] E. Brunet, I. M. Rouzine, and C. O. Wilke, "The Stochastic Edge in Adaptive Evolution," *Genetics*, vol. 179, pp. 603–620, May 2008.

[37] G. Sella and A. E. Hirsh, "The application of statistical physics to evolutionary biology," *PNAS*, vol. 102, pp. 9541–9546, July 2005.

[38] J. Berg and M. Lassig, "Stochastic evolution of transcription factor binding sites," *Biophysics*, vol. 48, no. 1, pp. 36–44, 2003.

[39] J. Berg, S. Willmann, and M. Lassig, "Adaptive evolution of transcription factor binding sites," *BMC Evolutionary Biology*, vol. 4, p. 42, Oct. 2004.

[40] V. Mustonen and M. Lassig, "Molecular Evolution under Fitness Fluctuations," *Physical Review Letters*, vol. 100, Mar. 2008.

[41] N. H. Barton and J. B. Coe, "On the application of statistical physics to evolutionary biology," *Journal of Theoretical Biology*, vol. 259, pp. 317–324, July 2009.

[42] V. Mustonen and M. Lassig, "Fitness flux and ubiquity of adaptive evolution," *PNAS*, vol. 107, pp. 4248–4253, Mar. 2010.

[43] A. Nourmohammad, S. Schiffels, and M. Lassig, "Evolution of molecular phenotypes under stabilizing selection," *Journal of Statistical Mechanics: Theory and Experiment*, vol. 2013, p. P01012, Jan. 2013.

[44] M. Mezard, G. Parisi, M. A. Virasoro, and D. J. Thouless, "Spin Glass Theory and Beyond," *Physics Today*, vol. 41, no. 12, p. 109, 1988.

[45] J. A. Mydosh, *Spin glasses, an experimental introduction.* Taylor and Francis, 1993.

[46] A. Young, *Spin glasses and random fields.* No. 12 in Series on Directions in Condensed Matter Physics, Singapore : World Scientific, 1997.

[47] M. D. Ediger, C. A. Angell, and S. R. Nagel, "Supercooled liquids and glasses," *The journal of physical chemistry*, vol. 100, no. 31, pp. 13200–13212, 1996.

[48] L. Berthier and G. Biroli, "Theoretical perspective on the glass transition and amorphous materials," *Reviews of Modern Physics*, vol. 83, pp. 587–645, June 2011.

[49] T. R. Kirkpatrick, D. Thirumalai, and P. G. Wolynes, "Scaling concepts for the dynamics of viscous liquids near an ideal glassy state," *Physical Review A*, vol. 40, no. 2, p. 1045, 1989.

[50] J.-P. Bouchaud, L. F. Cugliandolo, J. Kurchan, and M. Mezard, "Out of equilibrium dynamics in spin-glasses and other glassy systems," *arXiv:cond-mat/9702070*, Feb. 1997. arXiv: cond-mat/9702070.

[51] L. Berthier and J.-P. Bouchaud, "Geometrical aspects of aging and rejuvenation in the Ising spin glass: A numerical study," *arXiv preprint cond-mat/0202069*, 2002.

[52] J. Kurchan and L. Laloux, "Phase space geometry and slow dynamics," *J. Phys. A: Math. Gen.*, vol. 29, p. 1929, May 1996.

[53] J.-P. Bouchaud, "Weak ergodicity breaking and aging in disordered systems," *Journal de Physique I*, vol. 2, no. 9, pp. 1705–1713, 1992.

[54] I. LeuthÄusser, "Statistical mechanics of Eigen's evolution model," *J Stat Phys*, vol. 48, pp. 343–360, July 1987.

[55] P. Tarazona, "Error thresholds for molecular quasispecies as phase transitions: From simple landscapes to spin-glass models," *Phys. Rev. A*, vol. 45, pp. 6038–6050, Apr. 1992.

[56] D. Saakian and C.-K. Hu, "Eigen model as a quantum spin chain: Exact dynamics," *Phys. Rev. E*, vol. 69, p. 021913, Feb. 2004.

[57] D. B. Saakian and C.-K. Hu, "Solvable biological evolution model with a parallel mutation-selection scheme," *Phys. Rev. E*, vol. 69, p. 046121, Apr. 2004.

[58] D. B. Saakian and J. F. Fontanari, "Evolutionary dynamics on rugged fitness landscapes: Exact dynamics and information theoretical aspects," *Physical Review E*, vol. 80, Oct. 2009.

[59] K. Shekhar, C. F. Ruberman, A. L. Ferguson, J. P. Barton, M. Kardar, and A. K. Chakraborty, "Spin models inferred from patient-derived viral sequence data faithfully describe HIV fitness landscapes," *Phys. Rev. E*, vol. 88, p. 062705, Dec. 2013.

[60] S. Malik and L. Zhang, "Boolean satisfiability from theoretical hardness to practical success," *Communications of the ACM*, vol. 52, p. 76, Aug. 2009.

[61] F. Krzakala, A. Montanari, F. Ricci-Tersenghi, G. Semerjian, and L. Zdeborová, "Gibbs states and the set of solutions of random constraint satisfaction problems," *PNAS*, vol. 104, pp. 10318–10323, June 2007.

[62] T. Jörg, F. Krzakala, G. Semerjian, and F. Zamponi, "First-Order Transitions and the Performance of Quantum Algorithms in Random Optimization Problems," *Phys. Rev. Lett.*, vol. 104, p. 207206, May 2010.

[63] S. Kauffman and S. Levin, "Towards a general theory of adaptive walks on rugged landscapes," *Journal of Theoretical Biology*, vol. 128, pp. 11–45, Sept. 1987.

[64] S. A. Kauffman, "Metabolic stability and epigenesis in randomly constructed genetic nets," *Journal of Theoretical Biology*, vol. 22, pp. 437–467, Mar. 1969.

[65] S. A. Kauffman and E. D. Weinberger, "The NK model of rugged fitness landscapes and its application to maturation of the immune response," *Journal of theoretical biology*, vol. 141, no. 2, pp. 211–245, 1989.

[66] E. D. Weinberger, "Local properties of Kauffman's N-k model: A tunably rugged energy landscape," *Physical Review A*, vol. 44, no. 10, p. 6399, 1991.

[67] P. Sibani and A. Pedersen, "Evolution dynamics in terraced NK landscapes," *EPL*, vol. 48, p. 346, Nov. 1999.

[68] G. Woodcock and P. G. Higgs, "Population Evolution on a Multiplicative Single-Peak Fitness Landscape," *Journal of Theoretical Biology*, vol. 179, pp. 61–73, Mar. 1996.

[69] R. Mari and J. Kurchan, "Dynamical transition of glasses: From exact to approximate," *The Journal of Chemical Physics*, vol. 135, p. 124504, Sept. 2011.

[70] G. E. Crooks, "Entropy production fluctuation theorem and the nonequilibrium work relation for free energy differences," *Physical Review E*, vol. 60, no. 3, p. 2721, 1999.

[71] C. Jarzynski, "Nonequilibrium equality for free energy differences," *Physical Review Letters*, vol. 78, no. 14, p. 2690, 1997.

[72] D. J. Evans and D. J. Searles, "The Fluctuation Theorem," *Advances in Physics*, vol. 51, pp. 1529–1585, Nov. 2002.

[73] S. Mossa and F. Sciortino, "Crossover (or Kovacs) Effect in an Aging Molecular Liquid," *Physical Review Letters*, vol. 92, Jan. 2004.

[74] E. Vincent, "Aging, rejuvenation and memory : the example of spin glasses," *Proceedings "Ageing and the glass transition"*, 2006.

[75] K. Jonason, E. Vincent, J. Hammann, J. P. Bouchaud, and P. Nordblad, "Memory and chaos effects in spin glasses," *Physical Review Letters*, vol. 81, no. 15, p. 3243, 1998.

[76] D. J. Earl and M. W. Deem, "Parallel tempering: Theory, applications, and new perspectives," *Phys. Chem. Chem. Phys.*, vol. 7, pp. 3910–3916, Nov. 2005.

[77] L. C. E. Struik, "On the rejuvenation of physically aged polymers by mechanical deformation," *Polymer*, vol. 38, pp. 4053–4057, Aug. 1997.

[78] L. Berthier and C. W. Holdsworth, "Surfing on a critical line: Rejuvenation without chaos, memory without a hierarchical phase space.pdf," *EPL (Europhysics Letters)*, vol. 58, 2002.

[79] E. Kussell and S. Leibler, "Phenotypic Diversity, Population Growth, and Information in Fluctuating Environments," *Science*, vol. 309, pp. 2075–2078, Sept. 2005.

[80] K. Ishii, H. Matsuda, Y. Iwasa, and A. Sasaki, "Evolutionary stable rate in a periodically changing environment," *Genetics*, vol. 121, 1989.

[81] R. A. Neher and B. I. Shraiman, "Competition between recombination and epistasis can cause a transition from allele to genotype selection," *PNAS*, vol. 106, pp. 6866–6871, Apr. 2009.

[82] B. Derrida, "Random-Energy Model: Limit of a Family of Disordered Models," *Phys. Rev. Lett.*, vol. 45, pp. 79–82, July 1980.

[83] S. Franz, L. Peliti, and M. Sellitto, "An evolutionary version of the random energy model," *J. Phys. A: Math. Gen.*, vol. 26, p. L1195, Dec. 1993.

[84] R. A. Neher, M. Vucelja, M. Mezard, and B. I. Shraiman, "Emergence of clones in sexual populations," *Journal of Statistical Mechanics: Theory and Experiment*, vol. 2013, p. P01008, Jan. 2013.

[85] C. Cammarota and E. Marinari, "Spontaneous energy-barrier formation in entropy-driven glassy dynamics," *Physical Review E*, vol. 92, July 2015.

[86] A. S. Perelson and C. A. Macken, "Protein evolution on partially correlated landscapes," *Proceedings of the National Academy of Sciences*, vol. 92, no. 21, pp. 9657–9661, 1995.

[87] S. Seetharaman and K. Jain, "Evolutionary dynamics on strongly correlated fitness landscapes," *Phys. Rev. E*, vol. 82, p. 031109, Sept. 2010.

[88] L. F. Cugliandolo, J. Kurchan, and L. Peliti, "Energy flow, partial equilibration, and effective temperatures in systems with slow dynamics," *Physical Review E*, vol. 55, no. 4, p. 3898, 1997.

[89] Y.-C. Zhang, M. Serva, and M. Polikarpov, "Diffusion reproduction processes," *J Stat Phys*, vol. 58, pp. 849–861, Mar. 1990.

[90] M. Meyer, S. Havlin, and A. Bunde, "Clustering of independently diffusing individuals by birth and death processes," *Phys. Rev. E*, vol. 54, pp. 5567–5570, Nov. 1996.

[91] O. Hallatschek and D. R. Nelson, "Life at the front of an expanding population," *Evolution*, vol. 64, pp. 193–206, Jan. 2010.

[92] K. S. Korolev, M. Avlund, O. Hallatschek, and D. R. Nelson, "Genetic demixing and evolution in linear stepping stone models," *Rev. Mod. Phys.*, vol. 82, pp. 1691–1718, May 2010.

[93] O. Hallatschek, P. Hersen, S. Ramanathan, and D. R. Nelson, "Genetic drift at expanding frontiers promotes gene segregation," *PNAS*, vol. 104, pp. 19926–19930, Dec. 2007.

[94] M. Eden, "A two-dimensional growth process," *Dynamics of fractal surfaces*, vol. 4, pp. 223–239, 1961.

[95] J.-T. Kuhr, M. Leisner, and E. Frey, "Range expansion with mutation and selection: dynamical phase transition in a two-species Eden model," *New Journal of Physics*, vol. 13, p. 113013, Nov. 2011.

[96] M. Kardar, G. Parisi, and Y.-C. Zhang, "Dynamic scaling of growing interfaces," *Physical Review Letters*, vol. 56, no. 9, p. 889, 1986.

[97] J. Krug and H. Spohn, "Universality classes for deterministic surface growth," *Physical Review A*, vol. 38, no. 8, p. 4271, 1988.

[98] C. A. Tracy and H. Widom, "Asymptotics in ASEP with Step Initial Condition," *Communications in Mathematical Physics*, vol. 290, pp. 129–154, Aug. 2009.

[99] A. Sasaki and M. A. Nowak, "Mutation landscapes," *Journal of Theoretical Biology*, vol. 224, pp. 241–247, Sept. 2003.

[100] M. Lynch, "The Lower Bound to the Evolution of Mutation Rates," *Genome Biol Evol*, vol. 3, pp. 1107–1118, Jan. 2011.